US 20060116634A1

(19) United States

(12) Patent Application Publication (10) Pub. No.: US 2006/0116634 A1

Shachar (43) Pub. Date: Jun. 1, 2006

(54) SYSTEM AND METHOD FOR CONTROLLING MOVEMENT OF A SURGICAL TOOL

(76) Inventor: **Yehoshua Shachar**, Santa Monica, CA (US)

Correspondence Address:
KNOBBE MARTENS OLSON & BEAR LLP
2040 MAIN STREET
FOURTEENTH FLOOR
IRVINE, CA 92614 (US)

(21) Appl. No.: **11/331,781**

(22) Filed: **Jan. 13, 2006**

Related U.S. Application Data

(62) Division of application No. 10/621,196, filed on Jul. 15, 2003.

(60) Provisional application No. 60/396,302, filed on Jul. 16, 2002.

Publication Classification

(51) **Int. Cl.**
A61M 31/00 (2006.01)
A61B 5/05 (2006.01)

(52) **U.S. Cl.** **604/95.01**; 600/424

(57) **ABSTRACT**

A system whereby a magnetic tip attached to a surgical tool is detected, displayed and influenced positionally so as to allow diagnostic and therapeutic procedures to be performed rapidly, accurately, simply, and intuitively is described. The tools that can be so equipped include catheters, guidewires, and secondary tools such as lasers and balloons, in addition biopsy needles, endoscopy probes, and similar devices. The magnetic tip allows the position and orientation of the tip to be determined without the use of x-rays by analyzing a magnetic field. The magnetic tip further allows the tool tip to be pulled, pushed, turned, and forcefully held in the desired position by applying an appropriate magnetic field external to the patient's body. A Virtual Tip serves as an operator control. Movement of the operator control produces corresponding movement of the magnetic tip inside the patient's body. Additionally, the control provides tactile feedback to the operator's hand in the appropriate axis or axes if the magnetic tip encounters an obstacle. The output of the control combined with the magnetic tip position and orientation feedback allows a servo system to control the external magnetic field by pulse width modulating the positioning electromagnet. Data concerning the dynamic position of a moving body part such as a beating heart offsets the servo systems response in such a way that the magnetic tip, and hence the secondary tool is caused to move in unison with the moving body part. The tip position and orientation information and the dynamic body part position information are also utilized to provide a display that allows three dimensional viewing of the magnetic tip position and orientation relative to the body part.

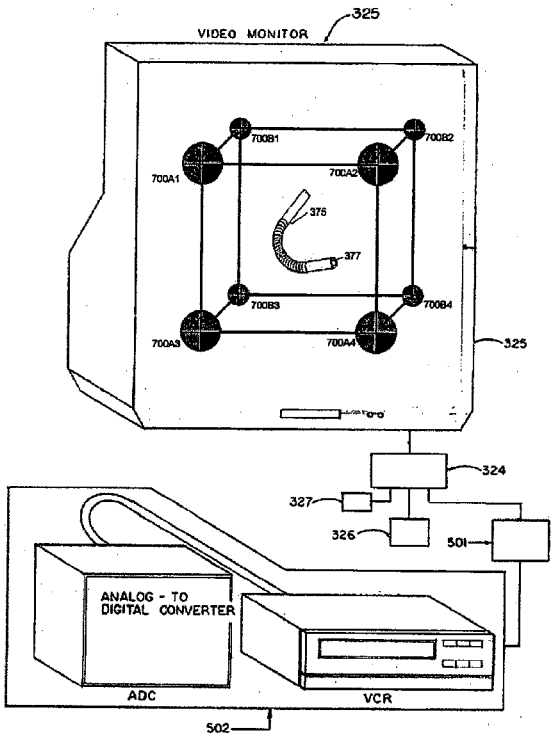

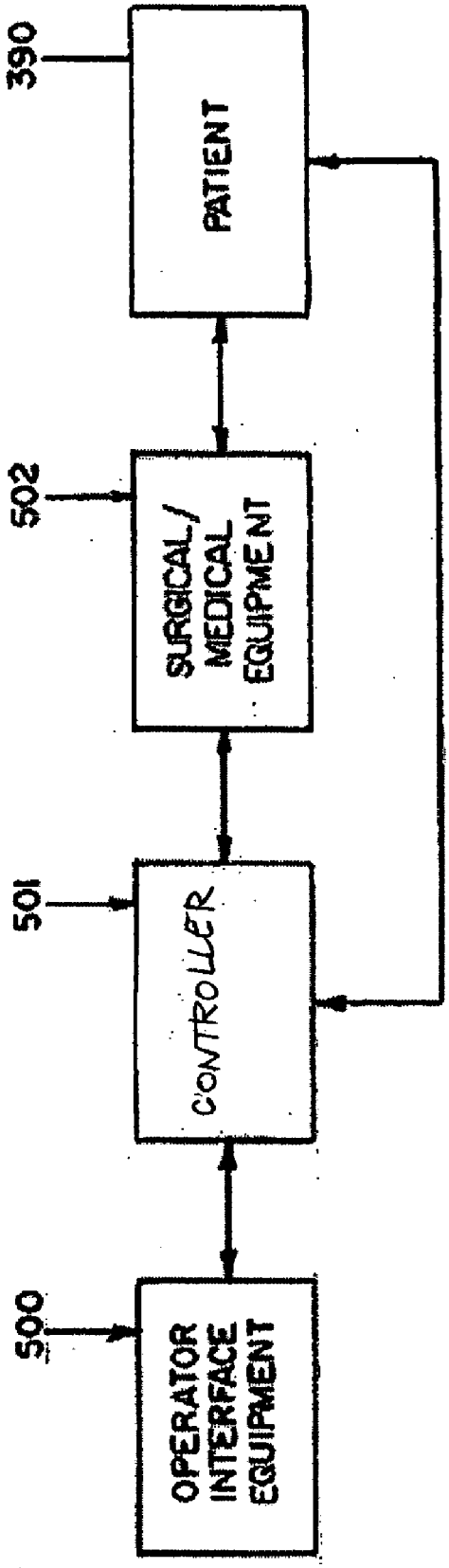
390
PATIENT
502
SURGICAL / MEDICAL EQUIPMENT
501
CONTROLLER
500
OPERATOR INTERFACE EQUIPMENT

FIG. 1A

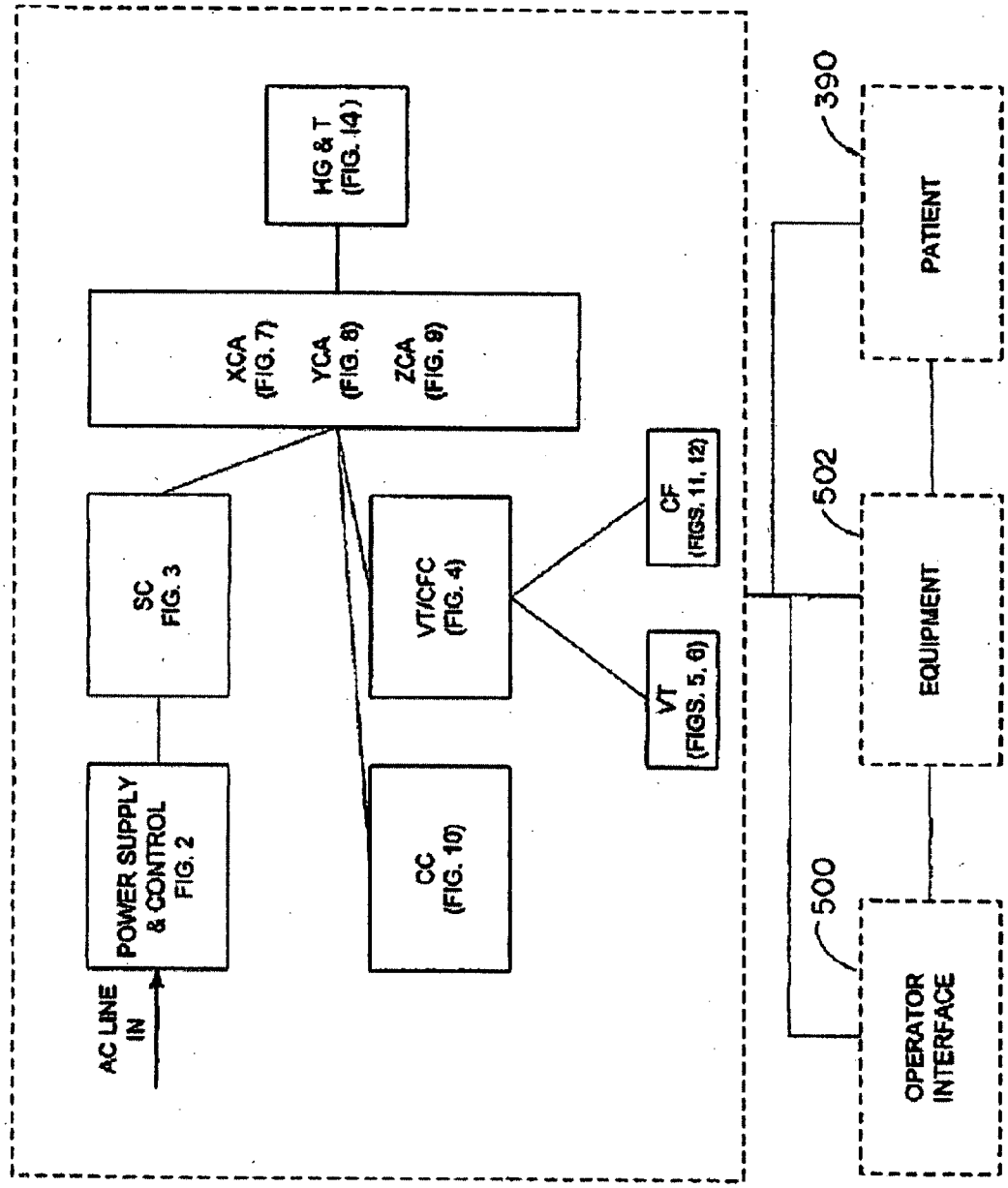
HG & T (FIG. 14)
XCA (FIG. 7)
YCA (FIG. 8)
ZCA (FIG. 9)
SC FIG. 3
VT/CFC (FIG. 4)
CF (FIGS. 11, 12)
VT (FIGS. 5, 6)
CC (FIG. 10)
POWER SUPPLY & CONTROL FIG. 2
AC LINE IN
390
PATIENT
502
EQUIPMENT
500
OPERATOR INTERFACE

FIG. 1B

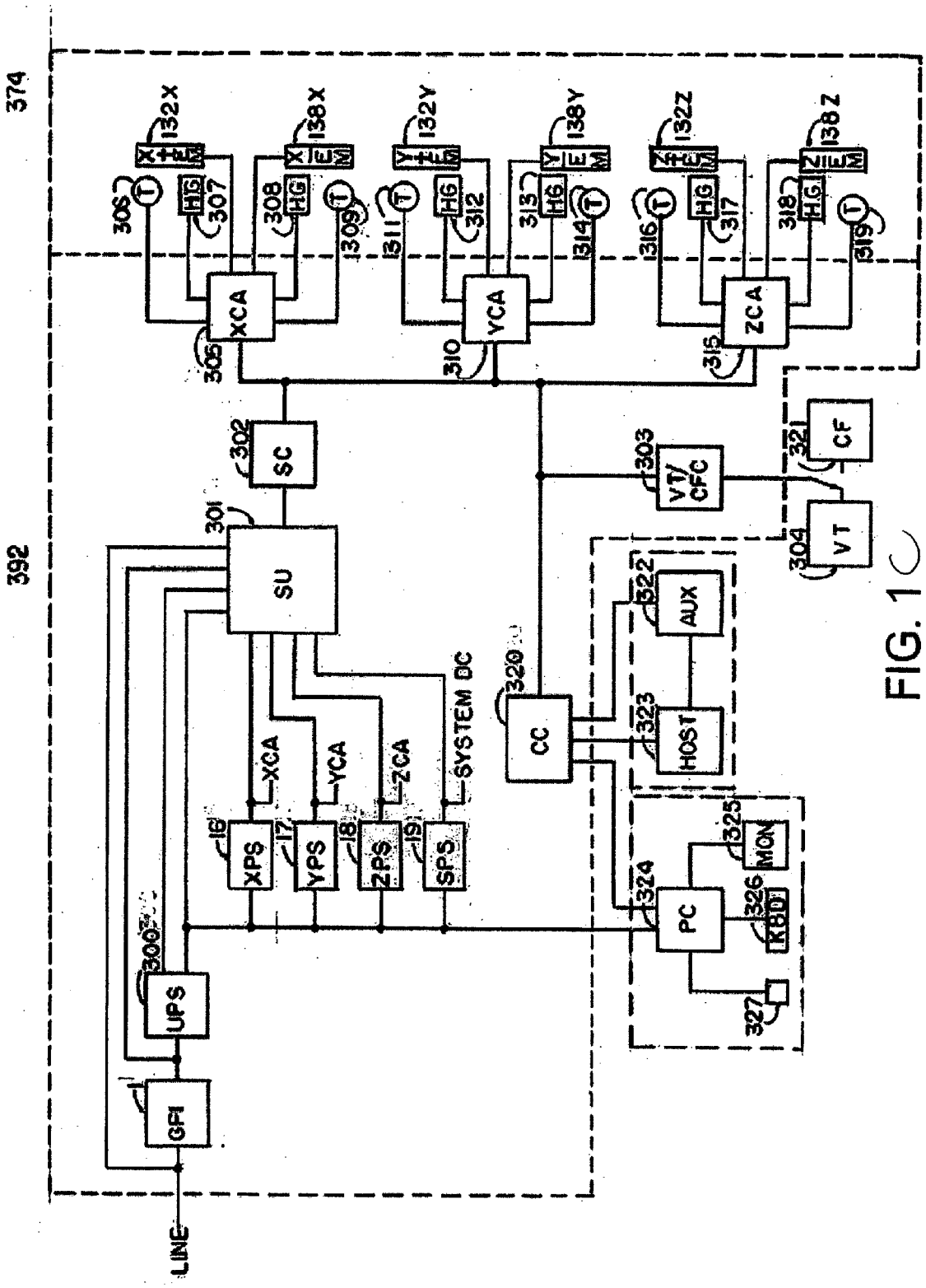
374
392
132X
138X
132Y
138Y
132Z
138Z
XCA
YCA
ZCA
SC
SU
VT/CFC
CF
VT
AUX
CC
HOST
PC
MON
KBD
XPS
YPS
ZPS
SPS
SYSTEM DC
UPS
GFI
LINE

FIG. 1

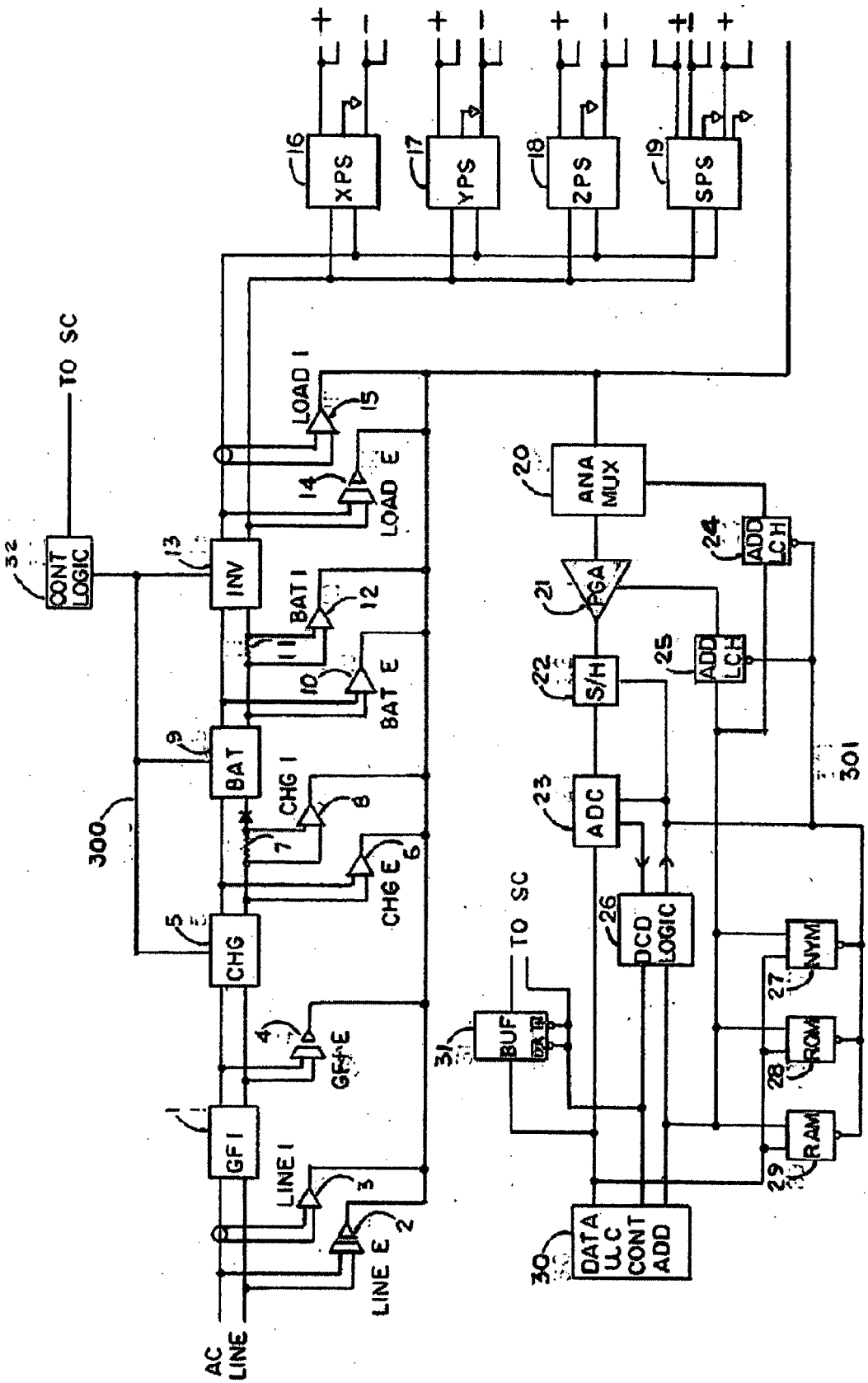
XPS
YPS
ZPS
SPS
TO SC
CONT LOGIC
INV
BAT
CHG
GF I
GF E
LINE I
LINE E
AC LINE
LOAD I
LOAD E
BAT I
BAT E
CHG I
CHG E
ANA MUX
PGA
S/H
ADC
ADD CH
DCD LOGIC
BUF
NVM
ROM
RAM
DATA ULC CONT ADD
300
301

FIG. 2

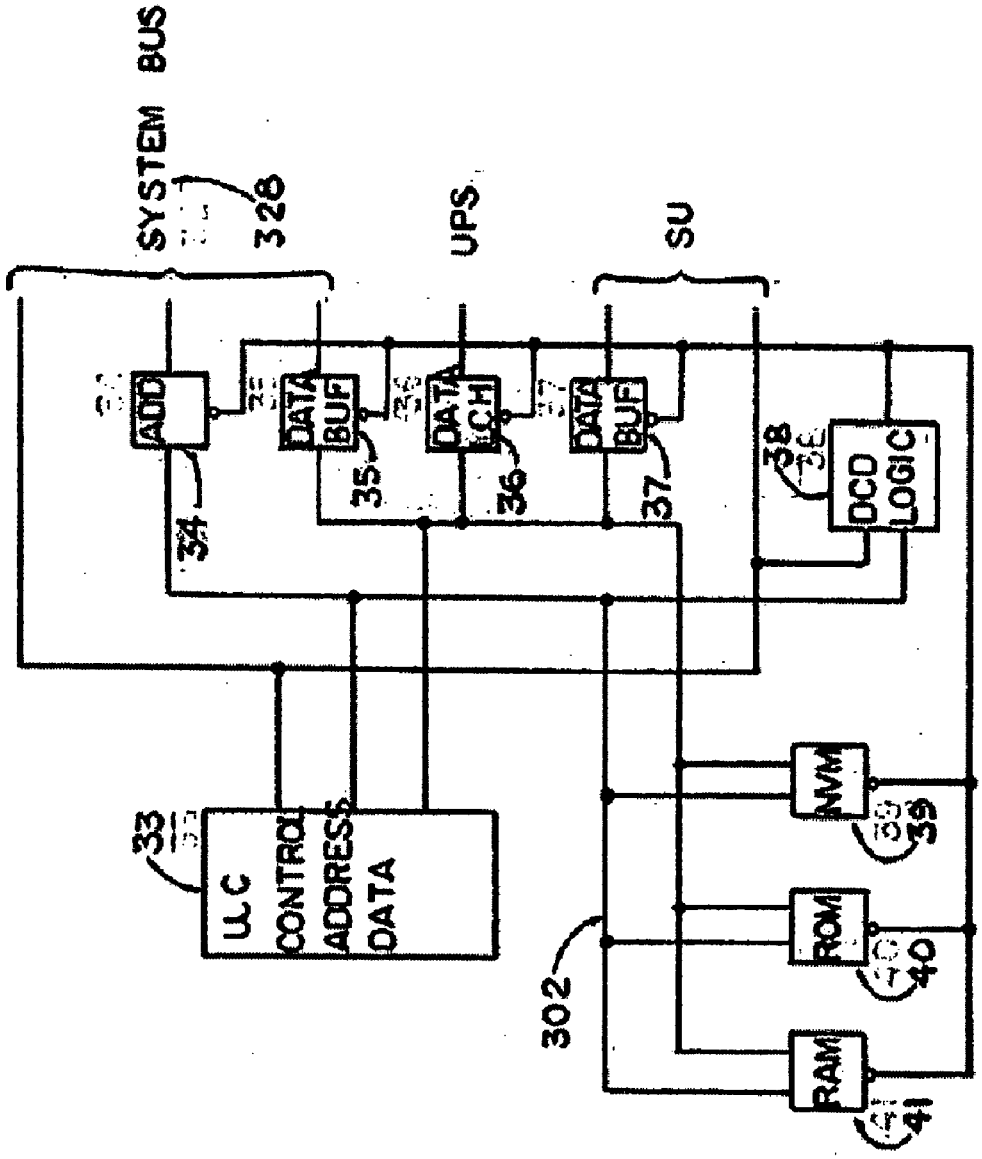
SYSTEM BUS
328
UPS
SU
ADD
DATA BUF
DATA LCH
DATA BUF
DCD LOGIC
34
35
36
37
38
33
U.C
CONTROL
ADDRESS
DATA
NVM
ROM
RAM
39
40
41
302

FIG. 3

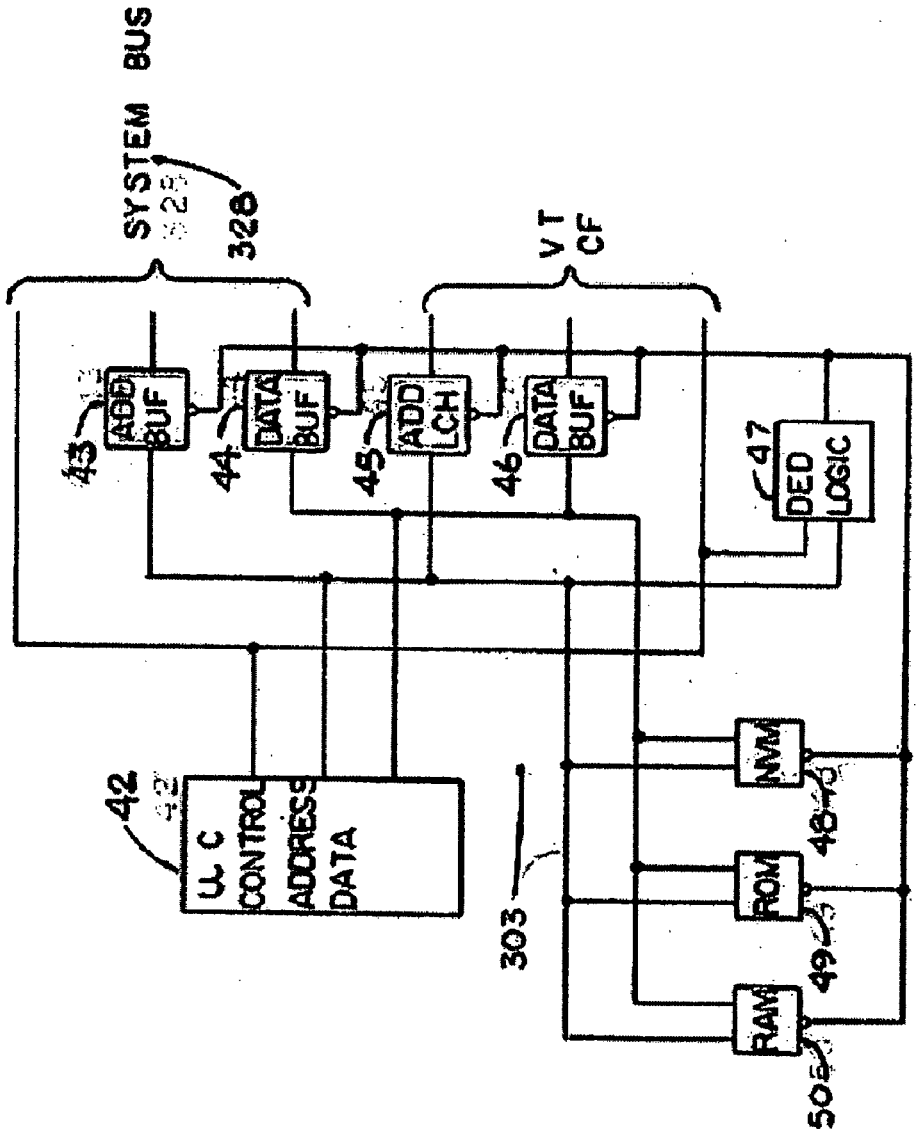
SYSTEM BUS
328
VT CF
ADD BUF
DATA BUF
ADD LCH
DATA BUF
DED LOGIC
43
44
45
46
47
42
U C
CONTROL
ADDRESS
DATA
303
NVM
ROM
RAM
48
49
505

FIG. 4

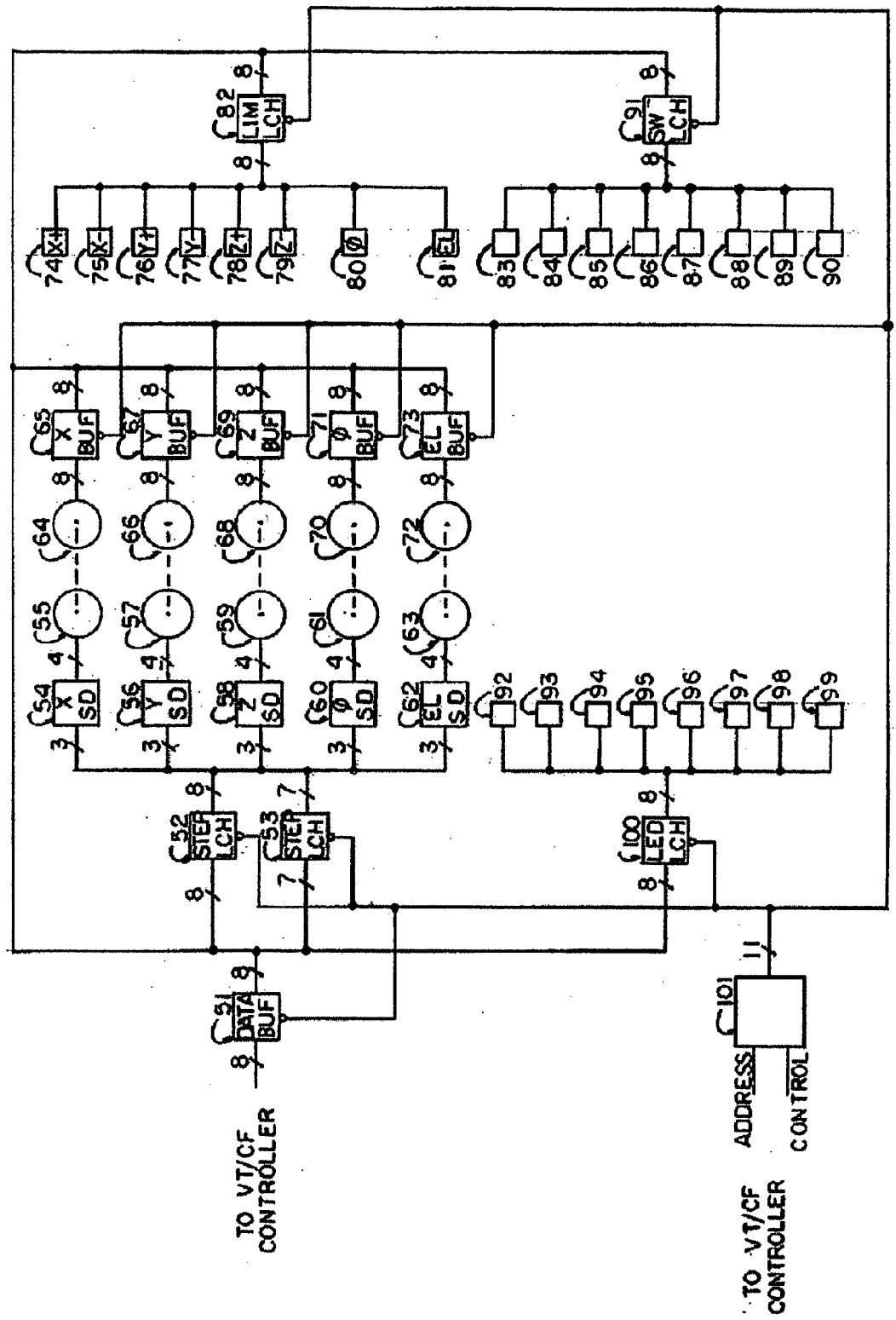
82 LIM LCH
91 SW LCH
74 X+
75 X-
76 Y+
77 Y-
78 Z+
79 Z-
80 Ø
81 EL
83
84
85
86
87
88
89
90
65 X BUF
67 Y BUF
69 Z BUF
71 Ø BUF
73 EL BUF
64
66
68
70
72
55
57
59
61
63
54 X SD
56 Y SD
58 Z SD
60 Ø SD
62 EL SD
92
93
94
95
96
97
98
99
52 STEP LCH
53 STEP LCH
100 LED LCH
51 DATA BUF
101
TO VT/CF CONTROLLER
ADDRESS
CONTROL
TO VT/CF CONTROLLER

FIG. 5

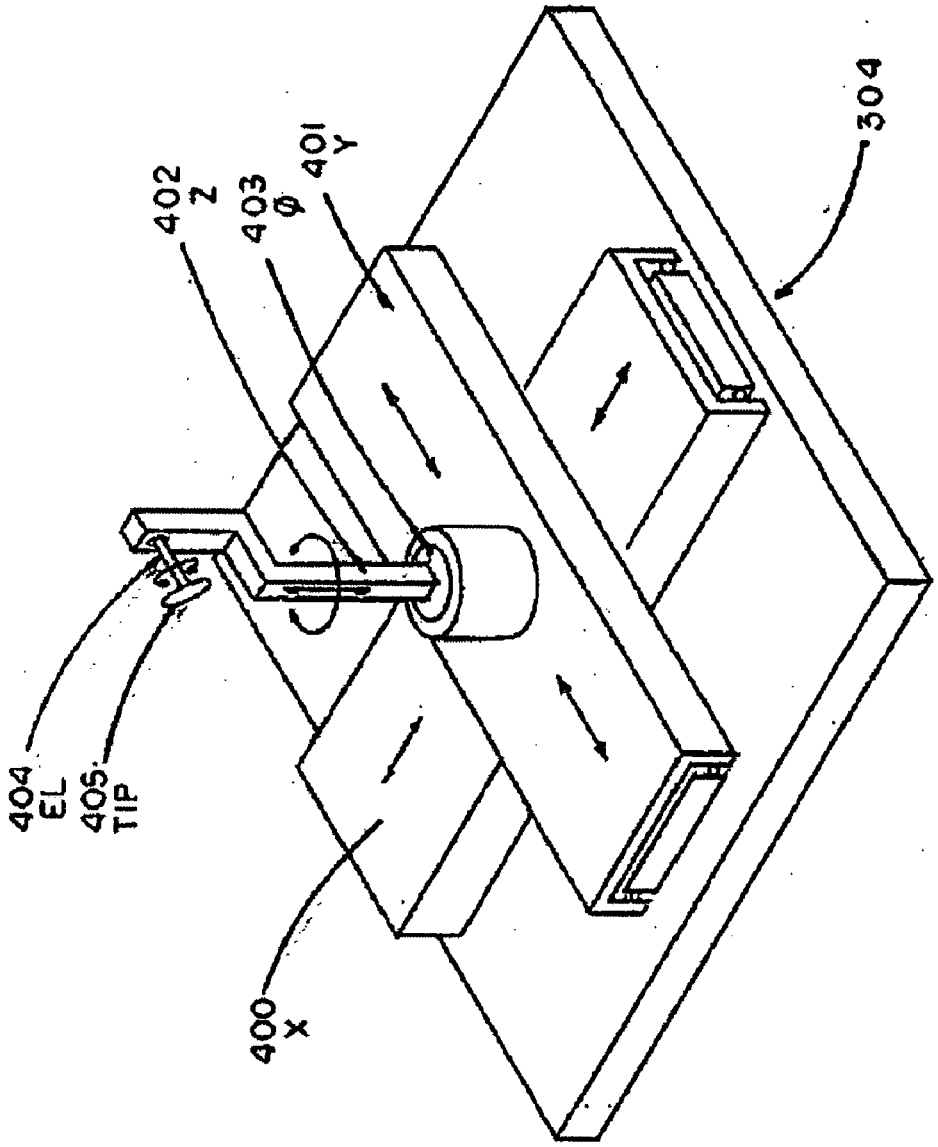

FIG. 6

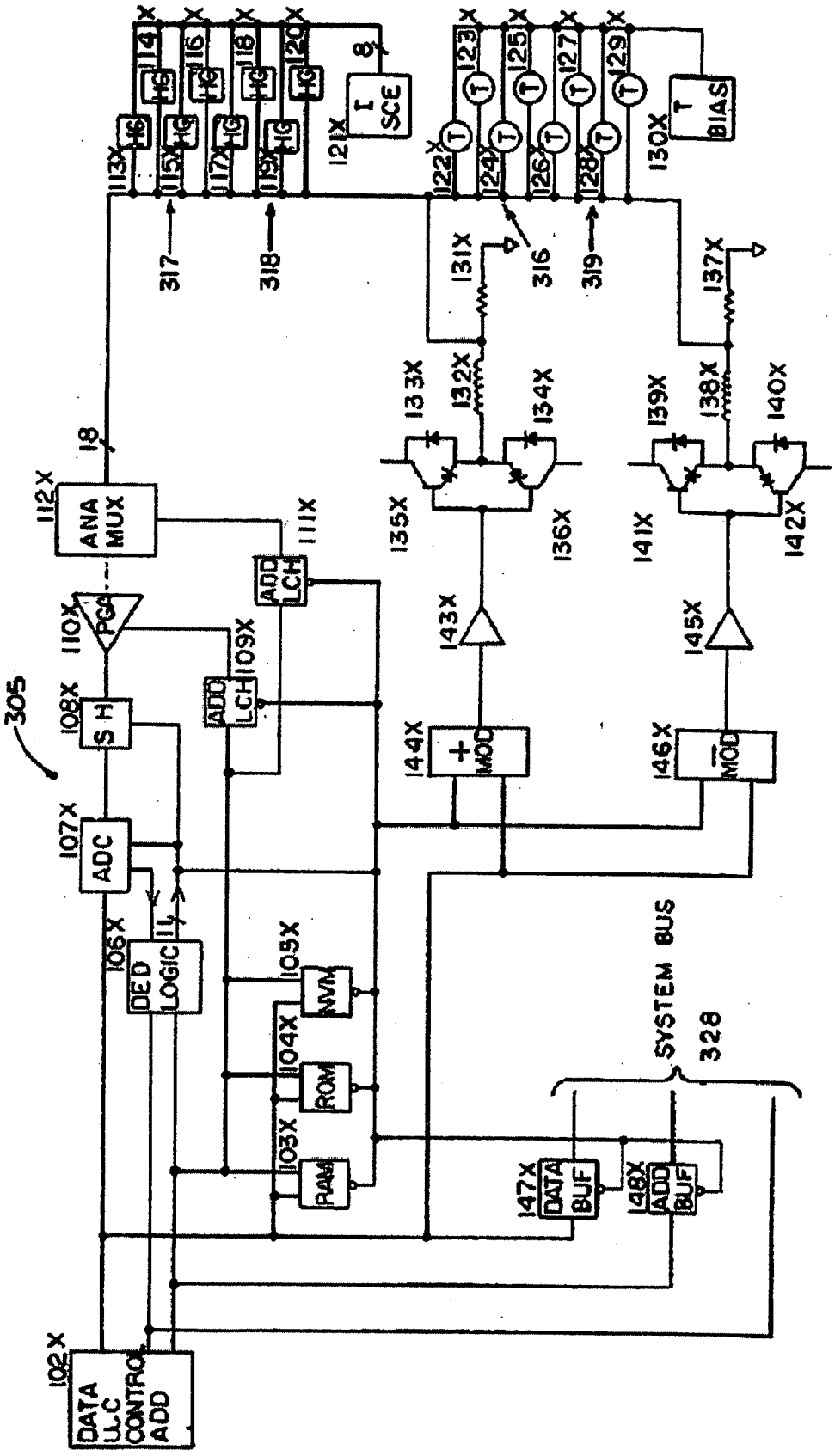
305
102X
DATA U.C. CONTROL ADD
107X
ADC
108X
S H
110X
PGA
112X
ANA MUX
18
111X
ADD LCH
109X
ADD LCH
106X
DED LOGIC
105X
NVM
104X
ROM
103X
RAM
113X
115X
117X
119X
121X
I SCE
8
122X
123X
124X
125X
126X
127X
128X
129X
130X
T BIAS
317
318
316
319
131X
137X
133X
132X
134X
135X
136X
139X
138X
140X
141X
142X
143X
145X
144X
+MOD
146X
-MOD
147X
DATA BUF
148X
ADD BUF
SYSTEM BUS
328

FIG. 7

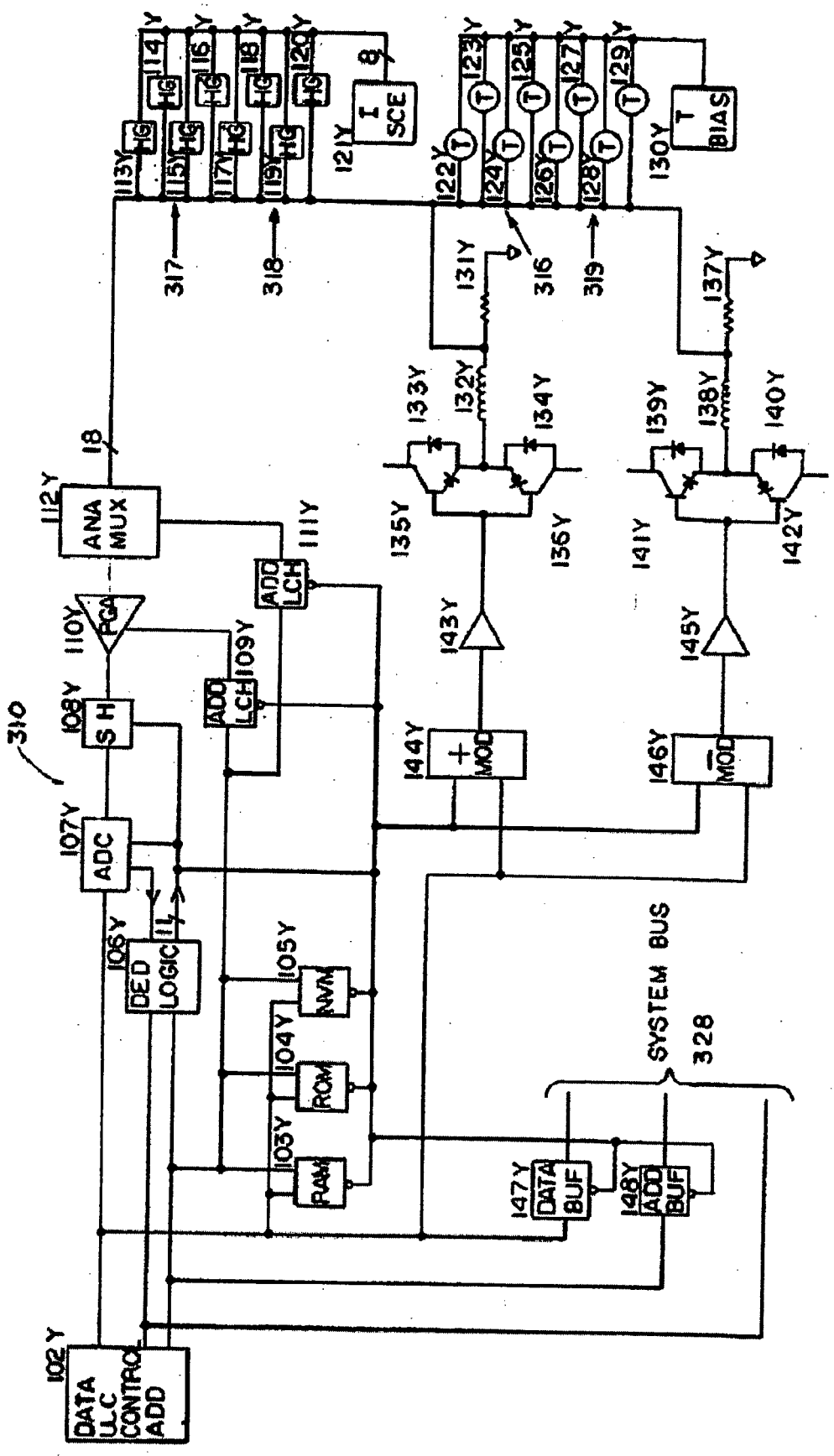
310
102Y
DATA
U.C
CONTRO
ADD
106Y
DED
LOGIC
107Y
ADC
108Y
S H
110Y
PGA
112Y
ANA
MUX
18
111Y
ADD
LCH
109Y
ADD
LCH
103Y
RAM
104Y
ROM
105Y
NVM
147Y
DATA
BUF
148Y
ADD
BUF
SYSTEM BUS
328
144Y
+
MOD
146Y
−
MOD
143Y
145Y
135Y
136Y
141Y
142Y
133Y
134Y
139Y
140Y
132Y
138Y
131Y
137Y
317
318
316
319
113Y
114Y
115Y
116Y
117Y
118Y
119Y
120Y
121Y
I
SCE
8
122Y
123Y
124Y
125Y
126Y
127Y
128Y
129Y
130Y
T
BIAS

FIG. 8

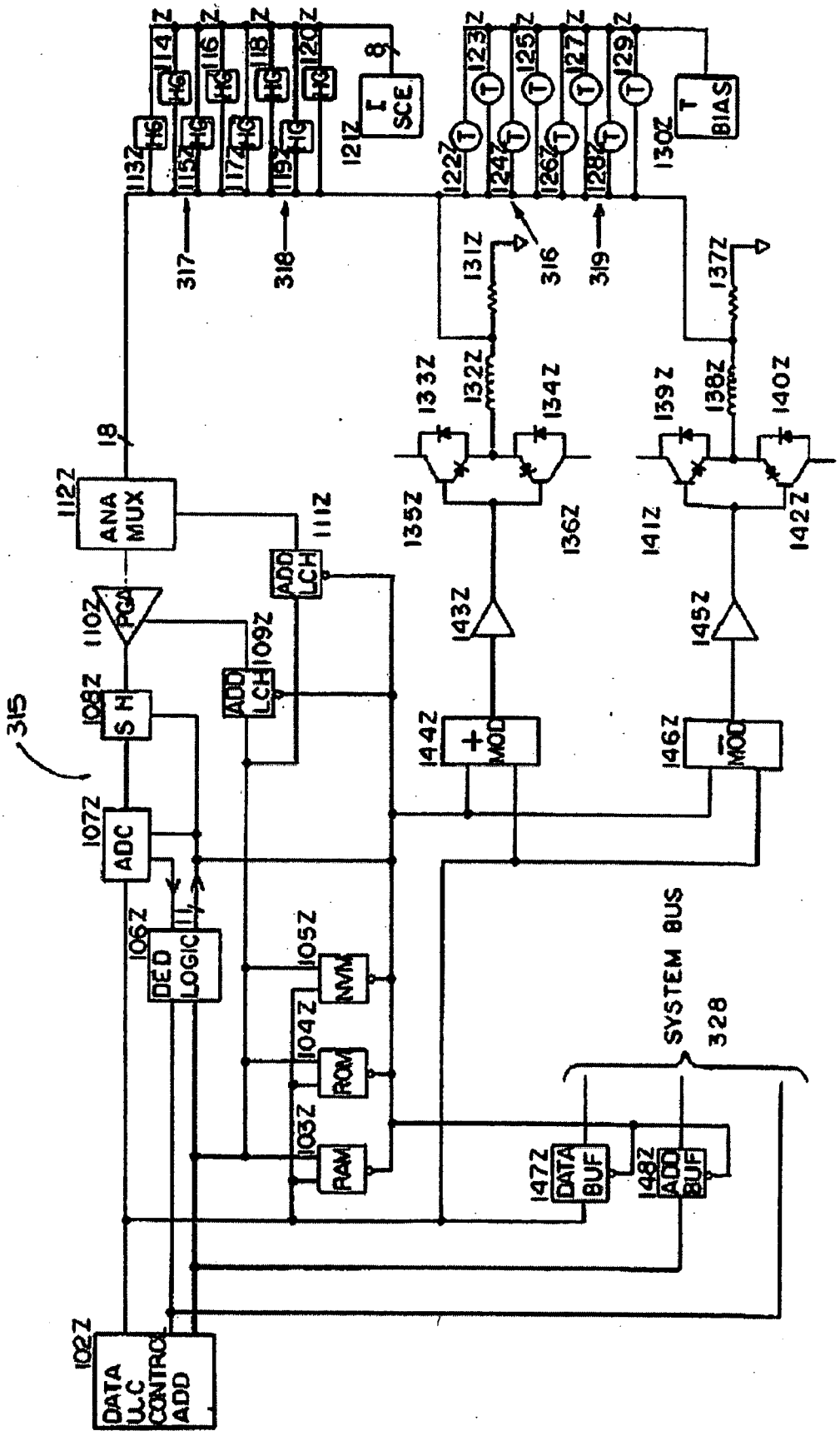
DATA U.C CONTROL ADD
102Z
DED LOGIC
106Z
ADC
107Z
S H
108Z
PGA
110Z
ANA MUX
112Z
18
ADD LCH
109Z
ADD LCH
111Z
RAM
103Z
ROM
104Z
NVM
105Z
+ MOD
144Z
− MOD
146Z
143Z
145Z
135Z
136Z
141Z
142Z
133Z
134Z
139Z
140Z
132Z
138Z
131Z
137Z
317
318
316
319
SYSTEM BUS
328
DATA BUF
147Z
ADD BUF
148Z
I SCE
121Z
T BIAS
130Z
HG
T
113Z
114Z
115Z
116Z
117Z
118Z
119Z
120Z
122Z
123Z
124Z
125Z
126Z
127Z
128Z
129Z
8
315

FIG. 9

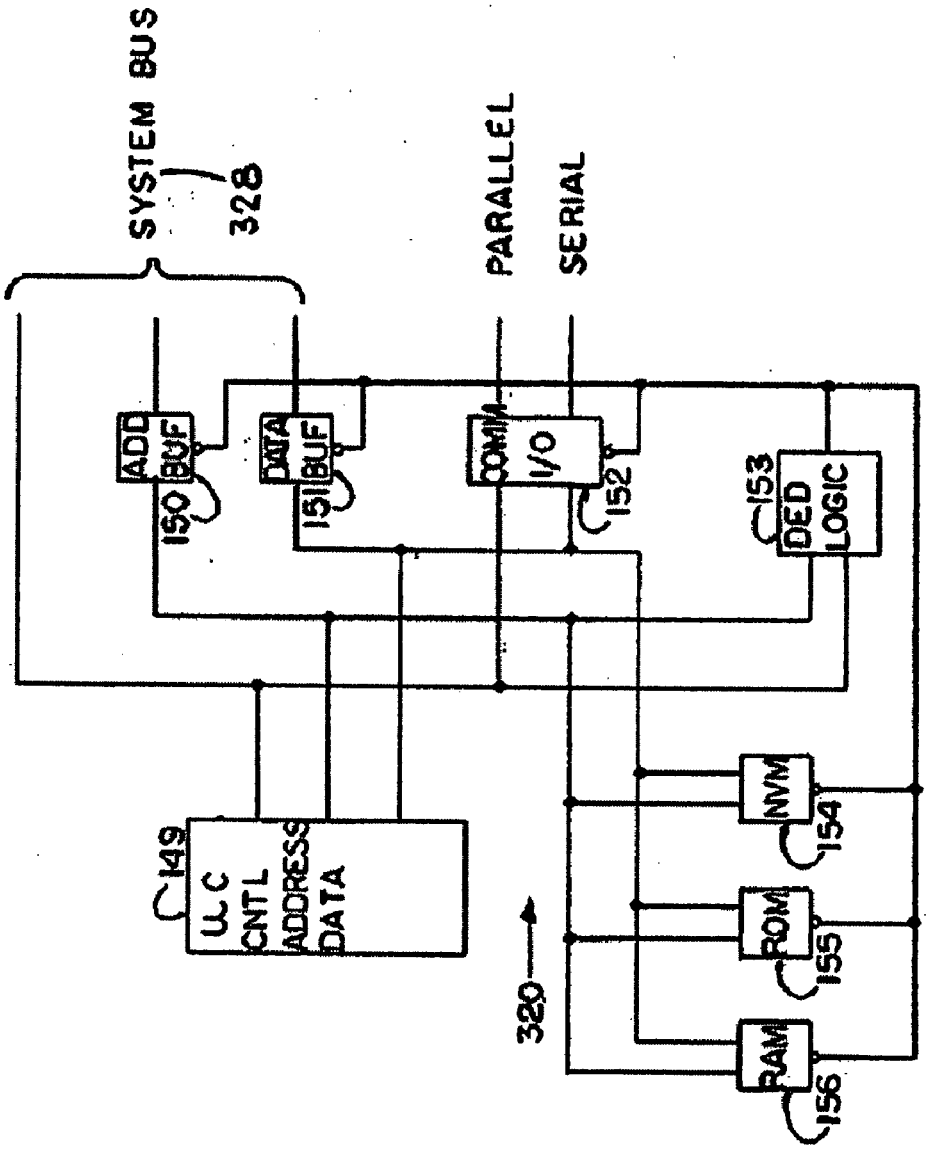
SYSTEM BUS
328
PARALLEL
SERIAL
ADD BUF
150
DATA BUF
151
COMM I/O
152
153
DED LOGIC
149
U.C CNTL
ADDRESS
DATA
320
NVM
154
ROM
155
RAM
156

FIG. 10

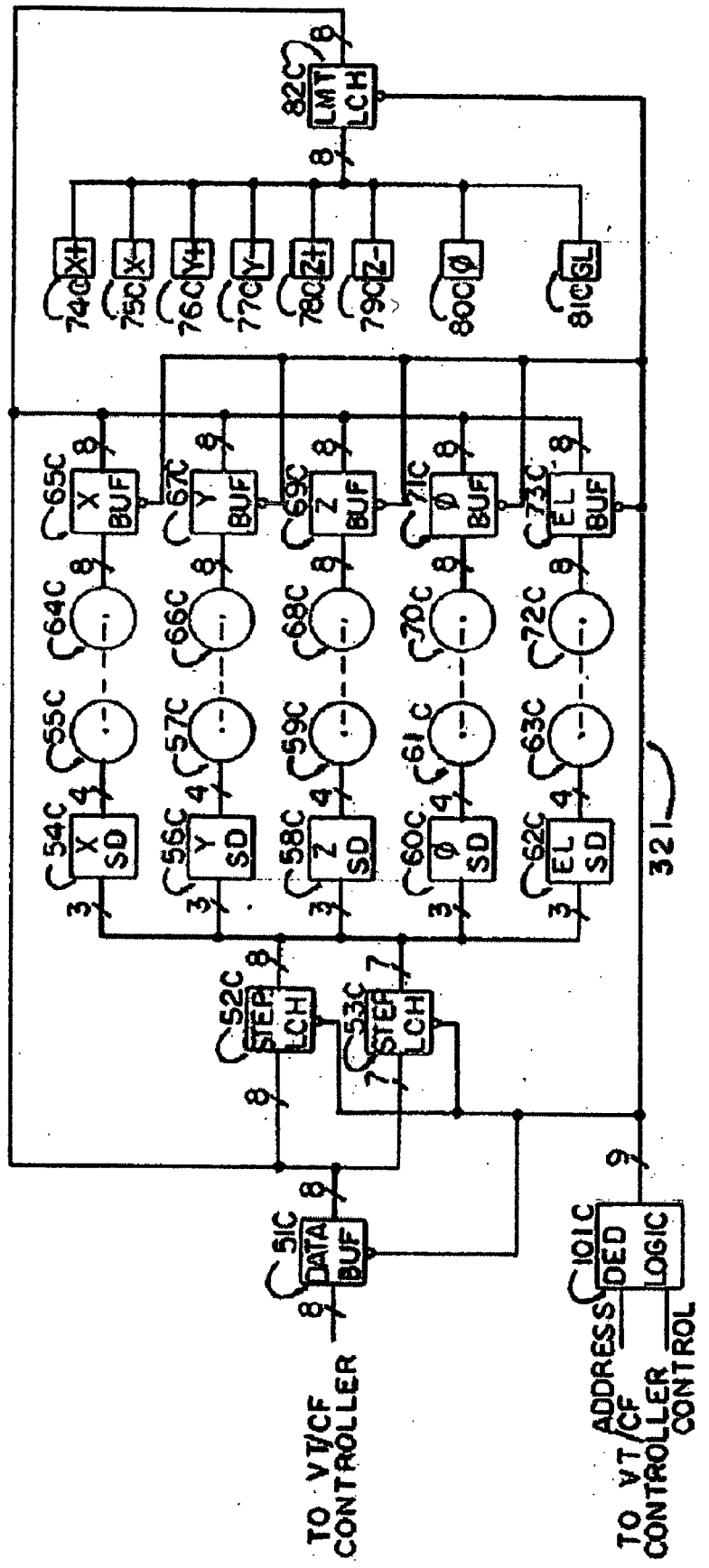
82C
LMT LCH
74C X+
75C X-
76C Y+
77C Y-
78C Z+
79C Z-
80C ø
81C GL
65C X BUF
67C Y BUF
69C Z BUF
71C ø BUF
73C EL BUF
64C
66C
68C
70C
72C
55C
57C
59C
61C
63C
54C X SD
56C Y SD
58C Z SD
60C ø SD
62C EL SD
321
52C STEP LCH
53C STEP LCH
51C DATA BUF
101C DED LOGIC
TO VT/CF CONTROLLER
ADDRESS
TO VT/CF CONTROLLER
CONTROL

FIG. 11

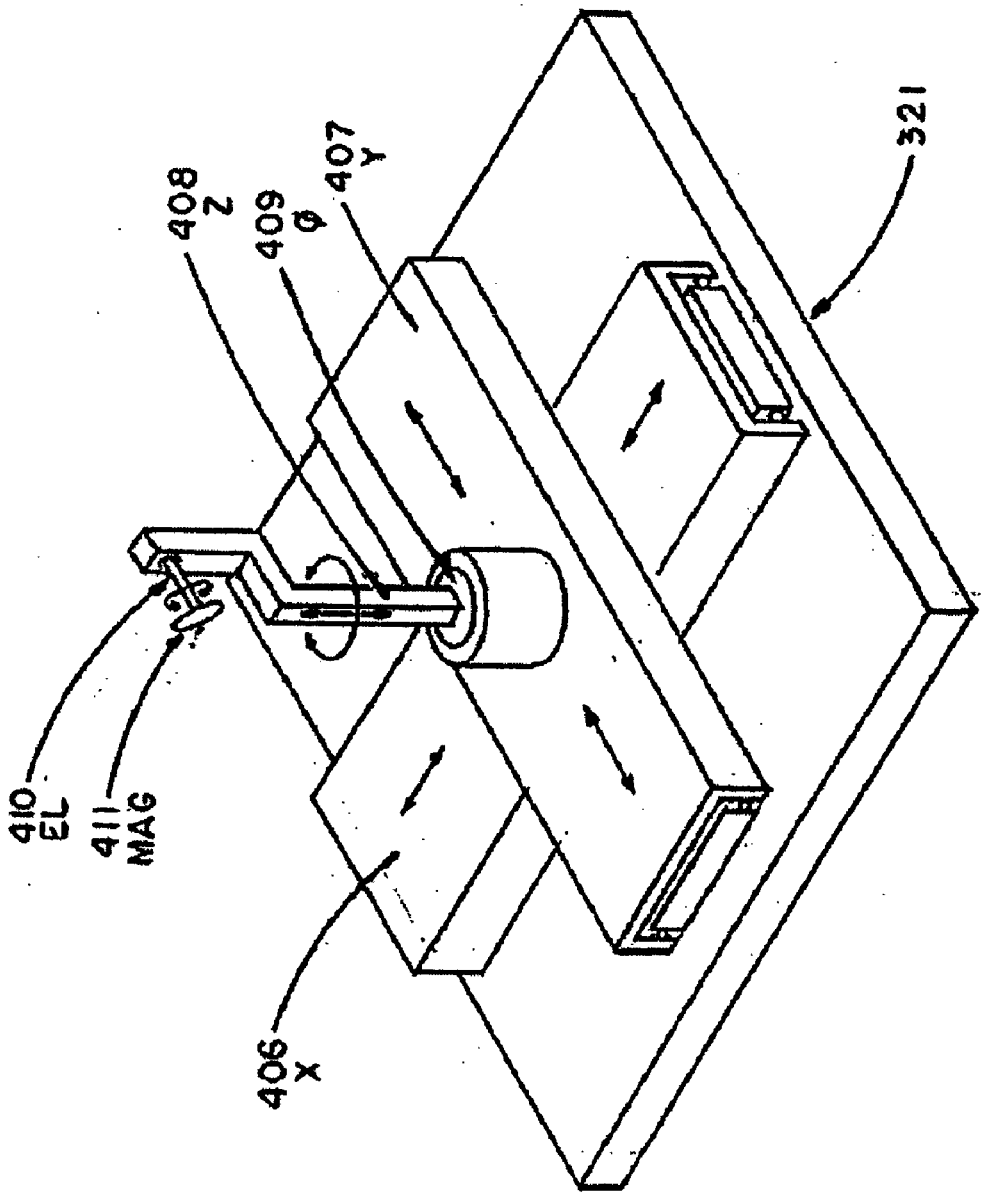

FIG. 12

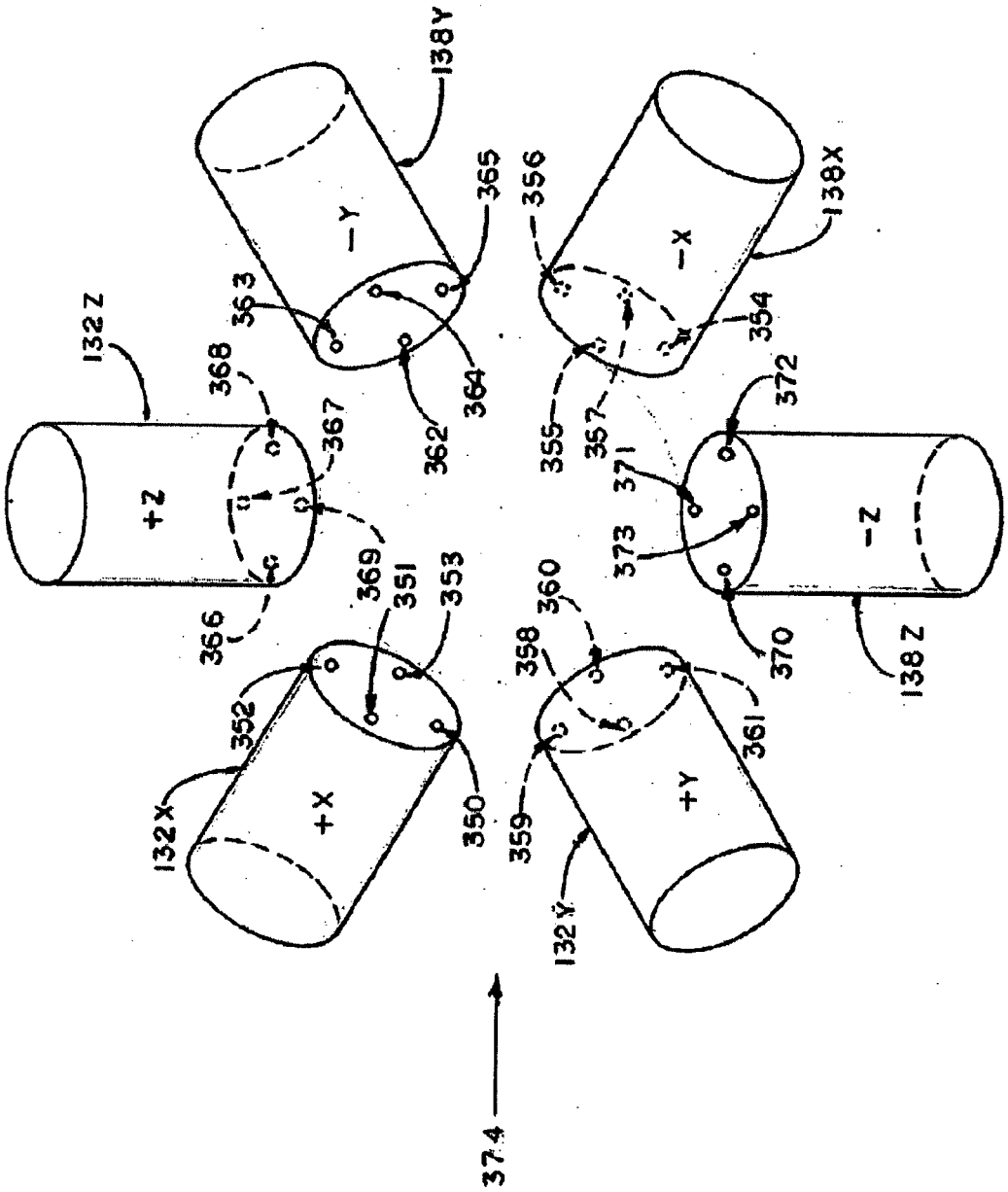
138Y
-Y
365
363
364
362
132Z
368
367
+Z
369
366
351
353
352
+X
132X
350
356
-X
138X
354
355
357
372
371
373
-Z
370
138Z
360
358
361
+Y
359
132Y
374

FIG. 13

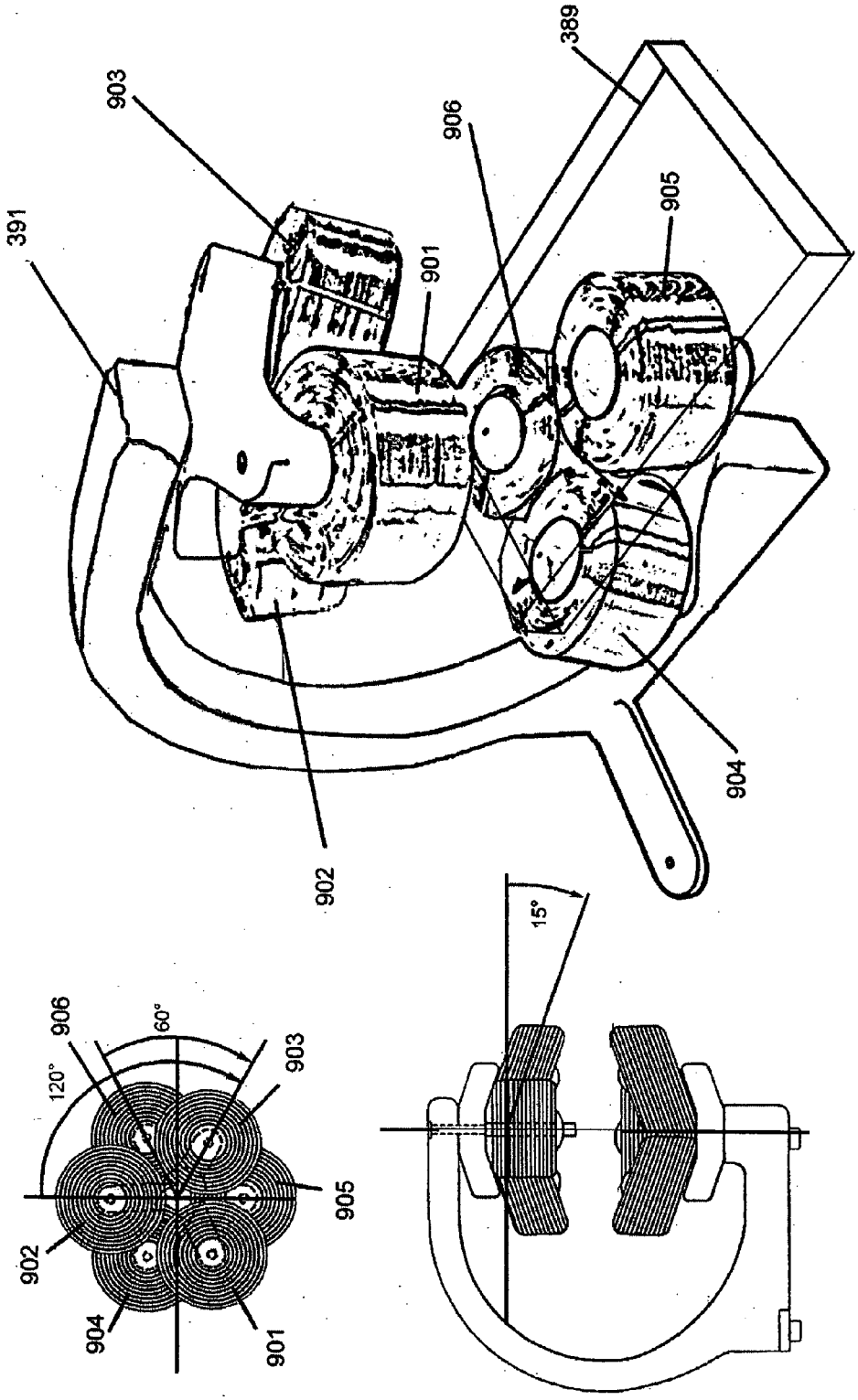

FIG. 13A

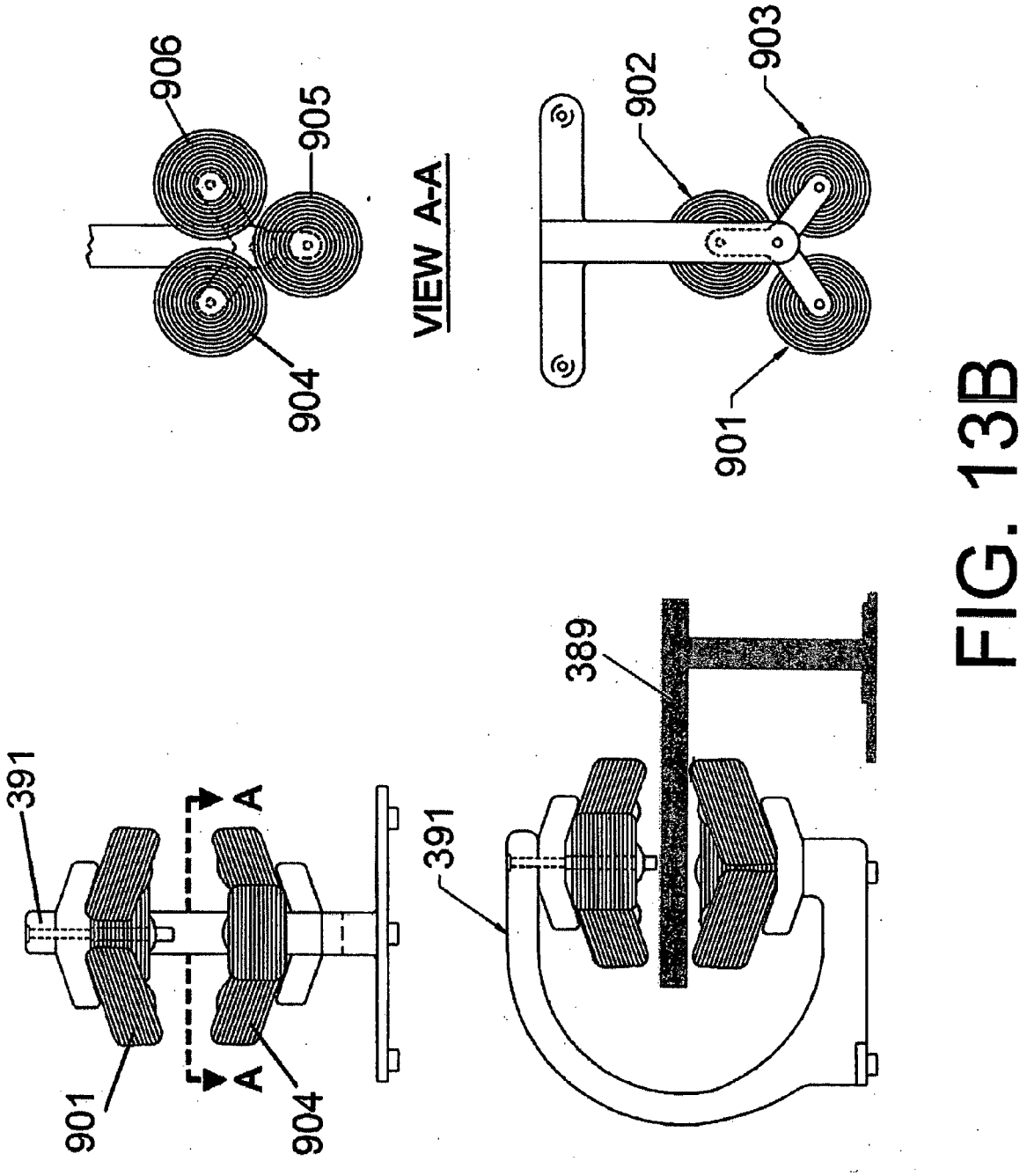

FIG. 13B

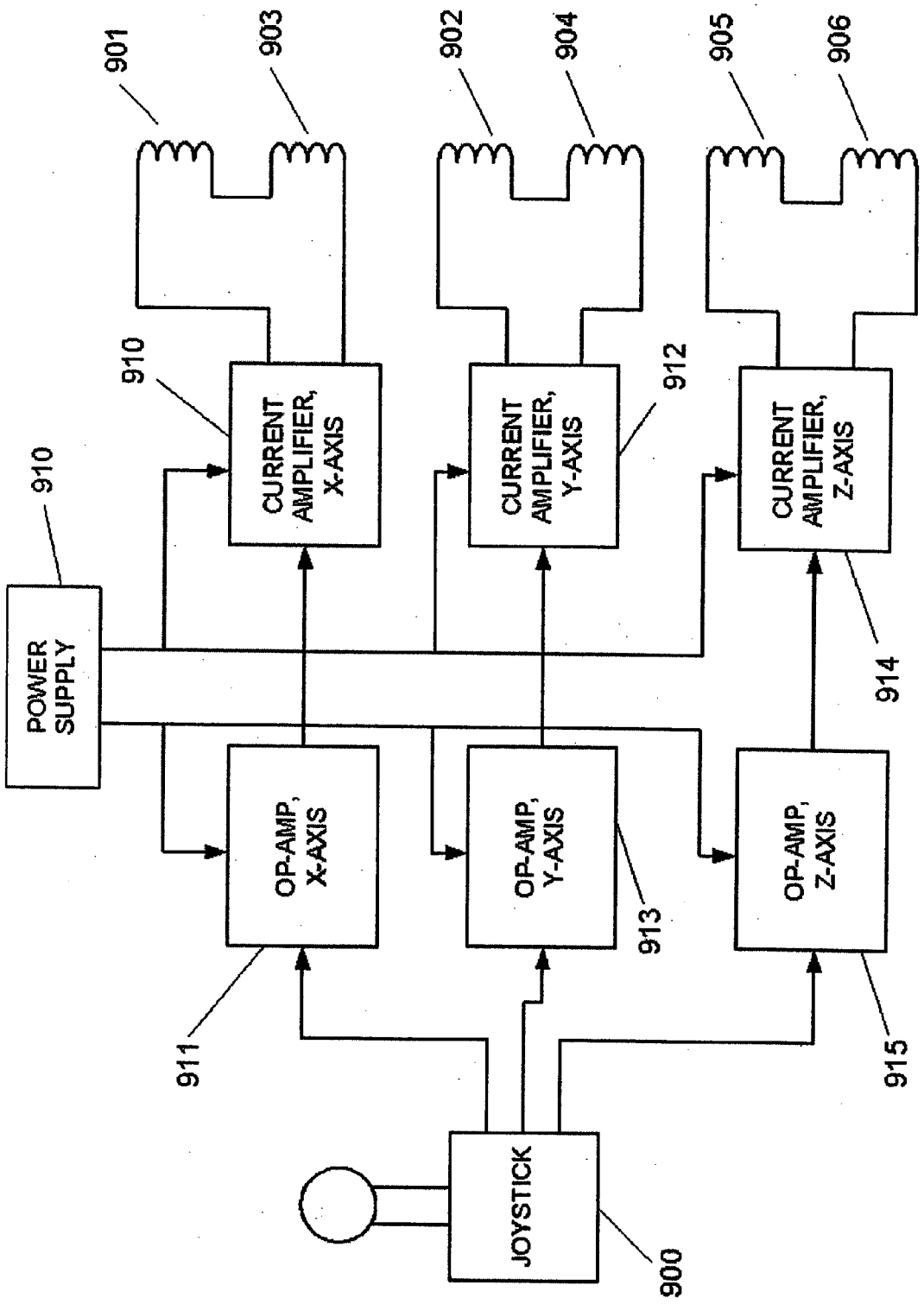
901
903
902
904
905
906
910
CURRENT AMPLIFIER, X-AXIS
CURRENT AMPLIFIER, Y-AXIS
912
CURRENT AMPLIFIER, Z-AXIS
910
POWER SUPPLY
914
OP-AMP, X-AXIS
OP-AMP, Y-AXIS
913
OP-AMP, Z-AXIS
911
915
JOYSTICK
900

FIG. 13C

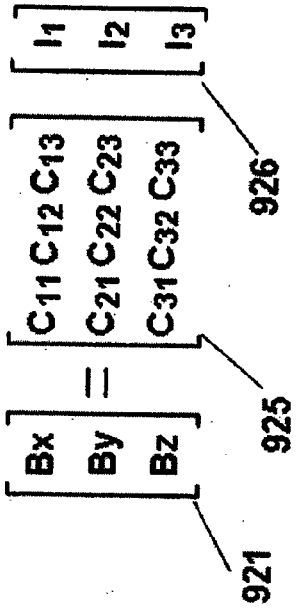

Fig. 13E

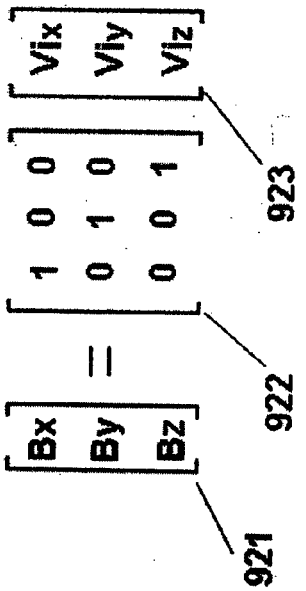

Fig. 13D

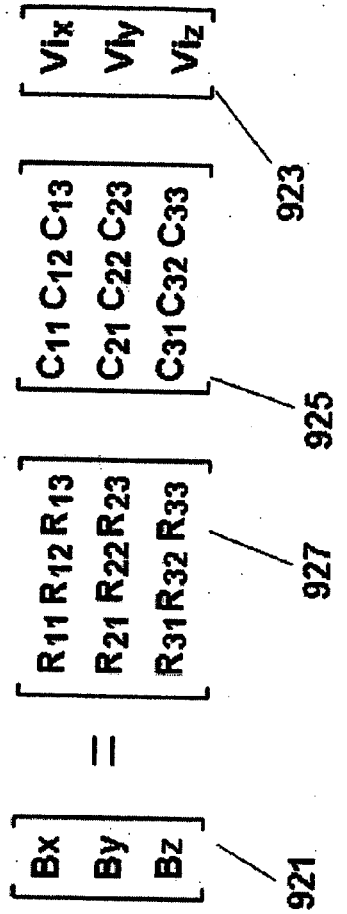

Fig. 13G

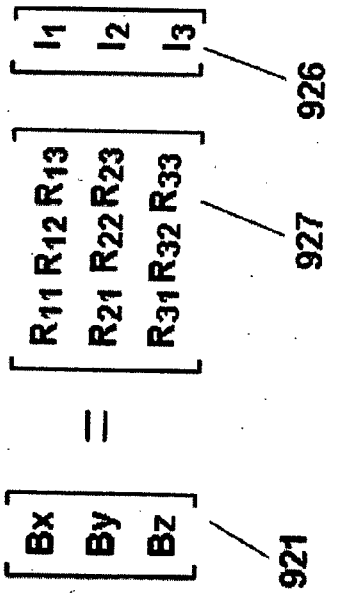

Fig. 13F

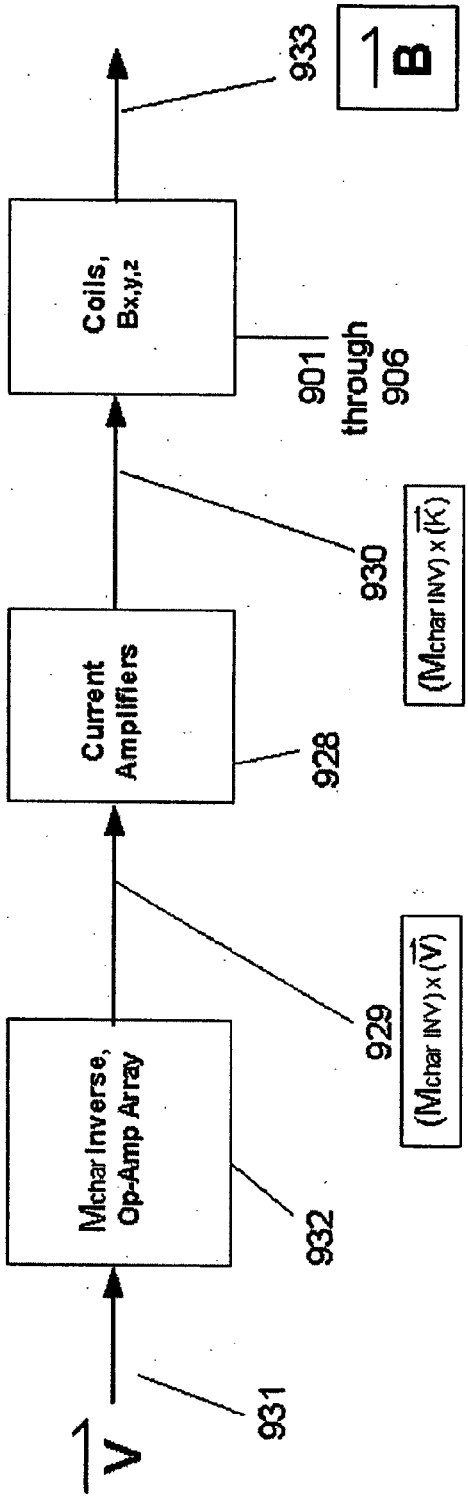
1 V
931
Mchar Inverse, Op-Amp Array
932
929
(Mchar INV) x ($\vec{V}$)
Current Amplifiers
928
930
(Mchar INV) x ($\vec{K}$)
Coils, Bx,y,z
901 through 906
933
1 B

Fig. 13H

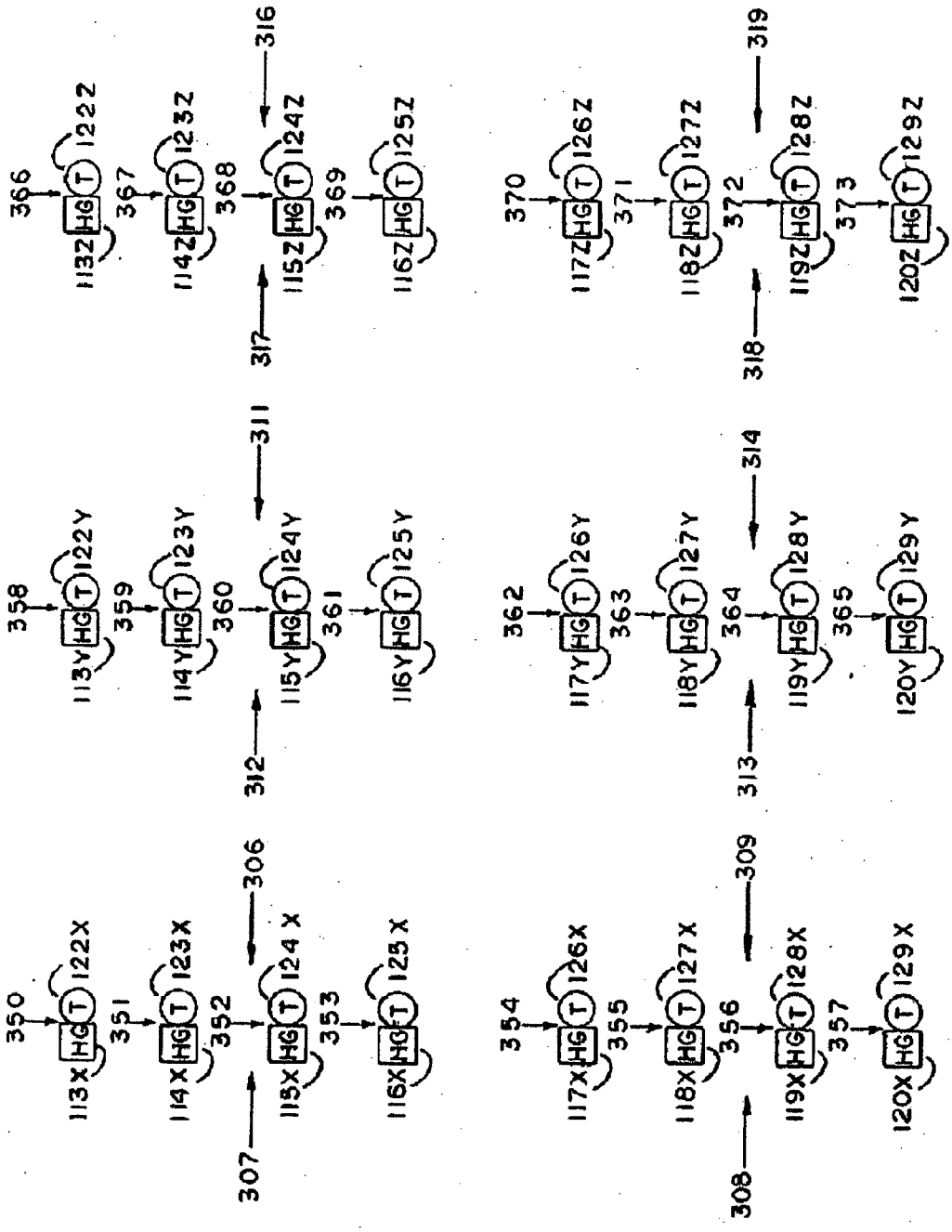
350
351
352
353
354
355
356
357
358
359
360
361
362
363
364
365
366
367
368
369
370
371
372
373
113X
114X
115X
116X
117X
118X
119X
120X
113Y
114Y
115Y
116Y
117Y
118Y
119Y
120Y
1132
1142
1152
1162
1172
1182
1192
1202
122X
123X
124X
125X
126X
127X
128X
129X
122Y
123Y
124Y
125Y
126Y
127Y
128Y
129Y
1222
1232
1242
1252
1262
1272
1282
1292
306
307
308
309
311
312
313
314
316
317
318
319

FIG. 14

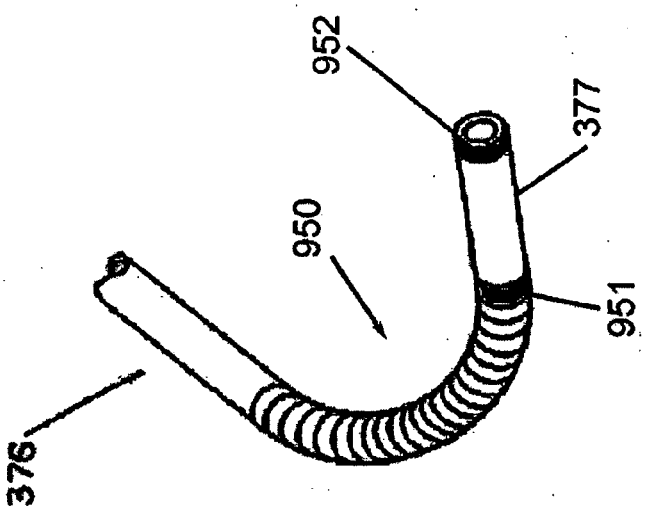

FIG. 15B

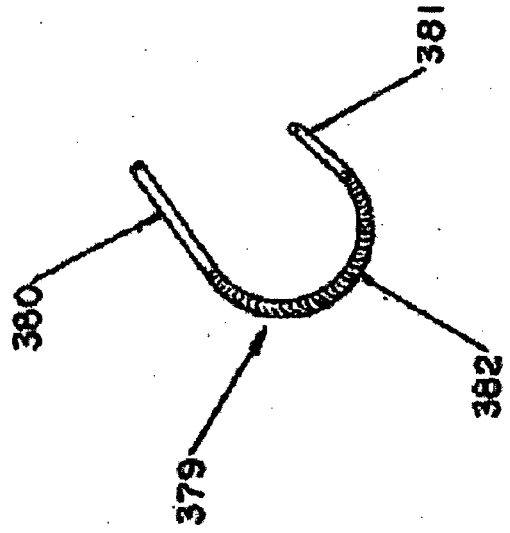

FIG. 15A

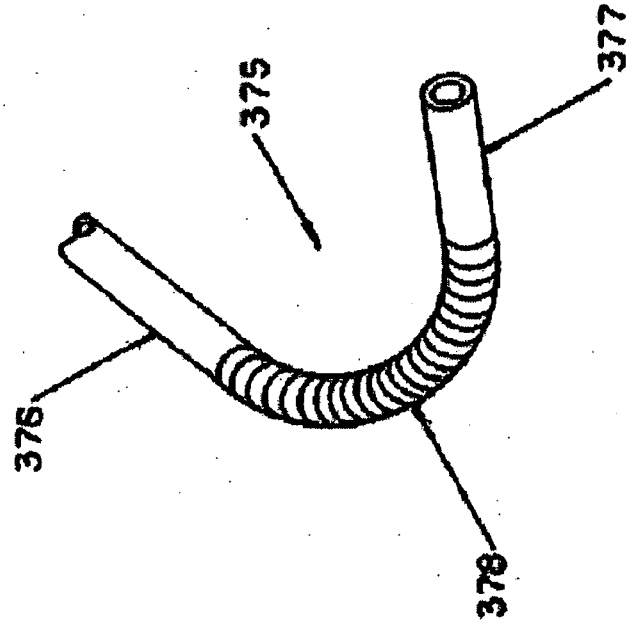

FIG. 15

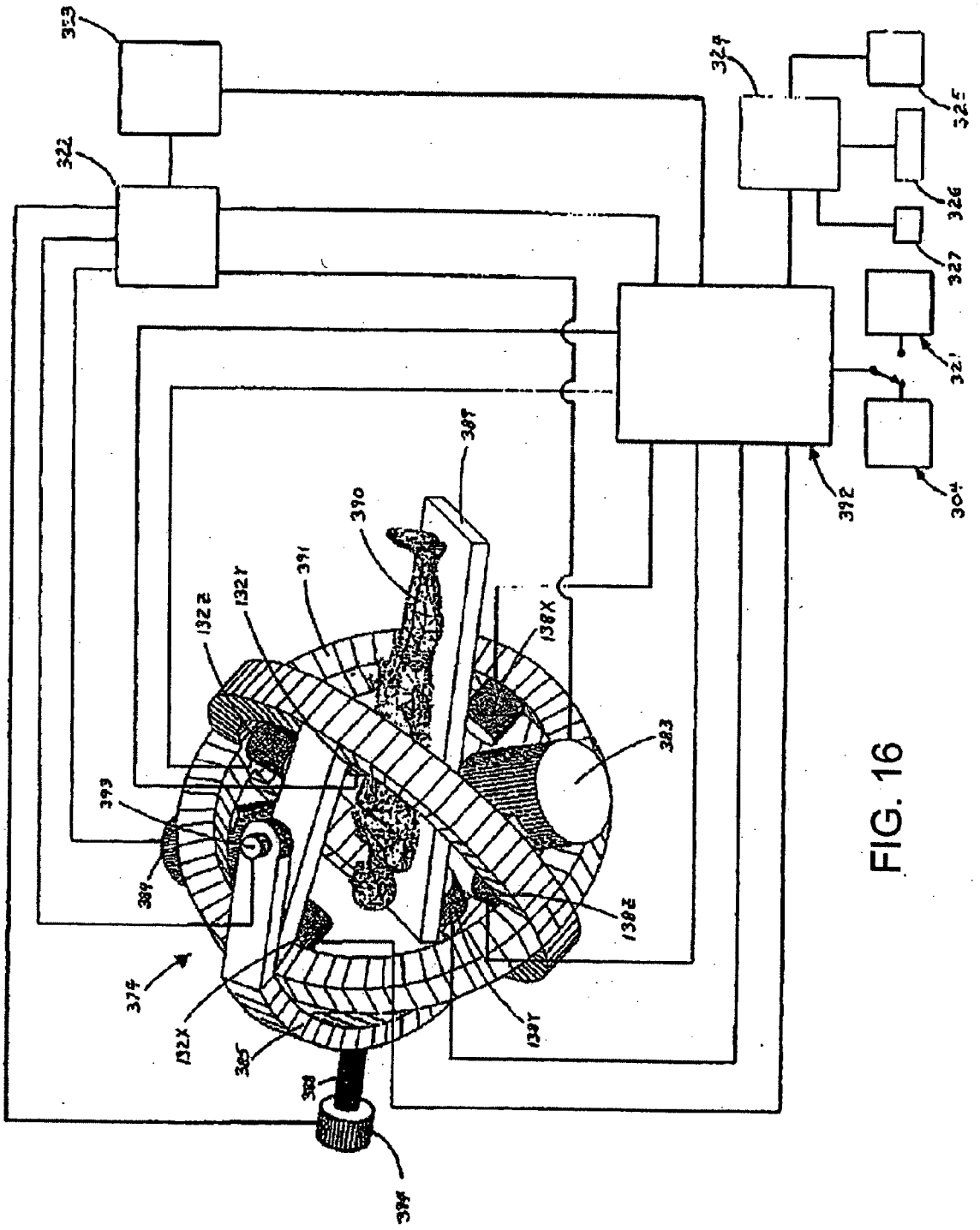
323
322
324
325
326
327
321
304
392
389
390
391
132Z
132Y
138X
383
393
389
138Z
374
132X
385
138Y
388
394

FIG. 16

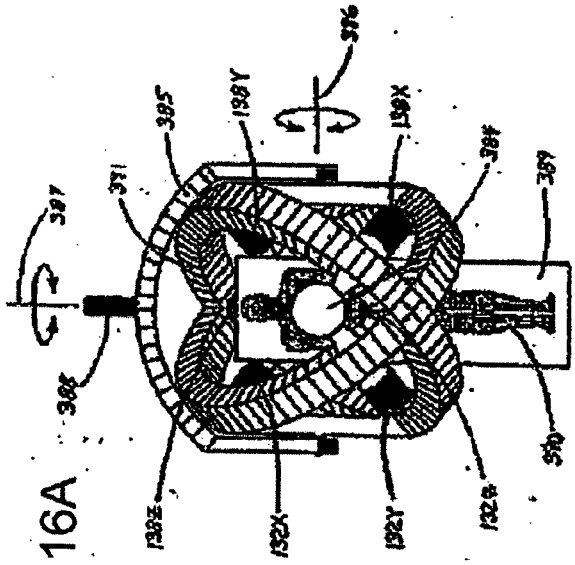

FIG. 16A

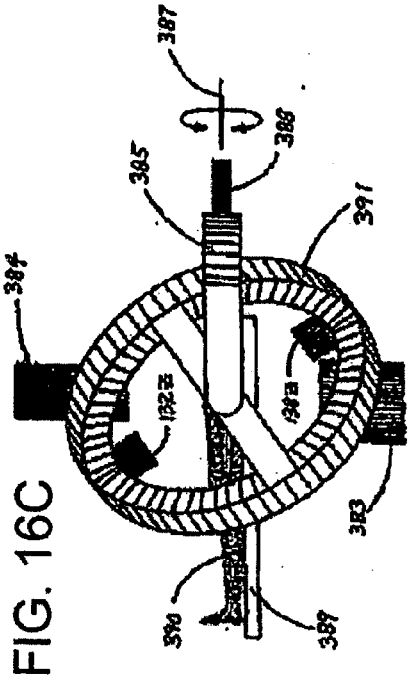

FIG. 16C

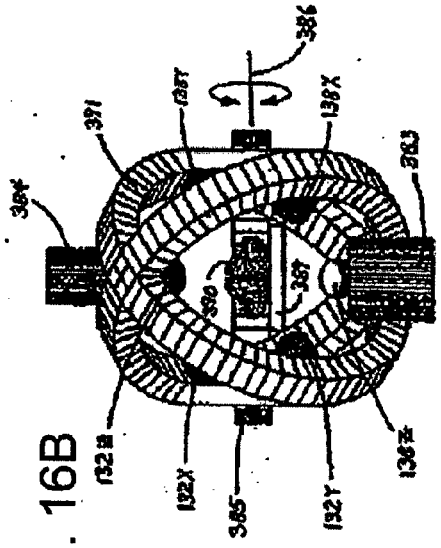

FIG. 16B

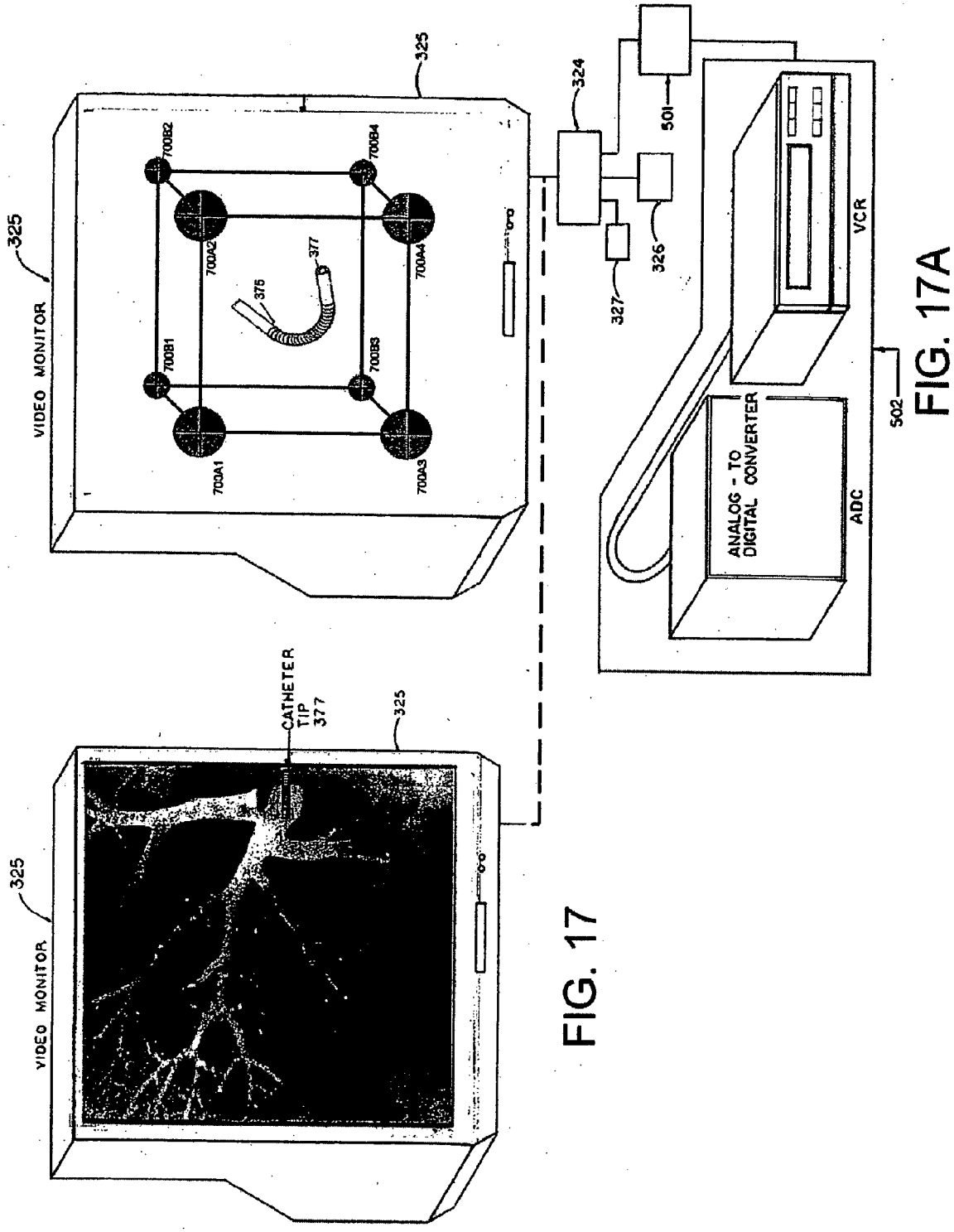

FIG. 17

FIG. 17A

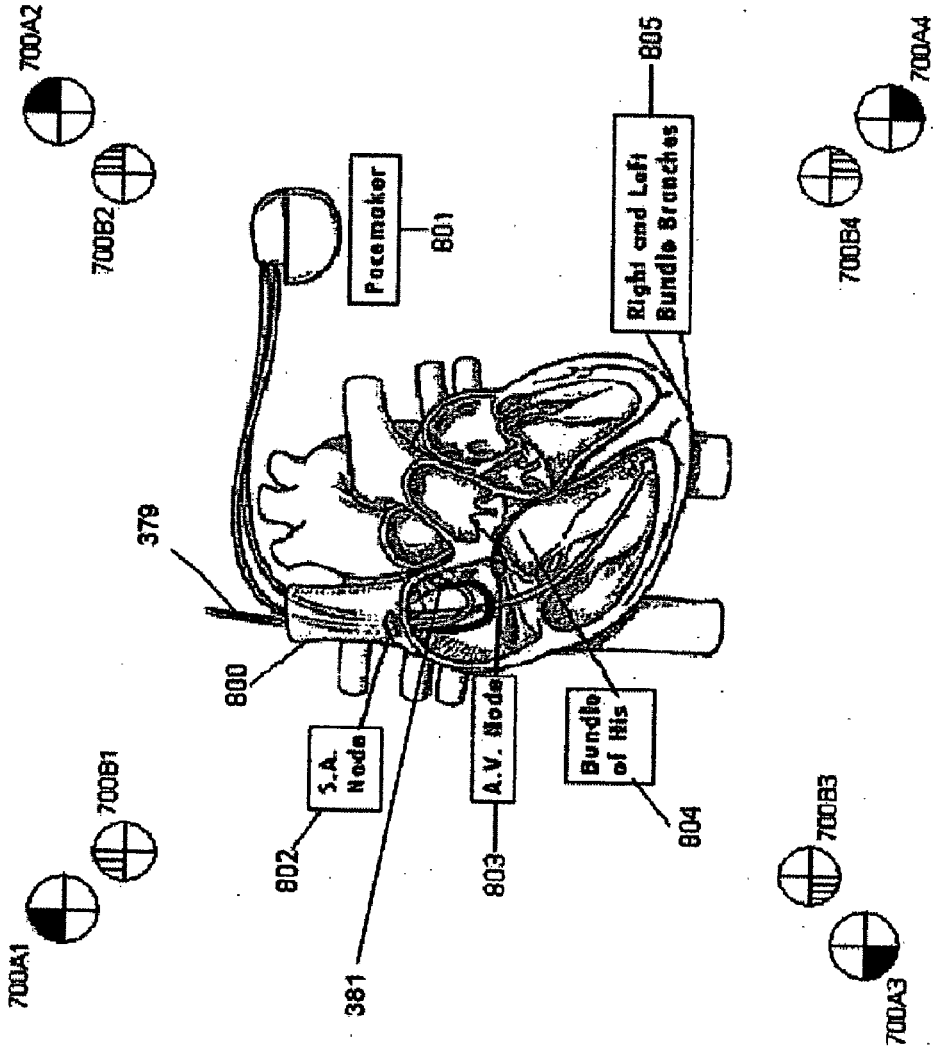
700A2
700B2
700A4
700B4
Pacemaker
801
805
Right and Left Bundle Branches
379
800
S.A. Node
802
A.V. Node
803
Bundle of His
804
381
700B1
700A1
700B3
700A3

FIG. 17B

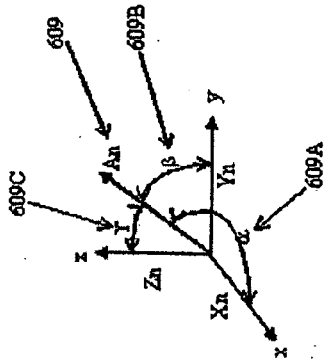

FIG. 18B

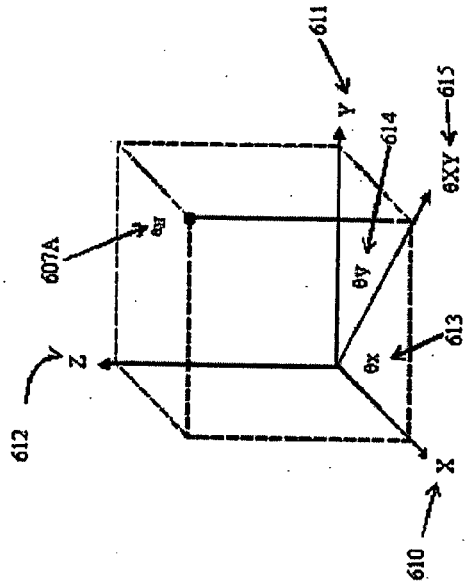

FIG. 18C

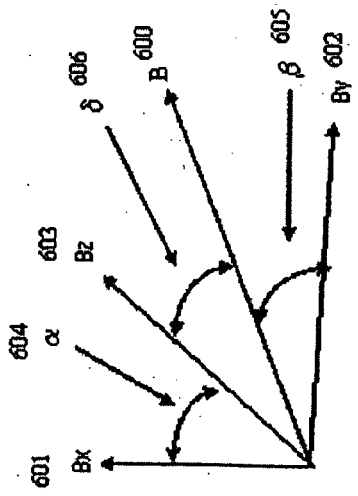

FIG. 18

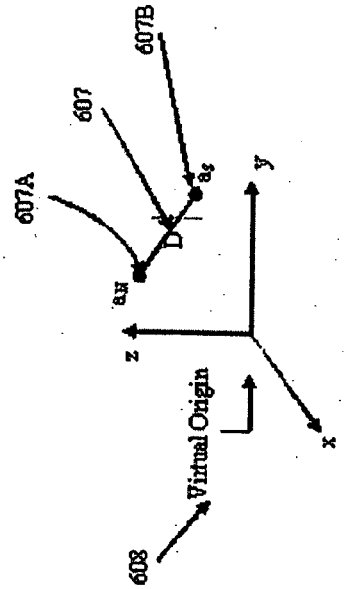

FIG. 18A

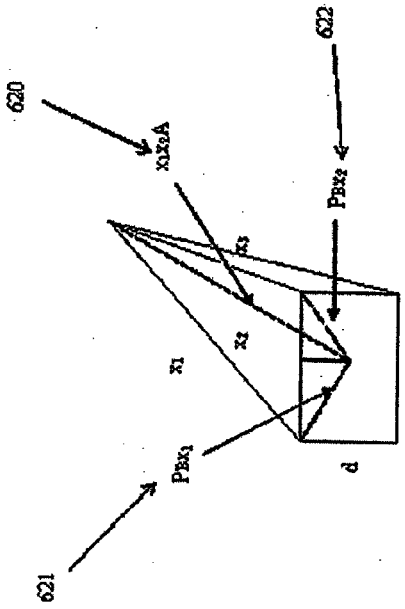

FIG. 20

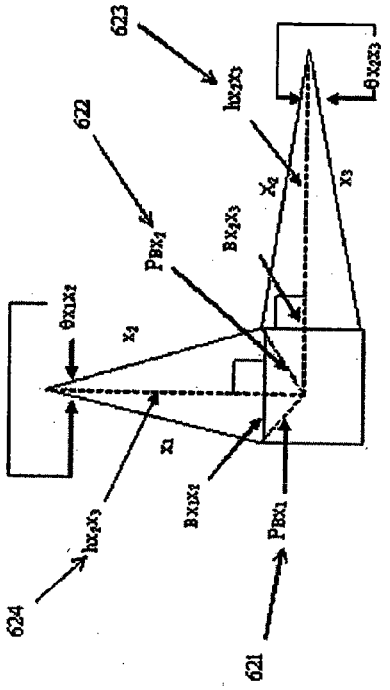

FIG. 20A

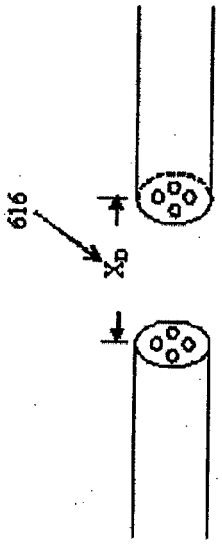

FIG. 19

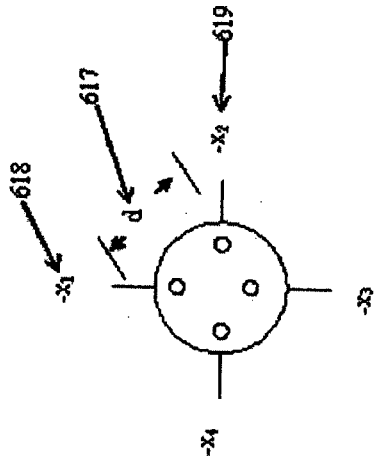

FIG. 19A

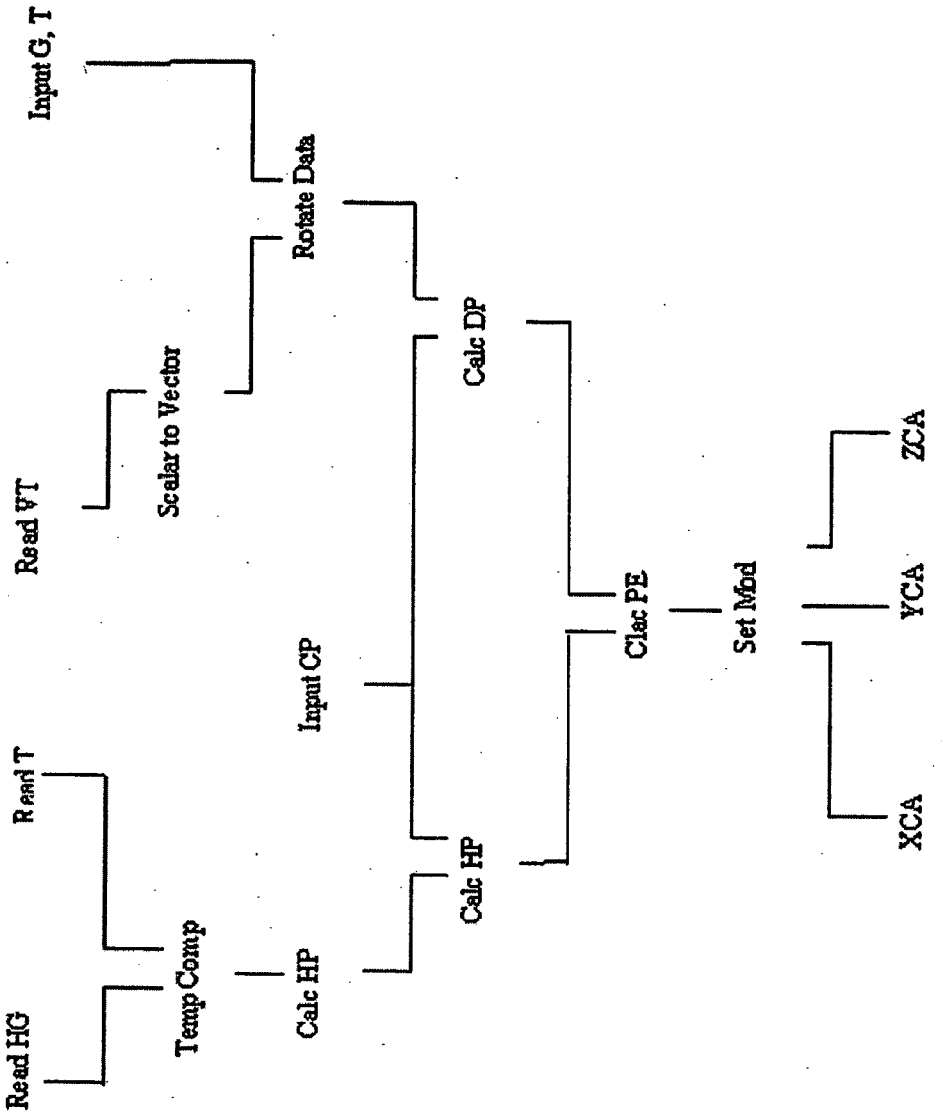

FIG. 23

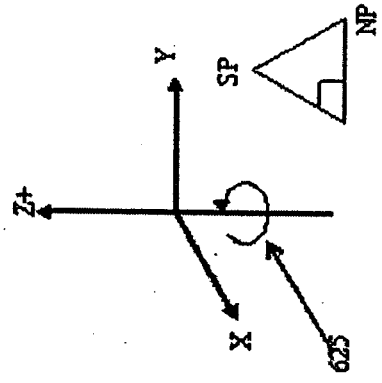

FIG. 21

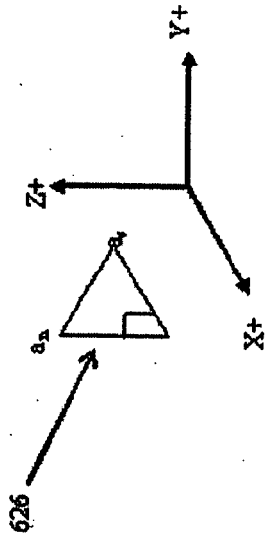

FIG. 22

SYSTEM AND METHOD FOR CONTROLLING MOVEMENT OF A SURGICAL TOOL

REFERENCE TO RELATED APPLICATIONS

[0001] The present application is a divisional of U.S. application Ser. No. 10/621,196 titled APPARATUS AND METHOD FOR A CATHETER GUIDANCE CONTROL AND IMAGING, which was filed Jul. 15, 2003 which claims priority from U.S. Provisional Patent Application No. 60/396,302, filed Jul. 16, 2002, titled "CATHETER GUIDANCE CONTROL AND IMAGING APPARATUS AND METHOD," the entire contents of which is hereby incorporated by reference.

BACKGROUND

[0002] 1. Field of the Invention

[0003] The present invention relates to systems and techniques for guiding, steering, and advancing invasive medical devices such as catheters and catheter-type devices.

[0004] 2. Description of the Related Art

[0005] In general, catheterization is performed by inserting an invasive device into an incision or a body orifice. Secondary tools such as guidewires and balloons are often advanced along the primary catheter to the area where the medical procedure is to be performed. These procedures rely on manually advancing the distal end of the invasive device by pushing, rotating, or otherwise manipulating the proximal end that remains outside of the body. Real-time x-ray imaging is a common method for determining the position of the distal end of the invasive device during the procedure. The manipulation continues until the distal end reaches the destination area where the diagnostic or therapeutic procedure is to be performed. This technique requires great skills on the part of the operator that can only be achieved after a protracted training period and extended practice. A high degree of manual dexterity is also required.

[0006] For example, angioplasty involves advancing a balloon catheter over a previously placed guidewire into a narrowed arterial section. Once properly positioned in the narrowed arterial section, the balloon is inflated and dilates this section: The time consuming technical difficulties encountered during angioplasty procedure are similar to those associated with angiography. If the artery to be treated is torturous with sharp bends, it may be difficult to advance the guidewire to the stenosis. If the stenosis is severe or the artery is totally blocked, it may be difficult or even impossible to properly position the guidewire. Alternatively, if the guidewire is successfully positioned in tight, hard plaque, the balloon catheter, being of a necessarily larger diameter than the guidewire, may encounter sufficient resistance to cause the guiding catheter to disengage from the ostium. This eliminates the support required to facilitate balloon advancement. These technical difficulties can render the procedure unfeasible.

[0007] Because of the difficulty involved in advancing a catheter into a desired location in the body, many diagnostic and therapeutic procedures employ a guidewire. The guidewire is first advanced into the heart or the artery and serves as a track and guide for a specific catheter. This technique is used to advance a catheter into the left ventricle and is especially important when studying aortic stenosis. Crossing the narrowed valve orifice is a challenge to the operator. Similarly, a guidewire is often manipulated into a blocked coronary artery and across the obstructive plaque. A therapeutic catheter, for example carrying a balloon, a laser, a stent, etc., is advanced over the guidewire, and placed at the site of the plaque. The narrowed site is then opened by inflating a balloon, operating a laser beam, or placing a stent. On occasions, the artery is torturous and severely narrowed and the plaque is irregular, calcified, or even totally occluding the artery. In these situations the placement of a guidewire beyond the narrowed site is very difficult and many times unsuccessful.

[0008] In some procedures, a catheter is used to cut through the intra-atrial septum in order to create a shunt (in transposition of the great vessels), to treat the mitral valve (mitral valvuloplasty), or to monitor directly the pressure in the left atrium.

[0009] The implantation of cardiac pacemakers is often essential for the survival of patients with heart rhythm or electrical conduction disturbances. This procedure is performed by the implantation of a small electrode in the heart cavity wall (ventricle or atrium). The other end of the electrode is attached to an electronic device which is implanted under the chest skin and that generates stimulation pulses to simulate the heart rhythm. Similar devices apply electrical shock when life-threatening heart electrical disturbances are detected by the electrodes (e.g., an Automatic Implantable Cardiac Defibrillator (AICD)). These electrodes are placed through a vein by pushing and manipulating under x-ray. Many times, the manipulation to place the electrodes in a proper position is difficult and the results are sub-optimal due to anatomical variations.

[0010] During electrophysiological study, electrical signals occurring in the myocardium (heart muscle) are measured and recorded. This is accomplished by advancing an electrode-carrying catheter into the heart. The catheter is manipulated until the electrode touches the endocardial region of interest. This can be a cumbersome and time-consuming procedure because multiple measurements are often required to perform a complete study. In addition, accurately positioning the electrode using manual manipulation is a difficult process.

[0011] Ablation of electrical pathways to eliminate heart rhythm disturbances eliminates potentially life threatening abnormal heart rhythms by ablating erroneous electrical pathways in the myocardium, that have been previously identified during an electrophysiological study. Ablation of these pathways using thermal or microwave energy delivered to a predetermined specific region by an energy-carrying catheter is the mainstay of the procedure. This catheter is placed in good contact with the selected endiocardial region, otherwise no ablation will occur. Additionally, the catheter must be precisely positioned in order to avoid damaging the normal electrical pathways. Given these exacting requirements, the imprecise nature of manual manipulation can cause this procedure to be especially difficult and time consuming.

[0012] Mitral valvuloplasty is used to treate mitral valve stenosis by dilating the narrowed valve with a balloon. The current method involves advancing a catheter through the vena cava into the right atrium. An incision is made in the intra-atrial septum and the catheter is forced through the cut

into the left atrium. A balloon is then advanced through the catheter into the mitral valve apparatus, and inflated to break the stenotic tissue. Notwithstanding a high success rate and a low risk of recurrent restenosis associated with this procedure, a known complication is an atrial septal defect induced by the puncture of the intra-atrial septum. Although much less aggressive than surgery, this procedure is lengthy, difficult, and requires special skills in addition to those normally requisite for catheterization.

[0013] Mitral valvuloplasty (aorta to left atrium method) is considered by some to be a preferred alternative to the vena cava approach because the intra-artrial septum puncture is eliminated, thereby eliminating the potential complication of atrial septal defect. This procedure differs from the current method of mitral valvuloplasty in that the catheter is advanced through the aorta, the left atrium, and the aortic valve, for positioning into the left ventricle. A balloon is then advanced through the catheter into the mitral valve apparatus and inflated to break the stenotic tissue. Because a relatively rigid balloon is required to break the tissue narrowing the mitral valve, it is almost impossible to bring the balloon into proper alignment via the aorta and left ventricle due to the sharp acute angle between the aortic route and the required approach to the mitral valve.

[0014] Myocardial revascularization is a therapeutic procedure that increases the blood supply to the heart muscle by inducing the formation of new small blood vessels in the myocardium. The surgery involves opening the chest wall and laser "drilling" multiple small channels from the heart external aspect (epicardium).

[0015] Percutaneous myocardial revascularization is a catheter-based procedure for promoting angioneogensis. It involves advancing a laser catheter into the heart and performing the channelling from the heart inner aspect (endocardium). This approach is particularly applicable to patients who constitute a high surgical risk and who are beyond conventional catheter based therapy. Due to the accuracy required when positioning and fixating the laser catheter, this procedure does not appear to be implementable with currently available catheter technology.

[0016] The foregoing procedures suffer from numerous disadvantages and limitations. A very high skill level is often required to properly manipulate the catheter into position. Extensive training is required to attain this skill level. Many of the procedures are tedious and time-consuming. This results in repeated and prolonged exposure of the patient and staff to the adverse effects of x-rays. The lengthy procedures also require the use of additional contrast material with associated risk to the patient. Procedures that require highly-accurate positioning of the catheter distal end (also referred to as the catheter tip) are difficult to perform and are not always feasible. The insertion, removal, and manipulation of secondary tools often causes the tip of the guiding catheter to be dislodged from the desired position. Time-consuming manipulation is required to correctly reposition the tip. The coronary arteries are sometimes torturous with sharp bends or blockages that make advancement of a guidewire or balloon difficult or even impossible. A principal source of catheter tip location information is the x-ray imaging system with its associated adverse side effects.

[0017] Therefore, there is a great and still unsatisfied need for an apparatus and method for guiding, steering, and advancing invasive devices and for accurately controlling their position; for providing three dimensional imaging; and for minimizing the use of x-rays or other ionizing-type radiation

SUMMARY

[0018] The present invention solves these and other problems by providing a magnetic catheter guidance and control apparatus that requires less training and less skill that prior art systems. The magnetic catheter guidance system can rapidly advance and position the catheter, thus minimizing x-ray and contrast material exposure. Moreover, the magnetic system used in the magnetic catheter guidance system can be used to locate the catheter tip to provide location feedback to the operator and the control system.

[0019] One embodiment includes a catheter and a guidance and control apparatus that can accurately, and with relative ease, allow the surgeon/operator to position the catheter tip inside a patient's body. The catheter guidance and control apparatus can maintain the catheter tip in the correct position. One embodiment, includes a catheter with guidance and control apparatus that can steer a guidewire or balloon through arteries and forcefully advance it through plaque or other obstructions. One embodiment includes a catheter guidance and control apparatus that displays the catheter tip location with significantly reduced x-ray exposure to the patient and staff. One embodiment includes a catheter guidance and control apparatus that is more intuitive and simpler to use, that displays the catheter tip location in three dimensions, that applies force at the catheter tip to pull, push, turn, or hold the tip as desired, and that is capable of producing a vibratory or pulsating motion of the tip with adjustable frequency and amplitude to aid in advancing the tip through plaque or other obstructions. One embodiment provides tactile feedback at the operator control to indicate an obstruction encountered by the tip.

[0020] In one embodiment, a catheter Guidance Control and Imaging (GCI) apparatus allows a surgeon to advance, accurately position and fixate a catheter, and to view the catheters' position in three dimensions with the x-ray imagery overlaying the display. In one embodiment, the apparatus includes an operator control called a "Virtual Tip" which, in addition to being a model representation of the actual or physical catheter tip advancing within the patient's body, possesses a positional relationship to the catheter tip.

[0021] The Virtual Tip includes a physical assembly, somewhat akin to a joystick, that can be manipulated by the surgeon and is also designed to deliver tactile feedback to the surgeon in the appropriate axis or axes if the actual tip encounters an obstacle. In other words, the Virtual Tip includes a joystick-type device that allows the surgeon to guide the actual catheter tip though the patient's body. Then the actual catheter tip encounters an obstacle, the Virtual Tip provides tactile force feedback to the surgeon to indicate the presence of the obstacle.

[0022] In one embodiment, the physical catheter tip (the distal end of the catheter) includes a permanent magnet that responds to a magnetic field generated externally to the patient's body. The external magnetic field pulls, pushes, turns, and holds the tip in the desired position. One of ordinary skill in the art will recognize that the permanent magnet can be replaced or augmented by an electromagnet.

[0023] The operator control provides the position and orientation command inputs to a servo system that controls the catheter tip position by regulating the magnetic force applied outside the patient's body. A measurement of the actual tip position and orientation is made via sensory apparatus that includes magnetic field sensors and temperature sensors. This measurement serves as a feedback to the servo system and the operator interface. In one embodiment, the servo system has a correction input that compensates for the dynamic position of a body part or organ, such as the heart, thereby offsetting the response such that the actual tip moves in unison with the beating heart.

[0024] The operation of the catheter guidance system is as follows: i) the operator adjusts the physical position of the virtual catheter tip, ii) a change in the virtual tip position is encoded producing input data received at a control system, iii) the control system generates commands sent to servo system control apparatus, iv) the servo system control apparatus operates the servo mechanisms to adjust the electromagnetic field of external magnets, which v) causes the position of the actual magnetic catheter tip within the patient's body to change, vi) the new position of the actual catheter tip is then sensed by magnetic field sensors and temperature sensor arrays, which vii) provide feedback to the servo system control apparatus and the monitoring system of the operator interface thereby updating the displayed image of the actual catheter tip position in relation to the overlaid patient x-ray image.

[0025] The operator can then make further adjustments to the virtual catheter tip position and the sequence of steps ii through vii are repeated in a way that is smooth and continuous to the user. In addition, throughout this procedure, feedback from the servo system control apparatus creates command logic when the actual catheter tip encounters an obstacle or resistance in its path. The command logic is used to control stepper motors physically coupled to the virtual catheter tip. The stepper motors are engaged to create resistance in the appropriate direction(s) that can be felt by the operator, and tactile feedback is thus provided to the surgeon.

BRIEF DESCRIPTION OF THE DRAWINGS

[0026] The various features of the present invention and the manner of attaining them will be described in greater detail with reference to the following description, claims, and drawings, wherein reference numerals are reused, where appropriate, to indicate a correspondence between the referenced items.

[0027] **FIG. 1A** is a high-level system block diagram for a surgery system that includes an operator interface, a catheter guidance system, surgical equipment (e.g., a catheter to be guided), and a patient.

[0028] **FIG. 1B** is a block diagram of one embodiment of the catheter guidance system from **FIG. 1A**.

[0029] **FIG. 1C** is a block diagram of the catheter guidance system of **FIG. 1B** showing additional details not shown in **FIG. 1B**.

[0030] **FIG. 2** is a schematic diagram of a ground fault interrupter, an uninterruptable power supply, DC supplies, and a supervisory unit for use in the apparatus of **FIG. 1B**.

[0031] **FIG. 3** is a schematic diagram of a system controller for use in the apparatus of **FIG. 1B**.

[0032] **FIG. 4** is a schematic diagram of a virtual tip and calibration fixture controller for use in the apparatus of **FIG. 1B**.

[0033] **FIG. 5** is an electrical block diagram of a virtual tip for use in the apparatus of **FIG. 1B**.

[0034] **FIG. 6** is a perspective view of the Virtual Tip device in connection with the electrical block diagram of **FIG. 5**.

[0035] **FIG. 7** is a schematic diagram of an X axis controller and amplifier for use in the apparatus of **FIG. 1B**.

[0036] **FIG. 8** is a schematic diagram of a Y axis controller and amplifier for use in the apparatus of **FIG. 1B**.

[0037] **FIG. 9** is a schematic diagram of a Z axis controller and amplifier for use in the apparatus of **FIG. 1B**.

[0038] **FIG. 10** is a schematic diagram of a communication controller for use in the apparatus of **FIG. 1B**.

[0039] **FIG. 11** is a schematic diagram of a calibration fixture for use in the apparatus of **FIG. 1B**.

[0040] **FIG. 12** is a perspective view of the calibration fixture (mechanical) of **FIG. 11**.

[0041] **FIG. 13** is an orthographic representation view illustrating a polar configuration of the electromagnets with their corresponding magnetic field sensors.

[0042] **FIG. 13A** is a possible polar configuration as a cluster of electromagnets forming the magnetic circuit with a C-Arm.

[0043] **FIG. 13B** is a representation of the geometrical layout of the coils, the arm and the table.

[0044] **FIG. 13C** is a block diagram representing the electronics scheme of clustered electromagnetic coils

[0045] **FIG. 13D** is a matrix representation of a vector

[0046] **FIG. 13E** is a representation of the characteristic matrix

[0047] **FIG. 13F** is a representation of the Inverse characteristic matrix

[0048] **FIG. 13G** is a representation of the product of the characteristic matrix with its Inverse matrix

[0049] **FIG. 13H** is a logical flow diagram of **FIG. 13G**

[0050] **FIG. 14** illustrates various magnetic field sensors and temperature sensor pairs for use in the apparatus of **FIG. 1B**.

[0051] **FIG. 15** and **15A** are fragmentary, perspective views of a catheter assembly and a guidewire assembly for use in the apparatus of **FIG. 1B**.

[0052] **FIG. 15B** a representation of a catheter fitted with a magnetic tip and two piezoelectric rings.

[0053] **FIG. 16** illustrates a bi-plane X-ray ring incorporating the apparatus of **FIG. 1B**.

[0054] **FIG. 16A** illustrates a top view of the apparatus of **FIG. 1B**.

[0055] **FIG. 16B** illustrates an end view of the apparatus of **FIG. 1B**.

[0056] **FIG. 16C** illustrates a side view of the apparatus of **FIG. 1B**.

[0057] **FIG. 17** illustrates the use of the apparatus of **FIG. 1B** with cineangiographic equipment.

[0058] **FIG. 17A** illustrates the use of fiduciary markers synchronizing the fluoroscopy image.

[0059] **FIG. 17B** illustrates the use of fiduciary markers in performing a pacemaker electrode implementation.

[0060] **FIG. 18** is a vectorial representation of the magnitude and direction of the resultant force vector applied by the electromagnets of **FIG. 13**.

[0061] **FIG. 18A** illustrates the polarity of the magnetic tip of the catheter in relation to the virtual origin of the coordinate system.

[0062] **FIG. 18B** illustrates the resultant vector as detected by the magnetic field sensors of **FIGS. 20 and 20**A.

[0063] **FIG. 18C** illustrates the angle of the resultant vector of **FIG. 18B** in three dimensions.

[0064] **FIG. 19** illustrates the distance between two opposing electromagnets for use in the apparatus of **FIG. 1B**.

[0065] **FIG. 19A** illustrates the distance between adjacent magnetic field sensors of **FIG. 19**.

[0066] **FIG. 20** is a representation of the process of deducing the location of the tip of **FIG. 18A** by the magnetic field sensors of **FIG. 19A**.

[0067] **FIG. 20A** illustrates the result of further calculations of the signals from the magnetic field sensors of **FIG. 19A**.

[0068] **FIG. 21** is a representation of the rotation of the magnetic tip of **FIG. 18A** in the Z axis (θ) direction.

[0069] **FIG. 22** is a representation of the translation of the magnetic tip of **FIG. 18A** in the Z axis (ΔZ) direction.

[0070] **FIG. 23** is a logical flow diagram of a controller forming part of the apparatus of **FIG. 1B**, for determining the position of the actual tip of **FIG. 18A** in response to a new move command.

DETAILED DESCRIPTION

[0071] **FIGS. 1A, 1B** and 1C show a system **700** that includes a guidance, control, and imaging (GCI) apparatus **501**. The system **700** further includes an operator interface equipment **500** and a surgical medical equipment **502**. **FIG. 1A** illustrates an embodiment of the GCI apparatus **501** that includes various functional units. **FIG. 1A** further illustrates the overall relationship between these functional units and the operator interface **500**, the auxiliary equipment **502** residing in the operating room, and the patient **390**. **FIG. 1B** provides further details of the inter-relationships of these functional units and some of their components.

[0072] **FIG. 1C** shows the inter-relation between the GCI apparatus **501**, surgical medical equipment **502**, operator interface equipment **500**, and a reference patient **390**. A more detailed description of the GCI apparatus **501** and other auxiliary equipment, such as the surgical medical equipment **502**, in the operating room will be described later in greater detail in connection with **FIGS. 16, 16A**, **16**B and **16**C. The system **700** is configured to guide a catheter or similar device having a distal end (also referred to herein as a tip) that enters the body.

[0073] **FIG. 2** is a block diagram that illustrates a first functional unit of GCI apparatus **501**, namely a power supply and control unit that includes a ground fault interrupter **1**, an uninterruptable power supply **300**, DC supplies **16**, **17**, **18**, and **19**, and a supervisory unit **301** for use in the system **700** of **FIG. 1B**.

[0074] Another functional unit of the GCI apparatus **501** is a system controller (SC) **302** which is illustrated in **FIG. 3**. Yet another functional unit of the GCI apparatus **501** is a virtual tip and calibration fixture controller (VT/CFC) **303** which is illustrated in **FIG. 4**. Still another functional unit of the GCI apparatus **501** is a virtual tip assembly (VT) **304** which is illustrated in **FIGS. 5 and 6**. Additional functional units of the GCI apparatus **501** include an X-Axis controller and amplifier (XCA) **305**, a Y-Axis controller and amplifier (YCA) **310**, and a Z-Axis controller and amplifier (ZCA) **315**. These functional units are each individually detailed by functional block diagrams in **FIGS. 7, 8**, and **9**, respectively. Still other functional units of the GCI apparatus **501** include a communication controller (CC) **320** which is depicted in detail in **FIG. 10**; a calibration fixture (CF) **321** which is depicted in detail in **FIGS. 11 and 12**; and magnetic field sensor (MFS) and temperature sensor (TS) pairs **374** that are illustrated in **FIG. 14**. The various magnetic field sensors and temperature sensor pairs **374** are used in the system **700** of **FIG. 1B**. The magnetic field sensor or sensors can be Hall-effect sensors, superconducting sensors, or other sensors that sense a magnetic field such as, for example, the magnetic field produced by a magnet (or electromagnet) at the distal end of the catheter. In one embodiment, the magnetic field sensors are Hall-effect sensors. The temperature sensors can be thermistors or other temperature-sensing devices. The temperature sensors are described herein because many magnetic field sensing devices, such as, for example, Hall-effect sensors are temperature-dependent. However, the temperature sensors are optional and can be omitted when the additional accuracy afforded by the temperature sensors is not needed or when knowledge of the temperature of the magnetic sensors is not needed.

[0075] Referring to **FIG. 1B**, the power supply and control system **392** includes: a Ground Fault Interrupter (GFI) **1**; an uninterruptable power supply (UPS) **300**; a supervisory unit (SU) **301**; individual DC power supplies XPS **16**, YPS **17**, and ZPS **18** that provide power to the X Axis Controller And Amplifier (XCA) **305**, the Y-axis Controller And Amplifier (YCA) **310**, and the Z-axis Controller And Amplifier (ZCA) **315**, respectively; and a DC system power supply (SPS) **19** that provides the DC power needed to operate other digital and analog circuitry of the GCI apparatus **501**. These components and their functional relationships are depicted in greater detail in **FIG. 2**.

[0076] Referring now to **FIG. 2**, the Ground Fault Interrupter (GFI) **1** acts as a safety device by monitoring the AC input current in the line and the neutral. If an imbalance is detected, it is assumed that a stray path to ground is present (posing a shock hazard to the user or the patient). This

detection will cause a trip that disconnects the load from the line. **100751** The uninterruptable power supply (UPS) **300** contains batteries **9**, a charging system **5**, an inverter **13**, and power switching circuitry. The UPS **300** automatically supplies the entire AC power requirements of the system **700** for the duration of a power failure, or until battery depletion occurs. A graceful system shutdown is initiated by a Supervisory Unit (SU) **301** and a system controller (SC) **302** if the power failure extends beyond battery capacity.

[**0077**] Still referring to **FIG. 2**, an amplifier **3** and its current transformer monitor the AC line current. An isolation amplifier **4** monitors the AC voltage output of Ground Fault Interrupter (GFI) **1**. Charger **5** produces the desired DC power to charge battery **9** of the uninterruptable power supply **300**. An amplifier **8** monitors the voltage drop across shunt **7** to determine the charge current of the battery **9**. An amplifier **10** monitors the output voltage of the battery **9**. An amplifier **12** monitors the voltage drop across shunt **11** to determine load current of the battery **9**. An inverter **13** generates the AC power used by components of the GCI apparatus **501**. An isolation amplifier **14** monitors the AC output voltage of inverter **13**. An amplifier **15** and its current transformer monitor the current output of inverter **13**.

[**0078**] A Supervisory Unit (SU) **301** monitors the signals from the following components: the AC line; and the outputs of the Ground Fault Interrupter (GFI) **1**, the uninterruptable power supply (UPS) **300**; and the DC power supplies **16**, **17**, **18**, and **19**. The Supervisory Unit (SU) **301** informs the System Controller (SC) **302** of an AC power failure, a Ground Fault Interrupter (GFI) trip, an Uninterruptable Power Supply (UPS) failure or failure of the DC power supplies **16**, **17**, **18**, and **19**.

[**0079**] As detailed in **FIG. 2**, the SU **301** includes an analog multiplexer **20** that connects a given signal to be monitored to a programmable gain amplifier **21**. A decode logic **26** in conjunction with an address latch **24** allow a microcontroller **30** to set the input channel of the analog multiplexer **20**. A microcontroller **30** executes a code resident in read only memory **28**. The decode logic **26** in conjunction with address latch **25** allow microcontroller **30** to set the gain of programmable gain amplifier **21**. Microcontroller **30** then strobes sample and hold circuit **22** via decode logic **26**. The output of sample and hold circuit **22** is thus a "snapshot" of the signal to be measured.

[**0080**] Analog to digital converter **23** is issued a convert command by microcontroller **30** via decode logic **26**. When conversion is complete, analog to digital converter **23** interrupts microcontroller **30** via decode logic **26** and the digital representation of the measured signal is input by microcontroller **30**. A random access memory **29** is used to store sampled data during operation of the SU **301**. A non-volatile memory **27** stores data during power down. It is by this method that the various voltages and currents are monitored by supervisory unit **301**. Microcontroller **30** communicates with system controller **302** via buffer **31**. Control logic **32** allows system controller **302** to coordinate the power up-power down sequence in accordance with system conditions.

[**0081**] With reference to **FIGS. 1B and 3**, System Controller (SC) **302** controls the power up-power down sequence in an orderly fashion and alerts the operator to the system status and any required corrective action via Communications Controller (CC) **320**, Computer **324**, and monitor **325**. In addition, System Controller (SC) **302** coordinates the operation of X Axis Controller and Amplifier (XCA) **305**, Y-Axis Controller and Amplifier (YCA) **310**, and Z Axis Controller and Amplifier (ZCA) **315**. Additionally, System Controller (SC) **302** communicates with Virtual Tip/Calibration Fixture Controller (VT/CFC) **321** and Communication Controller (CC) **320** via system bus **328**.

[**0082**] As illustrated in **FIG. 1B**, Servo Power Supply (XPS) **16** provides DC power to the X-Axis Controller and Amplifier (XCA) **305**. The XCA **305** energizes the electromagnets **132**X and **138**X that are located outside the patient's body. X Axis Controller and Amplifier (XCA) **305** monitors temperature sensor (TS) arrays **306**, **309**, and magnetic field sensor arrays **307**, **308**, and further drives Electromagnet (EM) **132**X and **138**X. Magnetic field sensor arrays **307** and **308** measure the magnetic flux in the X axis. Temperature sensor (TS) arrays **306** and **309** measure the temperature of magnetic field sensor arrays **307** and **308** so that X Axis Controller and Amplifier (XCA) **305** can apply temperature compensation factors to the magnetic field sensor outputs.

[**0083**] The sensory outputs of these arrays **306**, **307**, **308**, **309** provide feedback to XCA **305** concerning the position of the actual catheter tip **377** with reference to the X-axis. As it will become apparent from the present description, these electromagnets **132**X and **138**X affect the position of the actual catheter tip **377** inside the patient's body **390** in the X-axis.

[**0084**] Servo Power Supply (YPS) **17** provides DC power to the Y-Axis Controller and Amplifier (YCA) **310** for energizing the electromagnets (EM) **132**Y and **138**Y that are located outside the patient's body. YCA **310** monitors the sensor arrays of the Y-axis that include temperature sensor (TS) arrays **311**, **314**, and magnetic field sensor array **312**, **313**. Magnetic field sensor arrays **312** and **313** measure the magnetic flux in the Y-axis. Temperature sensor (TS) arrays **311** and **314** measure the temperature of magnetic field sensor arrays **312** and **313** so that Y Axis Controller and Amplifier (YCA) **310** can apply temperature compensation factors to the magnetic field sensor outputs. The sensory outputs of these arrays **311**, **312**, **313**, **314** provide feedback to the servo system controlled by YCA **310** concerning the position of the actual catheter tip **377** with reference to the Y-axis. As it will become apparent from the present description, these electromagnets **132**Y and **138**Y affect the position of the actual catheter tip **377** inside the patient's body **390** in the Y-axis.

[**0085**] The Z-Axis Power Supply (ZPS) **18** provides DC power to the Z-Axis Controller and Amplifier (ZCA) **315** for energizing the electromagnets (EM) **132**Z and **138**Z that are located outside the patient's body. ZCA **315** monitors the sensor arrays of the Z-axis that include the following components: temperature sensor (TS) arrays **316**, **318**, and magnetic field sensor arrays **317**, **319**. Magnetic field sensor arrays **317** and **319** measure the magnetic flux in the Z axis. Temperature sensor (TS) arrays **316** and **318** measure the temperature of magnetic field sensor arrays **317** and **319**, so that Z Axis Controller and Amplifier (ZCA) **315** can apply temperature compensation factors to the magnetic field sensor outputs. The sensory outputs of these arrays **316**, **317**, **318**, **319** provide feedback to the servo system controlled by

ZCA **315** concerning the position of the actual catheter tip **377** with reference to the Z-axis. As it will become apparent from the present description, these electromagnets **132**Z and **138**Z affect the position of the actual catheter tip **377** inside the patient's body **390** in the Z-axis.

[**0086**] Communication Controller (CC) **320** interfaces host system **323**, auxiliary equipment **322**, and the computer **324** to system bus **328**. The surgical and medical equipment **502** can include, for example, the host system **323** and auxiliary equipment **322**. The host system **323** contains data concerning the patient and the current procedure(s) and also archives data generated by the GCI apparatus **501**. Auxiliary equipment **322** can include the x-ray imaging system and other patient monitoring apparatus.

[**0087**] The operator interface **500** includes, for example, Computer **324**, monitor **325**, keyboard **326**, and mouse **327**. The computer **324** allows the operator to adjust the system parameters and to perform calibration and diagnostic routines. Monitor **325** displays the actual catheter tip **377** position data with overlaid X-ray imagery and operator prompts. Keyboard **326** and mouse **327** are used for operator-entered data input.

[**0088**] Virtual Tip/Calibration Fixture Controller (VT/CFC) **303** inputs encoder position, limit switch, and operator switch data from Virtual Tip assembly **304** to be used by XCA **305**, YCA **310**, and ZCA **315** in controlling the electromagnets **132**X, **138**X, **132**Y, **138**Y, **132**Z, and **138**Z. Also, Virtual Tip/Calibration Fixture Controller (VT/CFC) **303** outputs Tactile Feedback (TF) response and light emitting diode (LED) data to Virtual Tip (VT) **304** to be perceived by the operator as obstructions or resistance met by the actual catheter tip **377**.

[**0089**] **FIG. 3** illustrates the components of one embodiment of the system controller (SC) **302**. A detailed description of the functionality of these components will follow in the ensuing description of the drawings. SC **302** can be characterized as functioning in different modes: 1) a power-up/power-down mode, 2) a servo system controller mode, 3) a tactile feedback response mode, and 4) a calibration mode.

[**0090**] In the power-up/power down mode, SC **302** coordinates power-up/power-down sequencing of the components of the GCI apparatus **501**, performs built-in system diagnostic functions, and reports any errors detected during diagnostic functions which are sent to the communications controller (CC) **320** and stored in memory **41**. These tasks are accomplished by microcontroller **33**. Error data is stored in Random Access Memory (RAM) **41** during system operation and in Non Volatile Memory (NVM) **39** during power down. Microcontroller **33** communicates with other system components via system bus **328** by setting the appropriate address and control bits to decode logic **38** that enables address buffer **34** and data buffer **35**. Data latch **36** and data buffer **37** similarly connect microcontroller **33** to Uninterruptable Power Supply (UPS) **300** and to supervisory unit (SU) **301** via control logic **32**.

[**0091**] In the servo system controller mode, System Controller (SC) **302** calculates the actual tip (AT) position as further described in conjunction with **FIG. 23**. Then, using data from the virtual tip (VT) **405**, determines the appropriate position error, that is the difference between the actual tip position and the operator-desired tip position as indicated by the virtual tip position, to be sent to X Axis Controller and amplifier (XCA) **305**, Y-Axis Controller and amplifier (YCA) **310**, and Z-Axis Controller and amplifier (ZCA) **315** via the system bus **328**.

[**0092**] In the tactile feedback response mode, System Controller SC **302** initiates tactile feedback response by providing feedback data to the virtual tip (VT) **304** via the system bus **328**, as described in detail in **FIG. 23**.

[**0093**] During the calibration mode, System Controller (SC) **302** exercises Calibration Fixture (CF) **312** via Virtual Tip/Calibration Fixture controller (VT/CFC) **303** and correlates the position data from X-axis Controller and Amplifier (XCA) **305**, Y-axis Controller and Amplifier (YCA) **310**, and Z-axis Controller and Amplifier (ZCA) **305** with Calibration Fixture (CF) **321** encoders **64**C, **66**C, **68**C, **70**C, and **72**C.

[**0094**] **FIG. 4** illustrates the Virtual Tip And Calibration Fixture Controller (VT/CF) **303**. Data is stored in Random Access Memory (RAM) **50** during the system operation and in a Non Volatile Memory (NVM) **48** during power down. Microcontroller **42** communicates with System Controller (SC) **302** (**FIG. 3**) via system bus **328** by setting the appropriate address and control bits to decode logic **47**, which enables address buffer **43** and data buffer **44**. Address latch **45** and data buffer **46** similarly connect microcontroller **42** with virtual tip (VT) **405** or calibration fixture (CF) **321**, as described below.

[**0095**] Virtual Tip/Calibration Fixture (VT/CF) controller **303** inputs data from VT **304** or CF **321** concerning the encoder positions, limit "switch" closures, and operator input switch positions. Additionally, Virtual Tip/Calibration Fixture (VT/CF) controller **303** outputs data to Virtual Tip (VT) **304** to produce tactile feedback and to illuminate the LED indicators to alert the operator of various system conditions.

[**0096**] Referring to **FIG. 5**, the electronic circuitry function of the VT assembly **304** is as follows. A decode logic **101** responds to address and control bits originating from Virtual Tip/Calibration Fixture controller (VT/CFC) **303** (**FIG. 3**), enabling data buffer **51** and setting its direction for transferring data. Step latches **52** and **53** store incoming data sent from the VT/CFC **303** to be presented to stepper drivers **54**, **56**, **58**, **60** and **62** when strobed by decode logic **101**. Stepper motors **55**, **57**, **59**, **61**, and **63** respond to the stepper driver outputs to provide tactile feedback to the operator. The stepper motors **55**, **57**, **59**, **61**, and **63** create tactile feedback by producing resistance in the appropriate axial or angular coordinates as follows: stepper motor **55** in the X-axis **400**; stepper motor **57** in the Y-axis **401**, stepper motor **59** in the Z-axis **402**; stepper motor **61** in the angular direction of θ; and stepper motor **63** in the angular direction of EL.

[**0097**] Still referring to **FIG. 5**, the absolute encoders **64**, **66**, **68**, **70**, and **72** are mechanically coupled to the corresponding stepper motors **55**, **57**, **59**, **61**, and **63**, and provide position feedback to the VT/CFC **303** during Tactile Feedback (TF) as well as inform the VT/CFC **303** of the Virtual Tip (VT) position during manual adjustments of the VT **405** by the operator. Encoder outputs are buffered by **65**, **67**, **69**, **71**, and **73**, to temporarily store and transfer axial and angular position information to VT/CFC **303**. Limit

"switches"**74**, **75**, **76**, **77**, **78**, and **79** flag the ends of the three linear axes, in order to limit the mechanical motion of the virtual tip **405**, and to allow synchronization of the mechanics of the virtual tip assembly **304** and the electronics of **FIG. 5**. "Switches"**80** and **81** indicate when angular **0** and EL are at zero position, for synchronizing of the mechanics of the virtual tip assembly **304** and the electronics shown in **FIG. 5**. Latch **82** strobes decode logic **101** in order to store these data defining positional limits. Operator switches **83**, **84**, **85**, **86**, **87**, **88**, **89**, and **90** are read and latched by latch **91**, in order to store their command, since these switches are momentary (i.e., momentary contact as opposed to a stable switch position). LEDs **92**, **93**, **94**, **95**, **96**, **97**, **98**, and **99** are driven by LED latch **100**.

[**0098**] **FIG. 7** illustrates the X axis controller and amplifier (XCA) **305**. XCA **305** receives and amplifies signals in the form of sensory data from the x-axis magnetic field sensors sensor arrays **307** and **308** and temperature sensor arrays **306** and **309**. Using this sensory data, a code is executed in microcontroller **102**X to create positional feedback to the VT/CFC **303** and other system components via system bus **328**. Microcontroller **102**X also receives data from VT/CFC **303** and other system components via system bus **328** to use in generating commands that will control the excitation of the external electromagnets **132**X and **138**X to affect the position of the actual catheter tip in the X-axis. XCA **305** also generates error and correcting signals to be used during the calibration and normal system operation. These functions will now be described.

[**0099**] First, the method by which XCA **305** monitors the sensory data from the MFS arrays **307** and **308** and temperature sensor arrays **306** and **309** will be explained. Magnetic field sensors sensor array **307** includes magnetic field sensors **113***x*, **114***x*, **115***x* and **116***x*. Magnetic field sensors sensor array **308** includes magnetic field sensors **117***x*, **118***x*, **119***x*, and **120***x*. Temperature sensor array **306** includes temperature sensors **122***x*, **123***x*, **124***x*, and **125***x*. Temperature sensor array **309** includes temperature sensors **126***x*, **127***x*, **128***x*, and **129***x*. The physical positions of these sensors and relations to one another are described in conjunction with **FIG. 13**. Microcontroller **102***x* executes a mathematical procedure that is described in conjunction with **FIGS. 18, 18A**, **18**B and **18**C, that calculates positional data based on input from the sensor arrays **307** and **308**. Input and output data is stored in Random Access Memory (RAM) **103***x* during system operation. Non Volatile Memory (NVM) **105***x* stores data such as temperature compensation parameters which are used in combination with measured temperature sensor array **306** and **309** data to make necessary corrections to data from the magnetic field sensors **113**X, **114**X, **115**X, **116**X. **117**X, **118**X, **119**X, and **120**X.

[**0100**] The collecting of sensory data is initiated by decode logic **106***x* in conjunction with address latch **111***x* that allows microcontroller **102***x* to set the input channel of analog multiplexer **112***x*. Similarly, decode logic **106***x* in conjunction with address latch **109***x* allows microcontroller **102***x* to set the gain of programmable gain amplifier **110***x* in order to compensate for variations in signal strength from the sensor arrays **307**, **308**, **306**, and **309**. Microcontroller **102***x* strobes sample and hold circuit **108***x* via decode logic **106***x*, so that microcontroller **102***x* is able to perform other functions while periodically sampling the data temporarily stored in sample and hold circuit **108**X. The output of sample and hold circuit **108***x* is thus a "snapshot" of the signal to be measured.

[**0101**] Analog-to-Digital Converter (ADC) **107***x* is issued a "convert" command by microcontroller **102***x* via decode logic **106***x* to convert the data from the position sensors **307** and **308** from analog to digital, so that the digital system can interpret the data. When the conversion is complete, analog to digital converter **107***x* interrupts microcontroller **102***x* via decode logic **106***x* and the digital representation of the measured signal is input by microcontroller **102***x*. It is by this method that the magnetic field sensors **113***x*, **114***x*, **115***x*, **116***x*, **117***x*, **118***x*, **119***x*, and **120***x* as well as the temperature sensors **122***x*, **123***x*, **124***x*, **125***x*, **126***x*, **127***x*, **128***x*, and **129***x* are monitored. Similarly, the voltage drop across the shunts **131**X and **137**X is measured to determine the current flow through the electromagnets **132**X and **138**X.

[**0102**] Still referring to **FIG. 7**, current source **121***x* provides the control current to bias the magnetic field sensors **113**X, **114**X, **115**X, **116**X, **117**X, **118**X, **119**X, and **120**X since they operate best in a constant current mode and require stability for reliable sensing. Temperature sensor bias supply **130***x* supplies the voltage for the temperature sensors **122**X, **123**X, **124**X, **125**X, **126**X, **127**X, **128**X, **129**X.

[**0103**] The method by which XCA **305** generates commands to control the movement of the actual catheter tip **377** in the X-axis will now be explained. Microcontroller **102**X receives data from VT/CFC **303** and other system components via system bus **328** to use in generating commands that will control the movement. Microcontroller **102***x* in conjunction with decode logic **106***x* controls modulators **144***x* and **146***x* to provide the correct move signal and command. Preamplifiers **143***x*, and **145***x* amplify the modulators outputs and drive final amplifiers **135***x*, **136***x*, **141***x*, and **142***x*. Diodes **133***x*, **134***x*, **139***x*, and **140***x* protect the final amplifiers from a surge of back electromotive force due to the inductive nature of the electromagnet coils **132**X and **138**X.

[**0104**] Electromagnet coils **132***x* and **138***x* produce a magnetic field that affects the position of the actual catheter tip in the X-Axis.

[**0105**] Microcontroller **102**X communicates with VT/CFC **303** and other system components via system bus **328** by setting the appropriate address and control bits to decode logic **106***x*, which enables address buffer **148***x* and data buffer **147***x*.

[**0106**] Non Volatile Memory (NVM) **105***x* also stores calibration data to be used during calibration operations in conjunction with the calibration fixture **321** and VT/CFC **303**. These operations and the source of the calibration data will be described later in conjunction with **FIG. 23**. Further, Non Volatile Memory (NVM) **105***x* stores error codes to be used during power down operations controlled by the System Controls (SC) **302**.

[**0107**] **FIG. 8** illustrates The Y-axis controller and amplifier (YCA) **310** which operates in a similar manner to the XCA **305** of **FIG. 7**. YCA **310** receives and amplifies the signals from the Y-axis magnetic field sensor arrays **312** and **313** and temperature sensor arrays **311** and **314**. Using this incoming sensory data, a code is executed in microcontroller **102**Y to create positional feedback to the VT/CFC **303** and

other system components via system bus **328**. Microcontroller **102**Y also receives data from VT/CFC **303** and other system components via system bus **328** to use in generating commands that will control excitation of the external electromagnets **132**Y and **138**Y to affect the position of the actual catheter tip **377** in the Y-axis. YCA **310** also generates error and correcting signals to be used during the calibration and normal system operation. These functions will now be described.

[**0108**] First, the method by which YCA **310** monitors the sensory data from MFS arrays **312** and **313** and temperature sensor arrays **311** and **314** will first be explained. Magnetic field sensor array **312** includes magnetic field sensors **113***y*, **114***y*, **115***y* and **116***y*. Magnetic field sensor array **313** includes magnetic field sensors **117***y*, **118***y*, **119***y*, and **120***y*. Temperature sensor array **311** includes temperature sensors **122***y*, **123***y*, **124***y*, and **125***y*. Temperature sensor array **314** includes temperature sensors **126***y*, **127***y*, **128***y*, and **129**y. The physical positions of these sensors and relations to one another are described in conjunction with **FIG. 13**.

[**0109**] Microcontroller **102***y* executes a mathematical procedure, that described in conjunction with **FIGS. 18, 18A**, **18**B and **18**C, that calculates positional data based on input from the sensor arrays **312** and **313**. Input and output data is stored in Random Access Memory (RAM) **103***y* during system operation. Non Volatile Memory (NVM) **105***y* stores data such as temperature compensation parameters which are used in combination with measured temperature sensor array **311** and **314** data to make necessary corrections to data from the magnetic field sensors **113**Y, **114**Y, **115**Y, **116**Y, **117**Y, **118**Y, **119**Y, and **120**Y.

[**0110**] The collecting of sensory data is initiated by decode logic **106***y* in conjunction with address latch **111***y*, which allows microcontroller **102***y* to set the input channel of analog multiplexer **112***y*. Similarly, decode logic **106***y* in conjunction with address latch **109***y* allows microcontroller **102***y* to set the gain of programmable gain amplifier **110***y*, in order to compensate for variations in signal strength from the sensor arrays **311**, **312**, **313**, and **314**. Microcontroller **102***y* strobes sample and hold circuit **108***y* via decode logic **106***y*, to allow microcontroller **102***y* to perform other functions while periodically sampling the data temporarily stored in sample and hold circuit **108**Y. The output of sample and hold circuit **108***y* is thus a "snapshot" of the signal to be measured.

[**0111**] Analog to Digital Converter (ADC) **107***y* is issued a convert command by microcontroller **102***y* via decode logic **106***y* to convert the data from the position sensors **312** and **313** from analog to digital, so that the digital system can interpret the data. When the conversion is complete, analog to digital converter **107***y* interrupts microcontroller **102***y* via decode logic **106***y* and the digital representation of the measured signal is input by microcontroller **102**y. It is by this method that the magnetic field sensors **113***y*, **114***y*, **115***y*, **116***y*, **117***y*, **118***y*, **119***y*, and **120***y* as well as the temperature sensors **122***y*, **123***y*, **124***y*, **125***y*, **126***y*, **127***y*, **128***y*, and **129***y* are monitored. Similarly, the voltage drop across the shunts **131** Y and **137**Y is measured to determine the current flow through the electromagnets **132**Y and **138**Y.

[**0112**] Still referring to **FIG. 8**, current source **121***y* provides the control current to bias the magnetic field sensors **113**Y, **114**Y **115**Y, **116**Y, **117**Y, **118**Y, **119**Y, and **120**Y, since they operate best in a constant current mode and require stability for reliable sensing. Temperature sensor bias supply **130***y* supplies the voltage for the temperature sensors **122**Y, **123**Y, **124**Y, **125**Y, **126**Y. **127**Y, **128**Y, and **129**Y.

[**0113**] The method by which YCA **310** generates commands that will control the movement of the actual catheter tip in the Y-Axis will now be explained. Microcontroller **102**Y receives data from VT/CFC **303** and other system components via system bus **328** to use in generating commands that will control the movement of the actual catheter tip in the Y-axis will now be explained. Microcontroller **102***y* in conjunction with decode logic **106***y* controls modulators **144***y* and **146***y* to provide the correct move signal and command. Preamplifiers **143***y*, and **145***y* amplify the modulators outputs and drive final amplifiers **135***y*, **136***y*, **141***y*, and **142**y. Diodes **133***y*, **134***y*, **139***y*, and **140***y* protect the final amplifiers from a surge of back electromotive force due to the inductive nature of the electromagnet coils **132**Y and **138**Y. Electromagnet coils **132***y* and **138***y* produce the magnetic field which will affect the position of the actual catheter tip **377** in the Y-Axis.

[**0114**] Microcontroller **102**Y communicates with VT/CFC **303** and other system components via system bus **328** by setting the appropriate address and control bits to decode logic **106***y*, which enables address buffer **148***y* and data buffer **147***y*.

[**0115**] Non Volatile Memory (NVM) **105***y* also stores calibration data to be used during calibration operations in conjunction with the calibration fixture **321** and VT/CFC **303**. These operations and the source of the calibration data will be described later in conjunction with **FIG. 23**. Further, Non Volatile Memory (NVM) **105***y* stores error codes to be used during power down operations controlled by the System Controls (SC) **302**.

[**0116**] **FIG. 9** illustrates the Z-axis controller and amplifier (ZCA) **315** which operates in a similar manner to that of **FIGS. 7 and 8**. ZCA **315** receives and amplifies the signals from the z-axis magnetic field sensor arrays **312** and **313** and temperature sensor arrays **311** and **314**. Using the incoming sensory data, a code is executed in microcontroller **102**Z to create positional feedback to the VT/CFC **303** and other system components via system bus **328**. Microcontroller **102**Z also receives data from VT/CFC **303** and other system components via system bus **328**, to use in generating commands that will control the excitation of the external electromagnets **132**Z and **138**Z to affect the position of the actual catheter tip **337** in the Z-axis. ZCA **315** also generates error and correcting signals to be used during the calibration and normal system operation. These functions will now be described.

[**0117**] First, the method by which ZCA **315** monitors the sensory data from MFS arrays **317** and **318** and temperature sensor arrays **316** and **319** will first be explained. Magnetic field sensor array **317** includes magnetic field sensors **113***z*, **114***z*, **115***z* and **116***z*. Magnetic field sensor array **318** includes magnetic field sensors **117***z*, **118***z*, **119***z*, and **120***z*. Temperature sensor array **316** includes temperature sensors **122***z*, **123***z*, **124***z*, and **125***z*. Temperature sensor array **319** includes temperature sensors **126***z*, **127***z*, **128***z*, and **129***z*. The physical positions of these sensors and relation to one another are described in conjunction with **FIG. 13**.

[**0118**] Microcontroller **102***z* executes a mathematical procedure that is described in conjunction with **FIGS. 18, 18A**,

18B and 18C, and that calculates positional data based on input from the sensor arrays **317** and **318**. Input and output data is stored in Random Access Memory (RAM) **103***z* during system operation. Non Volatile Memory (NVM) **105***z* stores data such as temperature compensation parameters that are used in combination with measured data from the temperature sensor arrays **316** and **319**, to make necessary corrections to the data from the magnetic field sensors **113**Z, **114**Z, **115**Z, **116**Z, **117**Z, **118**Z, **119**Z, and **120**Z.

[**0119**] The collecting of sensory data is initiated by decode logic **106***z* in conjunction with address latch **111***z* that allows microcontroller **102***z* to set the input channel of analog multiplexer **112***z*. Similarly, decode logic **106***z* in conjunction with address latch **109***z* allows microcontroller **102***z* to set the gain of programmable gain amplifier **110***z*, in order to compensate for variations in signal strength from the sensor arrays **316**, **317**, **318**, and **319**.

[**0120**] Microcontroller **102***z* strobes sample and hold circuit **108***z* via decode logic **106***z*, to allow microcontroller **102***z* to perform other functions while periodically sampling the data temporarily stored in sample and hold circuit **108**Z. The output of sample and hold circuit **108***z* is thus a "snapshot" of the signal to be measured. Analog to Digital Converter (ADC) **107***z* is issued a convert command by microcontroller **102***z* via decode logic **106***z*, to convert the data from the position sensors **317** and **318** from analog to digital, so that the digital system can interpret the data. When the conversion is complete, analog to digital converter **107***z* interrupts microcontroller **102***z* via decode logic **106***z* and the digital representation of the measured signal is input by microcontroller **102***z*. It is by this method that the magnetic field sensors **113***z*, **114***z*, **115***z*, **116***z*, **117***z*, **118***z*, **119***z*, and **120***z* as we the temperature sensors **122***z*, **123***z*, **124***z*, **125***z*, **126***z*, **127***z*, **128***z*, and **129***z* are monitored. Similarly, the voltage drop across the shunts **131**Z and **137**Z is measured to determine the current flow through the electromagnets **132**Z and **138**Z.

[**0121**] Still referring to **FIG. 9**, current source **121***z* provides the control current to bias the magnetic field sensors **113**Z, **114**Z, **115**Z, **116**Z, **117**Z, **118**Z, **119**Z, and **120**Z since they operate best in a constant current mode, and require stability for reliable sensing. Temperature sensor bias supply **130***z* supplies the voltage for the temperature sensors **112**Z, **123**Z, **124**Z **125**Z, **126**Z, **127**Z, **128**Z, and **129**Z.

[**0122**] The method by which ZCA **315** generates commands that will control the movement of the actual catheter tip in the Z-axis will now be explained. Microcontroller **102**Z receives data from VT/CFC **303** and other system components via system bus **328**, to use in generating commands that will control the movement of the actual catheter tip in the Z-axis will now be explained. Microcontroller **102***z* in conjunction with decode logic **106***z* controls modulators **144***z* and **146***z* to provide the correct move signal and command. Preamplifiers **143***z*, and **145***z* amplify the modulators outputs and drive final amplifiers **135***z*, **136***z*, **141***z*, and **142***z*. Diodes **133***z*, **134***z*, **139***z*, and **140***z* protect the final amplifiers from a surge of back electromotive force due to the inductive nature of the electromagnet coils **132**Z and **138**Z. Electromagnet coils **132***z* and **138***z* produce the magnetic field which will affect the position of the actual catheter tip in the Z-axis.

[**0123**] Microcontroller **102**Z communicates with VT/CFC **303** and other system components via system bus **328** by setting the appropriate address and control bits to decode logic **106***z*, which enables address buffer **148***z* and data buffer **147***z*.

[**0124**] Non Volatile Memory (NVM) **105***z* also stores calibration data to be used during calibration operations in conjunction with the calibration fixture **321** and VT/CFC **303**. These operations and the source of the calibration data will be described later in conjunction with **FIG. 23**. Further, Non Volatile Memory (NVM) **105***z* stores error codes to be used during power down operations controlled by the System Controls (SC) **302**.

[**0125**] **FIG. 10** illustrates the communication controller (CC) **320** whose main function is to communicate with other system components via system bus **328**. The position data received from the XCA **305**, YCA **310**, and ZCA **315** is stored in Random Access Memory (RAM) **156** during system operation and in Non Volatile Memory (NVM) **154** during power down, in order to retain the position of the actual tip inside the patient's body. Microcontroller **149** communicates with other system components via system bus **328**, by setting the appropriate address and control bits to decode logic **153**, which enables address buffer **150** and data buffer **151**. Similarly, microcontroller **149** communicates with PC **324**, auxiliary equipment **322**, and host system **323** via communication I/O port **152**, by setting address and control bits to decode logic **153** or responding to an interrupt from port **152**. This is done for a number of reasons, such as the need to display the actual process and procedure of the operation on a CRT display.

[**0126**] **FIG. 11** illustrates the electrical circuitry of the calibration fixture (CF) **321** and **FIG. 12** illustrates the mechanical implementation of the calibration fixture (CF) **321**. The purpose of the CF, **321**, is to define the steps and limits of motion in each possible direction of the virtual tip **405**. This information is communicated to the VT/CFC **303** and used to synchronize the electronic circuitry and physical operations during normal operation of the GCI apparatus **501**.

[**0127**] The calibration magnet **411** is manipulated in relation to the five possible axes defined by the X-axis **406**, the Y-axis **407**, the Z-axis **408**, the θ axis **409**, and the EL axis **410**. These axes correspond exactly to the five directions of movement possible for the virtual tip **405**, which is the maximum number of degrees of freedom possible for the actual tip **377**. The manipulation of calibration magnet **411** is accomplished by the electronic circuitry of the calibration fixture **321** as implemented in **FIG. 11**.

[**0128**] The circuitry of **FIG. 11** operates as follows: A decode logic **101***c* responds to address and control bits originating from VT/CFC **303** and enables data buffer **51***c* and sets its direction. Step latches **52***c* and **53***c* store data to be presented to stepper drivers **54***c*, **56***c*, **58***c*, **60***c*, and **62***c* when strobed by decode logic **101***c*. Stepper motors **55***c*, **57***c*, **59***c*, **61***c*, and **63***c* respond to the stepper drive outputs to manipulate the magnetic calibration tip in the **5** axes. Absolute encoders **64***c*, **66***c*, **68***c*, **70***c*, and **72***c* are mechanically coupled to the corresponding stepper motors and provide position feedback to the VT/CFC **303**. The outputs of the encoders **64**C, **66**C, **68**C, **70**C and **72**C are buffered by data buffers **65***c*, **67***c*, **69***c*, **71***c* and **73***c* to temporarily store and transfer the data. Limit "switches"**74***c*, **75***c*, **76***c*, **77***c*, **78***c*, and **79***c* flag the ends of the three linear axes X, Y

and Z. "Switches"**80***c* and **81***c* indicate when θ and EL are at zero position. Limit latch **82***c* stores this data when strobed by decode logic **101***c*.

[0129] **FIG. 13** Illustrates the polar configuration **374** of the electromagnets **132**X, **132**Y, **132**Z, **138**Z, **138**Y, and **138**Z, the magnetic field sensors and temperature sensor pairs **350**, **351**, **352**, **353**, **354**,**355**, **356**, **357**, **358**, **359**, **360**, **361**, **362**, **363**, **364**, **365**, **366**, **367**, **368**, **369**, **370**, **371**, **372**, and **373**. The electromagnets **132***x*, **132***y*, **132***z* are arranged in three orthogonal axes X, Y, Z, or as shown in **FIGS. 13A and 13B**.

[0130] **FIG. 13A** and **FIG. 13B** illustrate a polar clustered configuration poles where the operating table **389** and electromagnets **901**, **902**, and **903** are configured relative to **904**, **905**, and **906**, as approximately shown and mounted by the use of support assembly **391** configured as a C-Arm to compliment and close the magnetic field circuit. The polar configuration **374** is further expressed as a non-symmetrical distribution of the polar arrangement where electromagnet **901** and its counterpart **903** are rotated to provide a lobed electromagnetic field. This arrangement further optimizes the magnetic circuit and provides for free access for the physician and the patient while the Z axis electromagnets **905** and **906** do not obstruct the available access space as approximately shown by **FIG. 13** and **FIG. 16**. Furthermore **FIG. 13** and **FIG. 13A** and **FIG. 13B** compliment each other and are an alternative to the bi-plane ring shown in **FIG. 16**, **FIG. 16A**, **FIG. 16B** and **FIG. 16C**. Both arrangements represent a possible approach provided in accommodating the imaging technology modalities such as x-ray, Cat-Scan, Pet-Scan and Ultrasound, while **FIG. 16** provides for the GCI apparatus **501** as a natural access for a fluoroscopic imaging on a bi-plane arrangement. **FIGS. 13, 13A** and **13**B enable geometry with a bore of approximately 25 inches which is capable of incorporating a computer tomography apparatus and/or the modality noted above. Further embodiment of using the geometrical arrangement noted in **FIGS. 13A and 13B** is expressed in the ensuing descriptions of **FIGS. 13C, 13D**, **13**E, **13**F, **13**G and **13**H. The two competing architectures shown in **FIGS. 16, 16A**, **16**B **16**C and **FIG. 13A, 13B**, provide for advantages and disadvantages in mounting the operating interface equipment **500**, surgical medical equipment **502**, and the GCI apparatus **501**. Further **FIGS. 13A and 13B** illustrate an alternative arrangement of the coils attached to the C-arm, **391**, and table **389**. In this arrangement coils **901** through **906** are shown in a cluster configuration. This geometry diverts from the intuitive orthogonal structure of coils commonly used when generating vectors or vector gradients with the aide of electromagnetic coils. **FIG. 13B** further illustrates the six coils, **901** through **906**, configured in a flower-like structure, or a cluster. Three of the coils are mounted at the top of the C-arm **391**, and three at the bottom. The three coils forming the upper cluster are further shifted by 120 degrees relative to each other, as are the bottom three coils. In addition, the coils of the cluster at the top of the C-arm are also tilted downward somewhat, at an angle of 15 to 20 degrees, as are the coils of the cluster at the bottom of the C-arm tilted upward, as shown in **FIG. 13B**. The entire cluster at the top of the C-arm is rotated with respect to the bottom cluster by an angle of 60 degrees.

[0131] In **FIG. 13B**, the coils at the top of the C-arm **391** are marked as **901**, **902**, and **903**, counting clockwise, and the bottom coils are marked **904**, **905** and **906**, counting in a counter clockwise direction. Coils **901** and **903** work as a pair and are designated as the X-axis pair of coils, coils **902** and **904** work as another pair and are designated as the Y-axis pair of coils, and coils **905** and **906** are the third pair and are designated as the Z- axis pair of coils.

[0132] **FIGS. 13C, 13D**, **13**E, **13**F, **13**G and **13**H, show an alternative architecture of the GCI apparatus **501** whereby the polar configuration noted in **FIGS. 16, 16A**, **16**B, and **16**C, is altered to accommodate the cluster configuration of the electro-magnet circuit as shown in **FIGS. 13A and 13B**. **FIG. 13B** is a simplified block diagram of the electrical scheme of the various components of the system. The system comprises a power supply, **910**, a joystick, **900**, feeding three channels, X, Y, and Z, where the three signals taken together form a matrix V, **923**, shown in **FIG. 13D**, comprising elements Vj_x, Vj_y and Vj_z. This arrangement is further explained in **FIGS. 13D, 13E**, **13**F, **13**G and **13**H. **FIG. 13C**, the X-axis channel, comprises an Op-Amp **911**, a current amplifier **910**, and coil pair **901**, **903**. The Y-axis channel comprises an Op-Amp **913**, a current amplifier **912**, and coil pair **902**, **904**. The Z-axis channel comprises an Op-Amp **915**, a current amplifier **914**, and coil pair **905**, **906**. As shown, each pair of coils is connected in series and further connected to the output of power amplifiers, **910**, **912**, and **914**, for the X, Y and Z axes, respectively. The alternative architecture to **FIG. 1** shown in **FIG. 13C** receives its input signal command from the joystick, **900**. Upon command from the operator using the joystick **900** to move in one or more axes, the joystick **900** sends its signal to an array of operational amplifiers, **911**, **913**, and **915**, corresponding to the X, Y, and the Z axes respectively. Op-Amps **911**, **913**, and **915** translate the signal received from joystick **900** and perform an Inverse operation on the matrix of the three signals for the three axes. The Op-Amp array **932** multiplies the signal from joystick **900** represented as vector V, **923**, by another matrix M-inverse, shown in **FIG. 13F and 13G** as **927**, such that the output of the Op-Amp array **932** is M-inverse times V, where M is the characteristic matrix **925** of the cluster arrangement comprising the six coils **901** through **906**. The output from the Op-Amp array **932**, comprising Op-Amps **911**, **913**, and **915**, is obtained, and is fed to power amplifiers **910**, **912**, and **914**, driving the six coils **901** through **906** to obtain the result of generating a motion in the desired direction, hence providing the apparatus **501** with the ability to translate the desired motion of the operator or the clinician as to move the catheter tip **377** in a body lumen of a patient, **390**. This scheme as shown in **FIGS. 13D, 13E**, **13**F, and **13**G, is reduced further in **FIG. 13H** where the input signal V, **931**, from Joystick **900**, is fed to an Mchar-Inverse Op-Amp array, **932**. The resultant output from the array **932** is the matrix product Mchar-Inverse by the vector V. This signal is fed to current amplifiers **928**, their signal output represented by the vector B, **933**, is then fed as the respective current to the coils **901** through **906**, thereby producing the result of translating the hand-movement of the clinician into the appropriate signal, thus moving the catheter tip to the desired location.

[0133] In summary, the alternative arrangement shown above provides GCI **501** a method in which a competing architecture to **FIG. 1** is employed where a non-symmetrical arrangement of the coils is linearized through the use of the

scheme shown in **FIG. 13H**, thereby producing the desired results. This is shown in **FIG. 13E**.

[0134] **FIG. 14** shows an arrangement of the magnetic field sensors and temperature sensor pairs into sensor arrays **306**, **307**, **308**, **309**, **311**, **312**, **313**, **314**, **316**, **317**, **318**, and **319**. Each orthogonal axis is divided into two poles by positioning a second electromagnet coaxially with the first. For example, electromagnet **132***x* is coaxial with electromagnet **138***x*, electromagnet **132***y* is coaxial with electromagnet **138***y*, and electromagnet **132***z* is coaxial with electromagnet **138***z*. Since the rotational movements of the virtual tip **405** defined by θ**403** and EL **404**, as shown in **FIG. 6** occur within the X-Y plane and the X-Z plane respectively, electromagnet poles along the X-, Y- and Z-axes are sufficient to affect movement of the actual catheter tip **377** in exactly the same five axes as defined for the virtual tip **405** as previously described in connection with **FIG. 6**.

[0135] In one embodiment, each magnetic field sensor contained in the MFS arrays **307**, **308**, **312**, **313**, **317**, and **319**, is paired with a temperature sensor (TS) contained in temperature sensor arrays **306**, **309**, **311**, **314**, **316**, and **318**. These paired combinations are detailed in **FIG. 14** and in the table below. The magnetic field sensors-temperature sensor (MFS/T) pairs are arranged in quadrants on the pole face of the electromagnets **132***x*, **132***y*, **132***z*, **138***x*, **138***y*, and **138***z*.

[0136] As shown in **FIG. 13**, the MFS/TS pairs **350**, **351**, **352**, and **353** are arranged in quadrants on electromagnet **132***x* pole face. Magnetic field sensor and temperature sensor (TS) pairs **354**, **355**, **356**, and **357** are arranged in quadrants on electromagnet **138***x* pole face. Magnetic field sensor and temperature sensor (TS) pairs **358**, **359**, **360**, and **361** are arranged in quadrants on electromagnet **132***y* pole face. Magnetic field sensor and temperature sensor (TS) pairs **362**, **363**, **364**, and **365** are arranged in quadrants on electromagnet **138***y* pole face. Magnetic field sensor and temperature sensor (TS) pairs **366**, **367**, **368**, and **369** are arranged in quadrants on electromagnet **132***z* pole face. Magnetic field sensor and temperature sensor (TS) pairs **370**, **371**, **372**, and **373** are arranged in quadrants on electromagnet **138***z* pole face.

[0137] **FIG. 14** illustrates the pairing of the magnetic field sensors and temperature sensors as mounted in **FIG. 13**. The magnetic field sensors and temperature sensors are mounted as isothermal pairs, and each pair functions in conjunction with each other. The magnetic field sensors measure the position of the actual tip **377** during the measurement phase, as controlled by microcontrollers **102***x*, **102***y* and **102***z* of XCA **305**, YCA **310** and ZCA **315**, respectively, during which time the electromagnets **132**X, **132**Y, **132**Z, **138**X, **138**Y, and **138**Z are de-energized. This is done in order to be able to take accurate and sensitive measurements with the magnetic field sensor arrays **307**, **308**, **312**, **313**, **317**, and **318**, as they would otherwise be saturated with the flux from the electromagnets. The temperature sensor arrays **306**, **309**, **311**, **314**, **316**, and **319** monitor the ambient temperature to detect an increase that may be uncomfortable for the patient or potentially damaging to surrounding tissues, and provide correctional data for calculating position based on the magnetic field sensors. The isothermal pairs are as follows:

[0138] magnetic field sensor **113**X and temperature sensor (TS) **122***x* form pair **350**. Magnetic field sensor **114***x* and temperature sensor (TS) **123***x* form pair **351**. Magnetic field sensor **115***x* and temperature sensor (TS) **124***x* form pair **352**. Magnetic field sensor **116***x* and temperature sensor (TS) **125***x* form pair **353**.Magnetic field sensor **117***x* and temperature sensor (TS) **126**X form pair **354**. Magnetic field sensor **118***x* and temperature sensor (TS) **127***x* form pair **355**. Magnetic field sensor **119***x* and temperature sensor (TS) **128***x* form pair **356**. Magnetic field sensor **120***x* and temperature sensor (TS) **129***x* form pair **357**. Magnetic field sensor **113***y* and temperature sensor (TS) **122***y* form pair **358**. Magnetic field sensor **114***y* and temperature sensor (TS) **123***y* form pair **359**. Magnetic field sensor **115***y* and temperature sensor (TS) **124***y* form pair **360**. Magnetic field sensor **116***y* and temperature sensor (TS) **125***y* form pair **361**. Magnetic field sensor **117***y* and temperature sensor (TS) **126***y* form pair **362**. Magnetic field sensor **118***y* and temperature sensor (TS) **127***y* form pair **363**. Magnetic field sensor **119***y* and temperature sensor (TS) **128***y* form pair **364**. Magnetic field sensor **120***y* and temperature sensor (TS) **129***y* form pair **365**. Magnetic field sensor **113***z* and temperature sensor (TS) **122***z* form pair **366**. Magnetic field sensor **114***z* and temperature sensor (TS) **123***z* form pair **367**. Magnetic field sensor **115***z* and temperature sensor (TS) **124***z* form pair **368**. Magnetic field sensor **116***z* and temperature sensor (TS) **125***z* form pair **369**. Magnetic field sensor **117***z* and temperature sensor (TS) **126***z* form pair **370**. Magnetic field sensor **118***z* and temperature sensor (TS) **127***z* form pair **371**. Magnetic field sensor **119***z* and temperature sensor (TS) **128***z* form pair **372**. Magnetic field sensor **120***z* and temperature sensor (TS) **128***z* form pair **373**.

[0139] **FIGS. 15 and 15**A show an improved catheter assembly **375** and guidewire assembly **379** to be used with the GCI apparatus **501**. The catheter assembly **375** is a tubular tool that includes a catheter body **376** which extends into a flexible section **378** that possesses increased flexibility for allowing a more rigid responsive tip **377** to be accurately steered through a torturous path.

[0140] The magnetic catheter assembly **375** in combination with the GCI apparatus **501** reduces or eliminates the need for the plethora of shapes normally needed to perform diagnostic and therapeutic procedures. This is due to the fact that during a conventional catheterization procedure, the surgeon often encounters difficulty in guiding the conventional catheter to the desired position, since the process is manual and relies on manual dexterity to maneuver the catheter through a tortuous path of, for example, the cardiovascular system. Thus, a plethora of catheters in varying sizes and shapes are be made available to the surgeon in order to assist him/her in the task, since such tasks require different bends in different situations due to natural anatomical variations within and between patients.

[0141] By using the GCI apparatus **501**, only a single catheter would be needed for most, if not all patients, because the catheterization procedure is now achieved with the help of an electromechanical system that guides the magnetic catheter and guidewire assembly **375** and **379** to the desired position within the patient's body **390** as dictated by the surgeon's manipulation of the virtual tip **405**, without relying on the surgeon pushing the catheter, quasi-blindly,

into the patient's body. The magnetic catheter and guidewire assembly **375**, **379** (i.e., the magnetic tip can be attracted or repelled by the electromagnets **132**X, **132**Y, **132**Z) provides the flexibility needed to overcome tortuous paths, since the GCI apparatus **501** overcomes most, if not all of the physical limitations faced by the surgeon while attempting to manually advance the catheter tip **377** through the patient's body.

[**0142**] The guidewire assembly **379** is a tool with a guidewire body **380** and a flexible section **382**, which possesses increased flexibility for allowing a more rigid responsive tip **381** to be accurately steered around sharp bends so as to navigate a torturous path. The responsive tips **377** and **381** of both the catheter assembly **375** and the guidewire assembly **379**, respectively, include magnetic elements such as permanent magnets. The tips **377** and **381** include permanent magnets that respond to the external flux generated by the electromagnets **132**X, **132**Y, **132**Z and **138**X, **138**Y, **138**Z.

[**0143**] The responsive tip **377** of the catheter assembly **375** is tubular, and the responsive tip **381** of the guidewire assembly **379** is a solid cylinder. The responsive tip **377** of catheter assembly **375** is a dipole with longitudinal polar orientation created by the two ends of the magnetic element positioned longitudinally within it. The responsive tip **381** of guidewire assembly **379** is a dipole with longitudinal polar orientation created by the two ends of the magnetic element **377** positioned longitudinally within it. These longitudinal dipoles allow the manipulation of both responsive tips **377** and **381** with the GCI apparatus **501**, as the electromagnets **132**X, **132**Y, **132**Z, **138**X, **138**Y, and **138**Z will act on the tips **377** and **381** and "drag" them in unison to a desired position as dictated by the operator.

[**0144**] **FIG. 15B** illustrates a further improvement of catheter assembly **375** and guide-wire assembly **379** to be used with the GCI apparatus **501**, where the catheter assembly **950** is fitted with an additional two piezoelectric rings, **951** and **952**, located as shown. An ultrasonic detector in combination with apparatus **501** provides an additional detection modality of the catheter tip whereby an ultrasonic signal is emitted as to excite the two piezoelectric rings and provide a measure of rotation of the catheter tip relative to the north pole axis of the magnet **377**. With the aide of the computer **324**, the GCI apparatus **501** is capable of defining the angle of rotation of the tip **377** and in a more elaborate scheme known to those familiar with the art the piezoelectric rings **951**, **952**, can provide additional position information to define the position, orientation, and rotation of the catheter tip **377** relative to the stereotactic framing as described further in **FIGS. 17 and 17**A.

[**0145**] **FIG. 16** illustrates a bi-plane x-ray ring incorporating the apparatus of **FIG. 1B**. **FIGS. 16A, 16B** and **16**C are further elaboration of **FIG. 16**, and show in further detail, elements that could not be depicted by the isometric view of **FIG. 16**, or were omitted from **FIG. 16** for clarity. Additionally, **FIGS. 16A, 16B**, and **16**C are top, end, and side views respectively of the electromagnet and imaging assembly **391** and support assembly **385**.

[**0146**] **FIG. 16** further illustrates the overall relationship between the operating table **389**, the patient **390**, a T-axis encoder **394**, a trunnion **388**, a support assembly **385**, a polar support **391**, a G-axis encoder **393**, the x-ray source **383**, an image intensifier **384**, the electromagnets **132**X, **132**Y, **132**Z, an overall arrangement referred to as polar configuration **374**, electromagnets **138**X **138**Y, **138**Z, the power supply and control system **392**, the auxiliary equipment **322**, the host system **323**, the PC **324**, the virtual tip assembly **304**, the calibration fixture **321**, the mouse **327**, the keyboard **326**, the monitor **325**, as they are approximately oriented for visual aid. The function of the components that has not yet been described will be explained in the ensuing paragraphs, with reference to **FIG. 16, 16A**, **16**B, and **16**C.

[**0147**] The T-axis encoder **394** and the G-axis encoder **393** provide the system with gantry position information for use in calculating the desired coordinate rotation prior to energizing the electromagnet. The trunnion **388** acts as a truss for the support assembly **385**. Polar support **391** pivots on the G-axis of support assembly **385**. The polar assembly **391** supports the x-ray source **383** and x-ray image intensifier **384** that produce x-ray images to be overlaid with the actual catheter position image on the monitor **325** of the operator interface **500**. Polar support **391** provides a mounting surface for electromagnets **132**X, **132**Y, **132**Z, **138**X, **138**Y, and **138**Z in their appropriate coaxial arrangements as was already described in **FIG. 13**.

[**0148**] **101441** The trunnion **388** is centered on an axis, namely the T-axis **387** depicted in **FIG. 16A**. The T-axis encoder **394** is mechanically coupled to the trunnion **388** to encode positional data of the support assembly **385** in the T-axis. A gimbal-axis (G-axis) **386**, depicted in **FIG. 16A**, intersects with the T-axis **378** at the center point of the polar support **391**. This center point coincides exactly with the center point of the X-ray field of view. A G-axis encoder **393** is mechanically coupled to the support assembly **385** along the G-axis **386**. A detailed description of the functionality of the above components will follow in the ensuing description.

[**0149**] **FIG. 16** Illustrates the x-ray support assembly **385** and **391** as configured on an anteroposterior projection with 20 degrees of caudal angulation (AP caudal). **FIG. 17** illustrates a general connection of the GCI apparatus **501** to cineangiographic equipment **502**. The cineoangiographic equipment **502** is interfaced with the GCI apparatus **501** through operator interface equipment **500**. The cineoangiography image of an arterial tree is shown on video monitor **325**, with the x-ray image of catheter tip **377** position superimposed. The display of these images is synchronized by the GCI apparatus **501** via the communications controller **320**, and is realized on the monitor **325** of the operator interface **500**.

[**0150**] **FIG. 17A** illustrates forming a stereotactic frame in support of position definition of the catheter tip relative to the frame. This method utilizes fiduciary markers formed as an approximate cube.

[**0151**] The solution presented herein is a method of capturing the Fluoroscopic Image generated by the x-ray Apparatus and/or ultrasonic imaging technique to create Referential Markers for synchronizing the image of the catheter tip or guide wire, which is generated by the GCI apparatus and superimpose that image onto the fiduciary markers which are represented digitally and are linked dynamically as to create one image which moves in unison with the area of interest. For example, the beating heart and its cardio-output, the pulmonary expansion and contraction, or a spasm of the patient, can be dynamically captured and linked

together as to achieve unison motion between the catheter's tip and the body's organ in question.

[0152] **FIG. 17A** further illustrates the image capture technique of superimposing the fiduciary markers **700A1**, **700A2**, **700A3**, **700A4**, **700B1**, **700B2**, **700B3**, and **700B4** onto the fluoroscopic/ultrasonic image, generated as shown in image **17**. The scheme provided identifies the dynamic location of the catheter tip **377** with reference to the fluoroscopic/ultrasonic image. The referential frame formed by the fiduciary markers **700**Ax defines the catheter's tip position relative to the stereotactic frame. Furthermore, by employing a technique of geometric projection this method provides for a synchronized image-capture relative to catheter tip, **377** thereby affording the superimposition of the fluoroscopic/ultrasonic image relative to both the fiduciary markers and the catheter tip on a dynamic basis, hence, providing position definition with a frame of reference.

[0153] **FIG. 17B** illustrates the implantation of cardiac pacemaker **801** with electrodes as shown, placed in area relative to the S.A. Node **802**, A.V. Node **803**, and a bundle of His **804**. Further illustrated are the right and left bundle branches **805**. Pacemaker implantation is essential for the survival of patients with heart rhythm or electrical conduction disturbances. This procedure is performed by the implantation of a small electrode in the heart cavity wall (ventricle or atrium). The other end of the electrode is attached to an electronic device **801** which is implanted under the chest skin and which generates stimulation pulses to simulate the heart rhythm. Similar devices apply electrical shock when life threatening heart electrical disturbances are detected by the electrodes (Automatic Implantable Cardiac Defibrillator (AICD). These electrodes are placed through a vein by pushing and manipulating under fluoroscopy. Through the use of the apparatus proposed GCI **501** and guidewire **379** fitted with magnetic tip **381** is used to carry and place the electrodes of pacemaker **801** in its proper position by using the method and apparatus described in this patent. By employing the fiduciary markers **700A1**, **700A2**, **700A3**, **700A4**, **700B1**, **700B2**, **700B3**, and **700B4** the physician navigates the guidewire **379** through the heart lumen while having a continuous dynamic referential frame identifying the guidewire tip **381** and as shown in **17** and further illustrated by **FIG. 17A**. Many times, the manipulation to place the electrodes in a proper position is difficult and the results are sub-optimal due to anatomical variations. The use of the proposed apparatus **501** provides simplicity in performing such a complex operation while the physician is capable of moving, pushing, and placing the electrodes of pacemaker **801** in its precise anatomical position without compromise due to the inability of navigating, guiding, controlling, and imaging the movement of the guidewire and the pacemaker electrodes accurately.

[0154] Having described the constituent components of the GCI apparatus **501**, its general and mathematical operations for controlling the position of the actual catheter tip **377** in relation to adjustments made to the virtual tip **405** and calculations to determine the new location of the actual catheter tip **377** will now be explained with reference to **FIGS. 18 through 23**.

[0155] Upon application of power, the built-in test routines residing in Supervisory Unit (SU) **301**, System Controller (SC) **302**, X-axis controller and amplifier (XCA) **305**, Y-axis controller and amplifier (YCA) **310**, Z-axis controller and amplifier (ZCA) **315**, Communication Controller (CC) **320**, Computer **324**, and Virtual Tip/Calibration Fixture Controller (VT/CFC) **303**, perform a series of self diagnostic tests. In addition, certain tests are performed on a continuous basis in the background. Exemplary background tests include DC power supply voltage and current monitoring, AC voltage and current monitoring and communication tests. These background tests are interleaved between normal functions in a manner that is transparent to the user.

[0156] The results of the test routines are reported to System Controller (SC) **302**. System Controller (SC) **302** compares these results to expected values stored in Non Volatile Memory (NVM) **39** (**FIG. 3**). Following a test failure or the detection of any anomalous behavior, System Controller (SC) **302** determines the severity of the situation. If an uncorrectable condition exists, System Controller (SC) **302** initiates a graceful power down. If, on the other hand, corrective action can be taken to alleviate or eliminate the problem, System Controller (SC) **302** instructs Computer **324** to sound an alarm, and instructs the monitor **325** to display an error prompt. Any detected failures are also stored as error codes in Non Volatile Memory (NVM) **39** for later review and troubleshooting.

[0157] In one embodiment, the Virtual Tip **405** and the Calibration Fixture (CF) **321** (**FIGS. 5, 6, 11**, and **12**) have **8** inches of travel in the X, Y, and Z axes. This corresponds to the 8"×8"×8" control area of the polar configuration **374** (**FIG. 13**). The Virtual Tip **405** and the Calibration Fixture **321** also have 360° of rotation in the θ and elevation axes.

[0158] Stepper motors **55**C, **57**C **59**C, **61**C, and **63**C with the coupled encoders **64**C, **66**C, **68**C, **70**C and **72**C revolve once during an **8**-inch excursion in the X, Y, or Z axes. Stepper motors **55**C, **57**C **59**C, **61**C, and **63**C have, for example, a resolution of **400** half steps per revolution, which equates to a positioning resolution of 0.022". Additionally, the encoders may have a resolution of 512 bits per revolution, which equates to a measurement resolution of 0.015625". In the θ and EL axes, the stepper motor resolution may be 0.9° and the encoder resolution may be 0.703125°.

[0159] During calibration, Calibration Fixture (CF) **321** is placed within the polar configuration **374** and connected to Virtual Tip/Calibration Fixture Controller (VT/CFC) **303**. Virtual Tip/Calibration Fixture Controller (VT/CFC) **303** then moves Calibration Fixture (CF) **321** by sending codes to drive stepper motors **55***c*, **57***c*, **59***c*, **61***c*, and **63***c*. Encoders **64***c*, **66***c*, **68***c*, **70***c*, and **72***c* are then read by Calibration Fixture (CF) **321** to determine the present position and orientation of magnet **411**. The position data from the encoders is compared to the position data derived from magnetic field sensor arrays **307**, **308**, **312**, **313**, **317**, and **318** (**FIGS. 1, 7, 8**, and **9**). The magnetic field sensor arrays **307**, **308**, **312**, **313**, **317** and **318** responses are thus characterized for the full range of the magnet **411** positions and orientations, and hence for the magnetic catheter tip **377** as well.

[0160] During normal operation, Virtual Tip **405** is connected to Virtual Tip/Calibration Fixture Controller (VT/CFC) **303**. As tip **405** is manipulated, Virtual Tip/Calibration Fixture Controller (VT/CFC) **303** reads encoders **64**, **66**, **68**, **70**, and **72**. The position data obtained from the Virtual Tip

405 is used by the System Controller **302** to determine the desired position (DP) of the actual tip (AT) and to control its motion as defined in the description of **FIG. 23**.

[0161] The electromagnetic field generated by electromagnets **132***x*, **132***y*, **132***z*, **138***x*, **138***y*, and **138***z* of **FIG. 13** will produce a resultant force on the actual catheter assembly tip **377** and guidewire assembly tip **381** (**FIGS. 15 and 15**A). This resultant force can be represented by force vector B **600** with a given magnitude and direction. This resultant force vector B together with its constituent vectors are illustrated in **FIG. 18**. Vector B is the resultant vector of the force vectors emanating from the six electromagnets **132***x*, **132***y*, **132***z*, **138***x*, **138***y*, and **138***z* together, upon a move command from the XCA **305**, YCA **310** and ZCA **315**. Vector Bx **601** is the projection of Vector B **600** on the X-axis, Vector By **602** is the projection of Vector B **600** on the Y-axis, and Vector Bz **603** is the projection of vector B **600** on the Z-axis. The angles α**604**, β**605**, and δ**606** are the corresponding angles between the vectors B **600** and Bx **601**, vectors B **600** and By **602**, and vectors B **600** and Bz **603**, respectively.

[0162] As stated earlier, and still referring to **FIG. 18**, the magnitude of the force vector B **600** resulting from the electromagnetic field is

$$B=\sqrt{Bx^2+By^2+Bz^2}$$

and its direction is given by the three angles below:

$$\alpha=\cos^{-1} Bx,\ \beta=\cos^{-1} By,\ \delta a=\cos^{-1} Bz$$

[0163] The force vector B is produced through commands sent from system controller **102** based on: 1) inputs from sensor arrays **307**, **308**, **312**, **313**, **317**, and **318** processed by XCA **301**, YCA **310** and ZCA **315** on the location of the actual catheter tip **377** within the patient's body **390**, and 2) inputs from VT/CFC **303** on the desired position of the actual catheter tip **377** as indicated by virtual tip **405** position. A code stored in ROM **40** of system controller **302** (**FIG. 3**) is processed by microcontroller **33** to generate the constituent vector components Bx **601**, By **602**, and Bz **603** of B **600**. The magnitude of each of these constituent vectors will be translated to the appropriate XCA **305**, YCA **310**, and ZCA **315** to cause changes in modulator outputs, which, in turn, change the electromagnetic field produced by electromagnets **132***x* and **138***x*, **132***y* and **138***y* , and **132***z* and **138***z*. The constituent vectors Bx, By and Bz will then be physically realized as electromagnetic fluxes along the X-, Y- and Z-axes and thereby produce a resultant force B **600** on the actual catheter tip **377** to effectively drag it to the desired position.

[0164] The new position of the actual catheter tip **377** is then determined in order to verify that is indeed in the desired position or if further adjustments are necessary or if an obstacle has been encountered. The methods by which system controller **302** determines the new actual catheter tip **377** position will be explained mathematically with reference to **FIGS. 18A through 22**.

[0165] The following notations were assigned to the variables associated with **FIGS. 18A, 19**, and **19**A and will be used in the ensuing discussion:

[0166] a_N: The most distal end of the magnetic element of the actual catheter tip assembly as indicated by its North dipole (see e.g., **FIG. 18A**).

[0167] a_S: The proximal end of the magnetic element of the actual catheter tip assembly **377** as indicated by its south dipole (see e.g., **FIG. 18A**).

[0168] a_D: Length of the actual catheter tip magnet **377** equal to the distance between the points a_N and a_S (refer to **FIG. 18A**).

[0169] X_D: Distance between opposite coaxial poles along the x-axis, that is the distance between the polar faces of electromagnets **132***x* and **138***x* (refer to numeral reference **616** in **FIG. 19**).

[0170] $-x_1$, $-x_2$, $-x_3$, $-x_4$: MFS and TS pairs **354**, **355**, **356**, **357**, respectively. (see **FIGS. 13 and 19**A).

[0171] d: The Distance between each consecutive MFS/TS pair, that is the distance between MFS/TS pair **354** and MFS/TS **355**, MFS/TS **355** and MFS/TS pair **356**, and so forth (refer to **FIG. 19A**).

[0172] x_1, x_2, x_3, x_4: MFS and TS Pairs **350**, **351**, **352**, **353**, respectively (refer to **FIGS. 13 and 19**A).

[0173] ROT: The angle of rotation θ in the X-Y plane (refer to numeral reference **625** in **FIG. 21**).

[0174] ELEV: The angle of EL in the X-Z plane (refer to numeral reference **626** in **FIG. 22**).

[0175] The electromagnetic field induced by electromagnets **132***x*, **132***y*, **132***z*, **138***x*, **138***y*, and **138***z* of **FIG. 13** produces a resultant force on the actual catheter assembly tip **377** and guidewire assembly tip **381** (**FIGS. 15 and 15**A). This resultant force can be characterized as a force vector with a given magnitude and direction, and is illustrated in **FIG. 18** along with its constituent vectors. Vector B **600** is the resultant vector of the force vectors emanating from the six electromagnets **132***x*, **132***y*, **132***z*, **138***x*, **138***y*, and **138***z* together, upon a move command from the XCA **305**, YCA **310** and ZCA **315**. Vector Bx **601** is the projection of Vector B on the X-axis, Vector By **602** is the projection of Vector B on the Y-axis, and Vector Bz **603** is the projection of vector B on the Z-axis. The angles α**604**, β**605**, and δ**606**, are the corresponding angles between the vectors B and Bx, vectors B and By, and vectors B and Bz, respectively.

[0176] **FIG. 18A** illustrates one embodiment of a magnetic catheter tip **607**. This magnetic tip **607** corresponds to the combination of the responsive tip **377** of the catheter assembly **375** and the responsive tip **381** of the guidewire assembly **379** (**FIGS. 15 and 15**A). The magnetic tip **607** is represented by its two poles a_N, **607**A and as **607**B in connection with a Virtual Origin **608**. The Virtual Origin **608** is defined by the center of travel of the Virtual Tip (VT) **405** in the X-, Y-, and Z-axes **400**, **401** and **402** (**FIG. 6**). The Virtual Origin **608** also coincides with the center of the travel of the calibration magnet **411** in the X-, Y-, and Z-axes **406**, **407** and **408**, during calibration (**FIG. 12**). The assumption is that the Virtual Origin **608** is in the center of the x-ray field of view, as well as the center of the sagnetic field sensors (MFS) sensing volume and the center of the electromagnet (EM) control volume. The Virtual Origin **608** also coincides with the center of travel of the Calibration Fixture (CF) in the X, Y, and Z axes, during calibration.

[0177] **FIG. 18B** illustrates the resultant position vector An **609** that defines the position of the catheter tip **607** as detected by the magnetic field sensor arrays **307**, **308**, **312**,

313, 317, and 318 and computed by microcontrollers 102*x*, 102*y* and 102*z* of XCA 305, YCA 310 and ZCA 315. The constituent vectors Xn, Yn, and Zn are the projections of the position vector An on the X-axis, Y-axis and Z-axis, respectively. The angles α609A, β609B, and γ609C, are the projected angles of the vector A_N on the X, Y, and Z axes, respectively. This orthogonal representation corresponds to the polar configuration 374 of FIG. 16.

[0178] FIG. 18C illustrates the angular representation of the resultant position vector of catheter tip 607 in 3 dimensions. The position vector An 609 shown in FIG. 18B define the location of a_N 607A which is one of the two poles of the magnetic tip 607, is projected on the X-Y plane. This projected vector θ_{XY} 615 can be defined by an angle θ_X 613 with relation to the X-axis, and an angle θ_Y 614 with relation to the Y-axis. The projection on the X-Z plane and Y-Z planes are not shown thus the angular relationship of location a_N with the Z-axis 612 is not shown for purposes of simplicity. These angular relationships of the position vector An defining the location a_N, as exemplified by θ_X 613 and θ_Y 614 are used in the calculations defining the positions of the actual catheter tip 377 as sensed by the magnetic field sensors sensor arrays 307, 308, 312, 313, 317, and 318. An explanation of these calculations will be provided later.

[0179] FIG. 19 illustrates the distance XD 616 between two opposite faces or poles of the electromagnets. The distance XD is used in calculations made during the operation of the system which will be explained in the following discussion.

[0180] FIG. 19A illustrates a distance d 617 between two adjacent X-axis magnetic field sensors. Magnetic field sensors –X1 and –X2618 and 619 respectively. Also shown in FIG. 19A are two additional magnetic field sensors, –X3 and –X4. The magnetic field sensors $-X_1$, $-X_2$, $-X_3$, $-X_4$ are the MFS and the temperature sensor (TS) pairs, corresponding to 354, 355, 356, and 357, respectively, and X_1, X_2, X_3, and X_4 are the MFS and TS pairs corresponding to 350, 351, 352, and 353, respectively.

[0181] FIG. 20 illustrates the geometrical process by which the system deduces the true location of the magnetic tip 607 from the data it receives from the magnetic field sensors X1, X2, X3, and X4. The resultant vector A 620 is further manipulated by the system to generate position co-ordinates 621 and 622 of the tip 607, thereby identifying the location of the actual tip 377. This geometrical process will become apparent in the following discussion.

[0182] FIG. 20A further illustrates components of the position vectors 622 and 621 obtained by additional mathematical manipulation and calculations done on the signals that are received from the magnetic field sensors X1, X2, X3, and X4. The location of the actual tip 377 is defined by the position co-ordinates shown as 621 and 622. Position 623 is the measured position of the actual catheter tip 377 as determined by the magnetic field sensors X1, X2, X3, and X4, and position 624 is its calculated position as determined by the system control 302. Under ideal conditions, the positions 623 and 624 are equal to each other.

[0183] FIG. 21 illustrates the rotation 625 of the tip 607 around the Z-axis (θ). The rotation is actually an arc motion occurring or oscillating in the X-Y plane. FIG. 22 illustrates the translation 626 of the tip 607 in the Z-axis.

[0184] The system controller (SC) 302 deduces the location of the actual catheter tip 377 from the signals generated by the magnetic field sensor arrays 307, 308, 312, 313, 317, and 318. This is done as described in the following paragraphs.

[0185] The following notations are assigned to the variables associated with FIGS. 18A, 19, and 19A:

[0186] a_N: North direction.

[0187] a_S: South direction.

[0188] a_D: Length of Tip Magnet.

[0189] X_D: Distance between opposite Poles 132*x* to 138*x*.

[0190] $-x_1$, $-x_2$, $-x_3$, $-x_4$: MFS and TS pairs 354, 355, 356, 357, respectively.

[0191] d: The Distance between magnetic field sensors and temperature sensor pairs 354 and 355, etc.

[0192] x_1, x_2, x_3, x_4: MFS and TS Pairs 350, 351, 352, 353, respectively.

[0193] ROT: θ AXIS

[0194] ELEV: EL AXIS

[0195] With reference to FIGS. 18*a*, 18*b*, and 18*c*, the positions of the actual tips 377 are defined by the orthogonal vectors a_N, A_N and as, A_S. These orthogonal vectors are the resultant vectors of their constituent x, y and z components:

$$A_N=(Xn, Yn, Zn),$$

[0196] where Xn, Yn, and Zn are the projections of orthogonal vector A_N on the X, Y, and Z axes (refer to FIG. 18B), and,

$$A_S=(Xs, Ys, Zs)$$

where Xs, Ys and Zs are the projections of orthogonal vector A_S on the X-, Y-, and Z-axes, respectively.

[0197] The directions of orthogonal vectors A_N and A_S from the origin are defined by the following angles (refer to FIG. 18B):

[0198] α is the angle to the X axis;

[0199] β is the angle to the Y axis; and

[0200] γ is the angle to the Z axis.

[0201] Similarly, the directions of the vector B are shown in FIG. 18 and defined by the three angles: α, β, and γ.

[0202] The distance of the vector A_N from the virtual origin to the point a_N 607A (FIG. 18C) is calculated by the following equation:

$$a_N=\sqrt{Xn^2+Yn^2+Zn^2},$$

[0203] and the angles defining the direction of vector AN are calculated by the following equations:

$$\alpha = \cos^{-1}\left[\frac{Xn}{An}\right] = \cos^{-1}\left[\frac{Xn}{\sqrt{Xn^2 + Yn^2 + Zn^2}}\right]$$

-continued

$$\beta = \cos^{-1}\left[\frac{Yn}{An}\right] = \cos^{-1}\left[\frac{Yn}{\sqrt{Xn^2 + Yn^2 + Zn^2}}\right]$$

$$\Upsilon = \cos^{-1}\left[\frac{Zn}{An}\right] = \cos^{-1}\left[\frac{Zn}{\sqrt{Xn^2 + Yn^2 + Zn^2}}\right]$$

[0204] With three orthogonal planes shown in **FIG. 18C** on which the positional vector A_N is projected, producing the constituent vectors in each plane and their respective angles. The vectors in these three planes, X-Y, X-Z, and Y-Z are as follows:

[0205] In the X-Y plane the angles of the projected vector θxy with respect to the X-axis and the Y-axis (refer to **FIG. 18C**) are expressed as follows:

$$\theta x = \arctan\left(\frac{Xn}{Yn}\right), \text{ and}$$

$$\theta y = \arctan\left(\frac{Yn}{Xn}\right),$$

where the magnitude of the projected vector Oxy in the X-Y plane is:

$$Axy = \sqrt{Xn^2 + Yn^2}.$$

[0206] Similarly, the angles of the projected vector θxy with respect to the X-axis and the Z-axis are expressed as follows:

$$\theta x = \arctan\left(\frac{Xn}{Zn}\right), \text{ and}$$

$$\theta z = \arctan\left(\frac{Zn}{Xn}\right),$$

[0207] and the magnitude of the projected vector θxz in the X-Z plane is:

$$Axz = \sqrt{Xn^2 + Zn^2}.$$

[0208] Similarly, the angles of the projected vector Oxy with respect to the Y-axis and the Z-axis are expressed as follows:

$$\theta y = \arctan\left(\frac{Yn}{Zn}\right), \text{ and}$$

$$\theta z = \arctan\left(\frac{Zn}{Yn}\right),$$

and the magnitude of the projected vector θyz in the Y-Z plane is:

$$Ayz = \sqrt{Yn^2 + Zn^2}.$$

[0209] It should be noted that the mathematical solution of the vector $A_S=(X_S,Y_S,Z_S)$ follows the mathematical solution of the vector $A_N=(X_N,Y_N,Z_N)$.

[0210] As shown in **FIG. 18A**, if the distance D **607** between a_N and a_S is known, then:

$$D = \sqrt{(Xn-Xs)^2+(Yn-Ys)^2+(Yn-Ys)^2}$$

[0211] To illustrate how system controller **302** determines the position of the actual catheter tip, the calculations used by microprocessor **102***x* of XCA **305** with respect to the X-axis and the virtual origin **608** will now be described, with the understanding that microprocessors **102***y* of YCA **310** and **102***z* of ZCA **315** will perform similar calculations, with each generating positional data concerning the Y- and Z-axes, respectively.

[0212] The transfer functions of the co-planar magnetic field sensors (x_1, x_2, x_3, x_4) are known from the calibration routine (fx_1, fx_2, fx_3, fx_4) as shown in **FIG. 20**, and they are as follows:

$$-X_1 = -(V_{-x_1}(f_{-x_1})) + X_1 = (V_{-x_1}(f_{-x_1}))$$

$$-X_2 = -(V_{-x_2}(f_{-x_2})) + X_2 = (V_{-x_2}(f_{-x_2}))$$

$$-X_3 = -(V_{-x_3}(f_{-x_3})) + X_3 = (V_{-x_3}(f_{-x_3}))$$

$$-X_4 = -(V_{-x_4}(f_{-x_4})) + X_4 = (V_{-x_4}(f_{-x_4}))$$

[0213] Each MFS/TS pair **354**, **355**, **356**, **357** mounted on the polar face of electromagnet **138***x* will provide location data to microprocessor **102***x* of XCA **305**. The measured distance to a_N **607**A, for example, from MFS/TS pair **354** will be referred to as $(-x_1)$; the distance measured by MFS/TS pair **355** will be referred to as $(-x_2)$; the distance measured by MFS/TS pair **356** will be referred to as $(-x_3)$; the distance measured by MFS/TS pair **357** will be referred to as $(-x_4)$.

[0214] Likewise, each MFS/TS pair **350**, **351**, **352**, **353** mounted on the polar face of electromagnet **132***x* will provide location data to microprocessor **102***x* of XCA **305**. The measured distance of a_N **607**A from MFS/TS pair **350** will be referred to as $(+x_1)$; the distance measured by MFS/TS pair **351** will be referred to as $(+x_2)$; the distance measured by MFS/TS pair **352** will be referred to as $(+x_3)$; the distance measured by MFS/TS pair **353** will be referred to as $(+x_4)$.

[0215] Since the MFS/TS pairs are arranged in a quadrant around the central X-axis, the individually measured distances of each MFS/TS temperature sensor are combined mathematically to determine the distance along the x-axis itself. This is done by determining a positional vectors Ax_1x_2, Ax_2x_3, Ax_3x_4, and Ax_1x_4. With reference to **FIG. 20**, the magnitude of positional vector Ax_2x_3, for example, is given by the following equation:

$$Ax_2x_3 = \frac{x_2x_3\,\mathrm{Sin}(\theta x_2x_3)}{d}.$$

[0216] The magnitude of the positional vectors Ax_1x_2, Ax_3x_4, and Ax_1x_4 are calculated in a similar way.

[0217] In addition, as shown in **FIG. 20A**, the angle θx_1x_2, which, for example, is the sum of the angles between Ax_1x_2 and x_1 and Ax_1x_2 and x_2, gives the direction of Ax_1x_2 as follows:

$$\theta x_1 x_2 = \cos^{-1}\left(\frac{d^2 - x_1^2 - x_2^2}{2x_1 x_2}\right)$$

[0218] The numerical solution, is graphically shown in **FIG. 20A** is achieved by using the canonical formalism described below. It should be noted that this numerical solution is performed in for example in a background mode by microprocessor **102***x* of XCA **305** and similarly for y axis and z axis.

$$hx_1 x_2 = \frac{x_1 x_2 \sin(\theta x_1 x_2)}{d}$$

$$Bx_1 x_2 = \sqrt{x_1^2 - hx_1 x_2^2}$$

$$\theta x_2 x_3 = \cos^{-1}\left(\frac{d^2 - x_2^2 - x_3^2}{2x_2 x_3}\right)$$

$$Ax_2 x_3 = \frac{x_2 x_3 \mathrm{Sin}(\theta x_2 x_3)}{d}$$

$$Bx_2 x_3 = \sqrt{x_2^2 - hx_2 x_3}$$

$$P_B x_1 = \sqrt{{}_B x_1 x_2^2 + {}_B x_2 x_3^2}$$

$$Ax_1 x_2 = \sqrt{x_1^2 - P_B x_1^2}$$

The angles of $\theta x_2 x_3$, ${}_{\theta x 3} x_4$, and $\theta x_1 x_4$ are calculated in a similar way.

[0219] Based on the distances Ax_1x_2, Ax_2x_3, Ax_3x_4, and Ax_1x_4 from the polar face **138***x* to the point a_N, an average distance $(-x_n)$ is determined as follows:

$$-x = \left(\frac{(-x_1 - x_2 A) + (-x_2 - x_3 A) + (-x_3 - x_4 A) + (-x_4 - x_1 A)}{4}\right).$$

[0220] Likewise, the distance from the polar face **132***x* to the point a_N is determined as follows:

$$+x = \left(\frac{x_1 x_2 A + x_2 x_3 A + x_3 x_4 A + x_4 x_1 A}{4}\right).$$

[0221] In one embodiment, when weighting the averages by using more accurate sensors yields better results (as determined during calibration), then a weighted average is used.

[0222] The distance of a_N from the virtual origin **608** is determined since the virtual origin is the common point of reference between the VT assembly **304** and the calibration fixture (CF) **321**. These distances are given for the three axes by the following sets of equations, where X_D **616** is the distance between two coaxial electromagnets **132***x* and **138***x* (refer to **FIG. 19**), Y_D is the distance between two coaxial electromagnets **132***y* and **138***y*, and Z_D is the distance between two coaxial electromagnets **132***z* and **138***z*:

$$\frac{X_D}{2} + (-X)$$

$$\frac{X_D}{2} + (+X)$$

where:

$$\left(\frac{X_D}{2} + (-X)\right) + \left(\frac{X_D}{2} + (-X)\right) = X_D$$

[0223] The same calculations apply to the y and z axes positions and with the three axes positions known will yield an absolute position. Therefore, relative to the virtual origin:

$$Xn = \begin{cases} \frac{X_D}{2} - (-Xn) \\ (+Xn) - \frac{X_D}{2} \end{cases} \quad Xs = \begin{cases} \frac{X_D}{2} - (-Xs) \\ (+Xs) - \frac{X_D}{2} \end{cases}$$

$$Yn = \begin{cases} \frac{Y_D}{2} - (-Yn) \\ (+Yn) - \frac{Y_D}{2} \end{cases} \quad Ys = \begin{cases} \frac{Y_D}{2} - (-Ys) \\ (+Ys) - \frac{Y_D}{2} \end{cases}$$

$$Zn = \begin{cases} \frac{Z_D}{2} - (-Zn) \\ (+Zn) - \frac{Z_D}{2} \end{cases} \quad Xs = \begin{cases} \frac{Z_D}{2} - (-Zs) \\ (+Zs) - \frac{Z_D}{2} \end{cases}$$

[0224] The system controller **302** deduces the following from the calculations to determine the center point of the magnetic element of the actual catheter tip:

$$Xc = \frac{Xn - Xs}{2}$$

$$Yc = \frac{Yn - Ys}{2}$$

$$Zc = \frac{Zn - Zs}{2}$$

[0225] Thus the GCI apparatus **501** derives the rotation in the X-Y plane as follows:

$$RotC = \tan^{-1}\left(\frac{Yn - Ys}{Xn - Xs}\right)$$

and the elevation in the X-Z plane as follows:

$$elevC = \tan^{-1}\left(\frac{Zn - Zs}{Xn - Xs}\right)$$

[0226] Using these results, system controller **302** can compare the actual catheter tip **377** location to the desired tip location. **FIG. 23** illustrates a logical computational flow

taken by the system controller (SC) **302** in determining the position of the actual tip **377**, using the following mathematical relations:

[**0227**] 1. System Controller (SC) **302** inhibits X-axis controller and amplifier (XCA) **305**, Y-axis controller and amplifier (YCA) **310**, and Z-axis controller and amplifier (ZCA) **315** modulator outputs.

[**0228**] 2. X-axis controller and amplifier (XCA) **305**, Y-axis controller and amplifier (YCA) **310**, and Z-axis controller and amplifier (ZCA) **315** read the magnetic field sensor array **307**, **308**, **312**, **313**, **317**, and **318** outputs.

[**0229**] 3. X-axis controller and amplifier (XCA) **305**, Y-axis controller and amplifier (YCA) **310**, and Z-axis controller and amplifier (ZCA) **315** read temperature sensor (TS) array **306**, **309**, **311**, **314**, **316**, and **319** outputs.

[**0230**] 4. X-axis controller and amplifier (XCA) **305**, Y-axis controller and amplifier (YCA) **310**, and Z-axis controller and amplifier (ZCA) **315** apply digital temperature compensation to the outputs of the magnetic field sensor arrays **307**, **308**, **312**, **313**, **317**, and **318** by referring to correction data (typically stored in Non Volatile Memory **105***x*, **105***y*, and **105***z*).

[**0231**] 5. System Controller (SC) **302** inputs the corrected magnetic field sensor data from X-axis controller and amplifier (XCA) **305**, Y-axis controller and amplifier (YCA) **310**, and Z-axis controller and amplifier (ZCA) **315**, and interpolates a 5-axis data set from the three orthogonal components (Bx, By, Bz) of the magnetic field produced by the actual tip. The tip position is calculated using the following two relations:

[**0232**] a) The magnitude of the force vector B **600** is given by the equation:

$$B=\sqrt{Bx^2+By^2+Bz^2};\ and$$

[**0233**] b) the direction of the force vector B is given by the three resultant angles, as:

$$\alpha=\frac{\cos^{-1}Bx}{B},\ \beta=\frac{\cos^{-1}By}{B},\ \delta=\frac{\cos^{-1}Bz}{B}$$

[**0234**] 6. System Controller (SC) **302** inputs the cardio position (CP) from the auxiliary equipment (x-ray, ultrasound, etc) **322** via Communication Controller (CC) **320**. The cardio position (CP) data set is dynamic due to the beating of the heart.

[**0235**] 7. System Controller (SC) **302** calculates the actual position (AP) by combining the cardio position (CP) and the HP data sets.

[**0236**] 8. System Controller (SC) **302** inputs Virtual Tip **405** position data from Virtual Tip/Calibration Fixture Controller (VT/CFC) **303**.

[**0237**] 9. System Controller (SC) **302** calculates the DP by combining the cardio position (CP) data set with that of the Virtual Tip (VT).

[**0238**] 10. System Controller (SC) **302** then determines the position error (PE) by comparing the DP with the AP.

[**0239**] 11. If the position error PE is less than an error threshold value, then the System Controller (SC) **302** enables X-axis controller and amplifier (XCA) **305**, Y-axis controller and amplifier (YCA) **310** and Z-axis controller and amplifier (ZCA) **315** with the continues to use the same modulation and polarity.

[**0240**] 12. If the position error PE is greater than the error threshold value, then the System Controller SC **302** alters the duty cycle and/or polarity of the modulation inputs to XCA **305**, YCA **310**, and ZCA **315** accordingly.

[**0241**] The System Controller (SC) **302** controls the stepper motors **55**, **57**, **59**, **61**, and **63** via the Virtual Tip/Calibration Fixture Controller (VT/CFC) **303** to produce tactile feedback if the position error (PE) exceeds a predetermined amount in a predetermined time in any axis or axes, thereby notifying the operator of an obstruction encountered by the catheter tip. That is, it is assumed that if the PE is not eliminated by the normal operation of the GCI apparatus **501** within an expected amount of time or cycles of steps 1 through 12 above, then an obstacle is likely to have been encountered by the actual catheter tip. This is perceived by the operator through tactile feedback generated by resistance produced the stepper motors **55**, **57**, **59**, **61**, and **63** acting on the virtual tip **405**.

[**0242**] The operation of the virtual tip **405** is relatively simple and intuitive to the user or surgeon. The surgeon simply pushes, pulls, or rotates the virtual tip **405** in the desired direction to cause a similar movement of the catheter tip **377** within the patient's body. If an obstruction is encountered by the catheter tip **377**, the virtual tip **405** responds with tactile feedback in the form of resistance to movement in the appropriate axis or axes. Thus, the surgeon can "feel" the actual tip as it is advanced. When tip **405** is released, the catheter tip **377** is forcefully held in its current position. System Controller (SC) **302** correlates the AT position with CP data obtained from auxiliary equipment **322** and via CC **320** it communicates with PC **324** in order to present monitor **325** with the combined tip and x-ray/ultrasonic imagery. The display of the three-dimensional AT position is continuously updated on a real-time basis with HP data. Relatively fewer frames of x-ray imagery are used to overlay the display with CP data. This correlation of AT and CP data is possible because the x-ray and the MFS arrays have a common reference point (i.e., both are stationary relative to the beating heart).The present technique significantly reduces x-ray exposure to the patient and staff while providing a superior method of observing the heart and catheter tip **377**.

[**0243**] Accordingly, it can be seen that the new catheter guidance and control apparatus and method provide an arrangement which is: relatively easy to use effectively; requires minimal training to master; rapidly advances and accurately positions the catheter tip; requires fewer types of catheters; forcefully fixates the catheter tip in the desired position; steers a guidewire through a torturous path; forcefully advances a guidewire or balloon through plaque; displays the catheter tip position in three dimensions; significantly reduces the amount of contrast material the patient

is exposed to; significantly reduces the amount of X-radiation the patient and medical staff are exposed to; is intuitive to use; and produces tactile feedback to indicate when the catheter tip encounters an obstruction.

[0244] Although the preceding description contains much specificity, this should not be construed as limiting the scope of the invention, but as merely providing illustrations of embodiments thereof. Many other variations are possible within the scope of the present invention. For example, the modulation of the electromagnets can be controlled in such a way as to cause a vibratory or pulsating motion of the tip to aid in crossing plaque; the responsive tip(s) can be electromagnetic rather than permanent magnets; the magnetic field external to the body can be generated by a permanent magnet or magnets; the control of the external magnetic field can be accomplished by manually administering the field generating devices; AC induction with its associated magnetic effects can be utilized by causing a coil or coils wound around the tip to respond to an impressed time variant field; materials with Curie temperatures within a few degrees of body temperature can be used as magnetic flux switches for selective tip control by irrigating them with fluids having appropriate temperatures; electrostatic phenomena can enhance magnetic effects; artificial intelligence can replace the operator control for producing command inputs; an expert system can replace or augment operator inputs; the apparatus can be used to incubate various body cavities and organs other than the heart; the apparatus can be used for human and animal procedures such as egg harvesting and embryo implantation; the responsive tip can be attached to a coherent fiber optic bundle to provide viewing of internal structures with unprecedented maneuverability; internal radioisotope therapy can be precisely performed by delivering a palletized source directly to a tumor using a guided catheter; internal tissue samples can be obtained without major surgery; a fiber optic light guide equipped with a responsive tip can be accurately positioned to deliver laser light to a specific internal location without major surgery; previously difficult liposuction and other subcutaneous surgical procedures can be performed accurately, and so forth. Thus, the scope of the invention is limited only by the claims.

What is claimed is:

1. A method for controlling movement of a tool having a distal end to be inserted in a body, comprising;

applying a force to said distal end by generating an external magnetic field;

regulating said force to move said distal end in a desired direction; and

locating said distal end by measuring a magnetic field of said distal end.

2. The method of claim 1, further comprising changing a visual representation of said distal end in substantially real time as said distal end moves through the body.

3. The method of claim 1, further comprising controlling one or more electromagnets to produce said external magnetic field.

4. The method of claim 1, further comprising measuring a temperature of one or more magnetic field sensors that measure said magnetic field of said distal end.

5. The method of claim 1, further comprising determining a current position of said distal end in comparison to a desired location.

6. The method of claim 5, wherein determining said current position of said tool distal end comprises:

inhibiting modulator outputs of a system controller;

inputting a dynamic cardio position via a communication controller; and

calculating said current position as a function of said cardio position.

7. The method of claim 1, further comprising computing a position error of said distal end.

8. The method of claim 7, further comprising altering at least one of a duty cycle and a polarity of modulation inputs to at least one of said X-axis controller, said Y-axis controller, and said Z-axis controller when said position error is greater than a specified minimum value.

9. The method of claim 7, further comprising producing a tactile feedback if said position error exceeds a predetermined amount along at least one axis.

10. The method of claim 1, wherein said system controller causes said tool distal end to move so that its position corresponds to position data from a Virtual Tip.

11. A method for controlling movement of a tool having a distal end to be inserted in a body, comprising;

calculating a desired direction of movement for said distal end;

computing a magnetic field needed to produce said movement;

controlling a plurality of electric currents to produce said magnetic field; and

locating said distal end by measuring a magnetic field of said distal end.

12. The method of claim 1, wherein said computing a magnetic field comprises:

determining a current position of said distal end with respect to one or more magnet poles; and

using a lookup table to find said magnetic field needed to produce said movement.

13. The method of claim 11, further comprising controlling one or more electromagnets to produce said external magnetic field.

14. The method of claim 11, further comprising measuring a temperature of one or more magnetic field sensors that measure said magnetic field of said distal end.

* * * * *